Effect of Hyperthyroidism and Hypothyroidism on Coronary Microvascular Geometry in Neonatal and Adult Rats

A Thesis Submitted to the School of Graduate Studies and Research of the University of Ottawa in Partial Fulfilment of the Requirements for the Degree of

Doctorate of Philosophy in Physiology

Candidate: Marcia Indranee Heron

Supervisor: Dr. K. Rakusan

ISBN 0-612-16444-6

UNIVERSITÉ D'OTTAWA
UNIVERSITY OF OTTAWA

DEDICATION

To my parents whose never-ending love and support have helped me to make my dreams come true. To my brother, who always kept me laughing - "Nub you". To my best friend, James, for always being there - "Love is a Many Splendid Thing". To Monty and Jasmine, all creatures great and small!

CARPE DIEM!

ACKNOWLEDGMENTS

I would like to thank my supervisor and friend, Dr. Karel Rakusan, for his guidance and counsel throughout the course of my graduate studies. You have challenged me, encouraged me, and taught me many things. I thank Ching-Ju Kuo and Barbara Hebert for all of their extremely valuable help, but especially for their very cherished friendship. Thank you to a partner in crime, David Silverman, who without fail questioned and challenged everything I said - "banker's hours forever". I thank my advisory committee, Dr. David Parry and Dr. William Ross, for their helpful insight and guidance. Finally, I wish to express my appreciation and gratitude to all of the professors and graduate students in the Department of Physiology, who have made my studies a truly enjoyable, learning experience.

TABLE OF CONTENTS

LIST OF FIGURES

LIST OF TABLES

LIST OF COLOR PLATES

ABSTRACT

The coronary microvasculature plays an essential role in myocardial oxygenation. The number and distribution of coronary capillaries determines the geometrical conditions for oxygen diffusion, whereas coronary arterioles regulate blood flow. Thus, the coronary microvascular response during pathological growth is important for the maintenance of adequate myocardial oxygenation. The aim of this research was to examine the coronary microvascular response to hyperthyroidism and hypothyroidism induced during the neonatal and adult periods.

Capillary geometry was examined in hyperthyroid, hypothyroid, and hypo-hyperthyroid adult male Sprague Dawley rats. Heart rates increased in hyperthyroid and hypo-hyperthyroid rats ($P<0.01$) but decreased in hypothyroid rats ($P<0.01$) compared to control. Adult-onset hyperthyroidism increased absolute and relative heart mass ($P<0.01$), whereas hypothyroidism decreased these parameters ($P<0.01$). In hypo-hyperthyroid rats, heart mass increased ($P<0.01$) compared to hypothyroid rats and relative heart mass increased compared to control ($P<0.01$).

Sections of left ventricular (LV) midmyocardium were processed using the following methods: (1) Alkaline phosphatase/Dipeptidyl peptidase IV (AP/DPP), which distinguishes between capillaries located in proximal and distal portions of the capillary network, enabling analysis of geometry in different regions of the capillary bed; (2) Silver-methenamine, which facilitates identification of capillaries and myocytes, enabling determination of capillary and myocyte numerical density and

myocyte-to-capillary ratios; and (3) immunohistochemical detection of Proliferating Cell Nuclear Antigen (PCNA) enabling the derivation of an index of cell proliferation.

Capillary numerical density was maintained in hyperthyroid and hypo-hyperthyroid rats despite increased LV mass, suggesting capillary proliferation. Hypothyroid rats had a larger than expected increase in capillary numerical density compared to control ($P<0.01$) thereby suggesting capillary proliferation. In hyperthyroid rats, the area of tissue surrounding an individual capillary (capillary domain) decreased for proximal capillaries, whereas in hypothyroid rats domain areas decreased in both proximal and distal regions compared to control ($P<0.01$). All groups had shorter capillary segment lengths (distance along a capillary between two consecutive branch points) in proximal and distal regions relative to control ($P<0.05$). PCNA labelling of endothelial cells was significantly increased only in hypo-hyperthyroid rats ($P<0.01$). These data suggest that both adult-onset hyper- and hypothyroidism induced capillary proliferation.

The effect of altered thyroid hormone status on the developing coronary microvasculature was examined in neonatal rats. Long-term effects of neonatal-onset hyper- and hypothyroidism on coronary microvascular geometry and cardiac function were examined in a subset of adult rats in which euthyroidism had been re-established. Neonatal-onset hyperthyroidism enhanced maturation, while hypothyroidism attenuated maturation. Serum T_3 levels and heart rates ($P<0.01$) increased in hyperthyroid but decreased in hypothyroid rats compared to control. After discontinuing treatment,

heart rates were similar between control and previously hypothyroid rats. Occasionally, heart rates remained elevated in previously hyperthyroid rats compared to control ($P<0.05$). Hyperthyroidism produced ventricular hypertrophy while hypothyroidism slowed cardiac growth ($P<0.01$). Both neonatal thyroid conditions induced a long-term deficit in LV growth ($P<0.01$) after euthyroidism was re-established.

Sections of LV midmyocardium were processed using the following methods: (1) *Bandeiraea simplicifolia I* lectin, for determination of capillary numerical density; (2) AP/DPP staining; (3) PCNA immunohistochemistry, and (4) Silver-methenamine staining for morphometric analysis of coronary arterioles. Capillary and arteriolar numerical density, as well as proximal and distal capillary segment lengths, were maintained in hyperthyroid rats despite LV hypertrophy suggesting enhancement of capillary and arteriolar proliferation. Total arteriolar length was greater in hyperthyroid than control rats ($P<0.05$). With hypothyroidism, capillary numerical density was either maintained or increased compared to control. Total arteriolar length was significantly lower in hypothyroid rats ($P<0.01$) suggesting slowed arteriolar growth. After cessation of treatment, total arteriolar length in previously hyperthyroid rats did not change despite increased LV mass. Previously hyperthyroid rats had increased RV and LV systolic pressure, LV developed and end-diastolic pressure, and +(dP/dt)max ($P<0.05$). An increased percentage of small arterioles (i.e. 10-30μm) was observed in previously hypothyroid rats.

In summary, adult-onset hypothyroidism and hyperthyroidism induced coronary capillary growth despite opposite changes in cardiac mass. In neonatal rats, hypothyroidism attenuated cardiac and arteriolar growth, yet its effect on capillary growth was variable. In contrast, neonatal-onset hyperthyroidism enhanced cardiac, capillary, and arteriolar growth. A long-term deficit in LV growth was induced by both neonatal thyroid conditions. Neonatal hypothyroidism resulted in subsequent growth of small arterioles after return to euthyroidism. Neonatal hyperthyroidism inhibited subsequent arteriolar growth and induced long-term positive inotropic, and possibly chronotropic, effects on cardiac function.

PREFACE

The principal goal of this dissertation is to quantify the response of the coronary capillary and arteriolar networks to hypo- and hyperthyroidism, induced during two different developmental stages - the neonatal period and adulthood. The coronary capillaries and arterioles, which will be referred to collectively as the coronary microvasculature, were analyzed as capillaries represent the major sites of O_2 exchange between blood and tissue, whereas arterioles, while also a site of O_2 exchange, function mainly to regulate blood flow and consequently O_2 supply. Thus the spatial organization and morphology of the coronary microvascular bed are important determinants of myocardial O_2 supply. The neonatal and adult stages were examined as the response of the coronary microvasculature to altered hemodynamic load has been shown to differ between young and adult mammals. Finally, use of both hyper- and hypothyroid models enabled comparison of the microvascular response to a hypertrophic (hyperthyroidism) or atrophic (hypothyroidism) condition.

By morphometrically analyzing the microvascular network in these two models at two different stages, one can assess the conditions under which microvascular growth or rarefaction are elicited and determine whether the microvascular response maintains the geometrical conditions for oxygen supply. Moreover, analysis of these two different periods may provide insight into the possible factors that are involved in the elicited microvascular response during different developmental stages.

Some of the terminology used in this dissertation - growth, proliferation,

development, and maturation - are closely related but can mean different things to different people, and have sometimes been used interchangeably in the literature. To avoid confusion, their usage, in the context of this dissertation will be defined. Growth, whether in reference to total body, cardiac, or microvascular, simply means an increase in the dimensional parameters of an organ. This growth may result from an enlargement in the existing elements of the unit or from an increase in the number of these elements. An increase in the number of elementary parts is termed proliferation. For example, cardiac growth generally refers to an increase in heart mass. This increase may arise from an increase in the volume of individual cardiac myocytes (hypertrophy) or in their absolute number (hyperplasia). Development refers to the natural progression from a previous, lower stage to a later, more complex stage. Closely related to this concept of development is maturation. Maturation involves progression through a series of physiological, biochemical, and morphological changes with increasing age, in the attainment of an adult phenotype. Thus, each stage of development (e.g. neonatal, adulthood) is associated with a given level of maturation.

The Introduction (Chapter 1) of this dissertation is essentially divided into three main areas. The first, outlines the importance of the different aspects of coronary microvascular geometry (e.g. morphology, numerical density, and spatial distribution within the myocardium) for myocardial O_2 supply. The second, reviews the pertinent features of normal postnatal growth of the coronary capillary and arteriolar networks providing a basis against which pathological growth may be compared. The current

state of knowledge regarding the coronary microvascular response to thyroid hormone-induced cardiac hypertrophy and hypothyroid-induced cardiac atrophy is then described. The third, discusses some of the unique histochemical techniques used in this research and introduces a novel immunohistochemical approach to assess cell proliferation. Notably, our laboratory was among one of the first to apply this immunohistochemical method to frozen cardiac tissue sections for the detection and quantitation of cell proliferation.

The subsequent three chapters outline and discuss the results of morphometric studies designed to examine the response of the coronary capillary network to adult-onset hypo- and hyperthyroidism (Chapter 2), and the developing coronary capillary (Chapter 3) and arteriolar networks (Chapter 4) to neonatal-onset hypo- and hyperthyroidism. All morphometric analysis were performed in the left ventricular myocardium of male rats. While we are aware that rats are born comparably more immature than humans, a rat model was used in order to compare the results of this research to other studies in the literature. Moreover, if maturation does play a role in the response of the microvascular network to a pathological stimulus, then thyroid hormone changes would be more pronounced in rats. At the end of each chapter the results of that particular study are briefly discussed. The final chapter of this dissertation (Chapter 5) summarizes the principal findings of these studies and discusses their implications.

Various portions of this dissertation have already been, or will shortly be published. The following list summarizes the present status of the research presented:

TOPIC	REFERENCE	STATUS
Evaluation of coronary capillaries in longitudinal sections (Introduction)	Oxygen Transport to Tissue XVI, p. 407-415 (1994)	Published
PCNA detection of cellular proliferation (Introduction)	J. Mol. Cell. Cardiol. 27(7):1393-1403 (1995)	Published
Capillary geometry in adult-onset hypo- and hyperthyroidism (Chapter 2)	Am. J. Physiol. 267:H1024-H1031 (1994)	Published
Capillary geometry in neonatal-onset hypo- and hyperthyroidism (Chapter 3)	Cardiovasc. Res.	Submitted
Arteriolar geometry in neonatal-onset hypo- and hyperthyroidism (Chapter 4)	Am. J. Physiol.	In press

CHAPTER 1

INTRODUCTION

1.1 Physiological perspective

The coronary microvascular network plays an essential role in the transport and distribution of O_2, CO_2, nutrients, heat, etc. between cardiac tissue and blood. In the case of myocardial oxygen supply, this role is especially important. Coronary arterioles regulate blood flow and thus oxygen supply into the capillary networks. In comparison, the coronary capillaries are the main sites of oxygen exchange, and as such the number and distribution of these vessels within the myocardium determines the geometrical conditions for oxygen diffusion between the blood and tissue. As a consequence, changes in the normal geometry of the coronary microvasculature can affect myocardial oxygenation. Therefore, the response of the coronary arterioles and capillaries to a pathological growth stimulus is very important, particularly with respect to its impact on the geometrical arrangement of the microvascular network and consequently maintenance of myocardial oxygen supply.

1.2 Coronary capillary geometry and myocardial oxygen supply

1.2.1 Krogh model of oxygen supply to tissue

A model for conceptualizing the relationship between the number or density of capillaries within a tissue cross-section and the diffusion of oxygen to muscle cells was first introduced by August Krogh (1919). In Krogh's model of oxygen supply

(Fig. 1.1), each capillary is considered a straight tube from which oxygen diffuses radially, supplying a surrounding concentric cylinder of tissue (Krogh, 1919).

The average cross-sectional area of the "Krogh" tissue cylinder can be determined by counting the number of capillaries within a known cross-sectional area (i.e. the capillary numerical density), and then dividing this known area by the number of capillaries. The cross-sectional area of the Krogh cylinder represents the amount of tissue that in theory, is supported by an individual capillary. From the average cross-sectional area the average radius of the Krogh tissue cylinder, an important determinant of myocardial oxygenation, can be estimated. Notably, oxygen is consumed as it traverses radially through the tissue and along the capillary from arteriole to venule, thus tissue at the margins of the Krogh cylinder are more susceptible to hypoxia especially toward the venous end.

A mathematical equation was developed for the Krogh model by the Danish mathematician, Erlang (Krogh, 1919). The Krogh-Erlang equation, based on Fick's First law of diffusion, enables calculation of the pressure difference necessary to supply a muscle with oxygen:

$$\Delta P = Pc - Px = \frac{M}{K}\left(\frac{R^2}{2}\ln\frac{x}{r} - \frac{(x^2 - r^2)}{4}\right)$$

The Krogh-Erlang equation

Where Pc = capillary PO_2 (mmHg); Px = tissue PO_2 at a distance x, from the center of the capillary (mmHg); M = oxygen consumption (mL O_2 / gm tissue / min); K = Krogh's diffusion coefficient or oxygen conductivity (mL O_2 / cm•min•mmHg); R = radius of the Krogh tissue cylinder (cm); r = capillary radius (cm); x = distance from center of capillary to a point in the tissue (cm).

Figure 1.1 Krogh's model of cylindrical tissue supply. r = capillary radius (cm); R = radius of the Krogh tissue cylinder (cm); Pc = capillary PO_2 (mmHg); Px = tissue PO_2 at any distance x (cm), for the centre of the capillary (mmHg); L = length of the capillary. (Modified from Rakusan, 1971; Fig. 1).

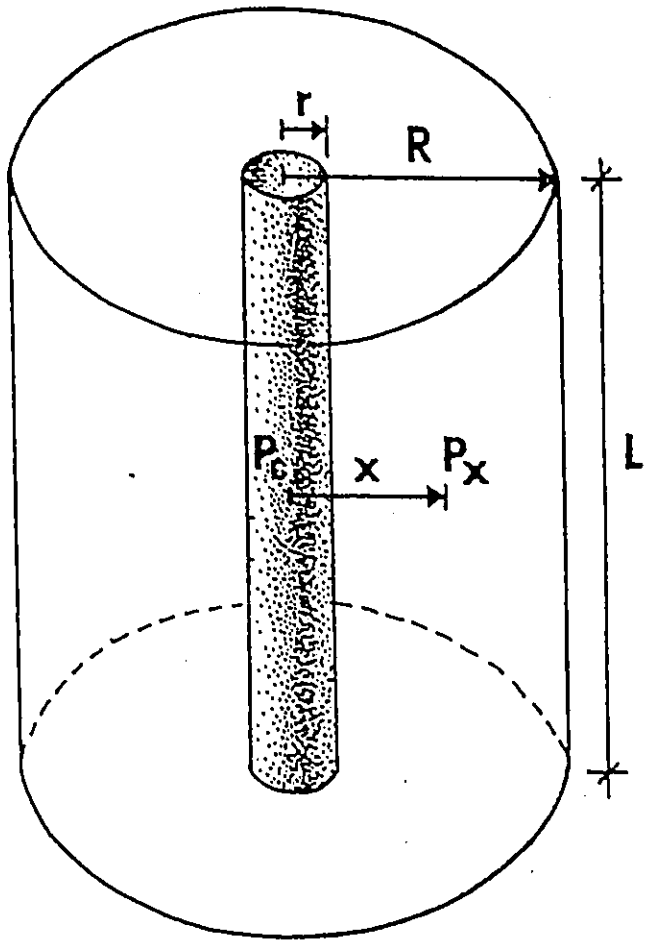
r
R
P_c
x
P_x
L

1.2.2 Determinants of myocardial oxygenation

The Krogh-Erlang equation, which is based on a number of simplifications and assumptions (for a review please see Kreuzer, 1982), cannot be applied rigidly to oxygen diffusion in the heart. However, this equation still provides a reliable indication of the oxygen supply from capillaries into the surrounding tissue. Many factors influence myocardial oxygenation, however the following discussion focuses on the importance of the radius of the Krogh cylinder and the heterogeneity in capillary spacing as these are the most relevant to our research.

Using the Krogh-Erlang equation, Rakusan (1971) evaluated the effect that independently changing individual oxygen determinants (i.e. myocardial oxygen consumption, myocardial blood flow, the diffusion coefficient or conductivity of oxygen, oxygen content of arterial blood, radius of the Krogh tissue cylinder, and capillary radius) would have on myocardial oxygenation or myocardial PO_2. In the analysis, capillary PO_2 (Pc) at any point along the capillary was estimated using the following equation:

$$Pc = Co = Ca - \left(\frac{M}{F}\right)\left(\frac{Lo}{L}\right)$$

Where Co= O_2 content in the capillary blood (mL O_2 / mL blood); Ca = O_2 content in arteriolar blood (mL O_2 / mL blood); M = myocardial O_2 consumption (mL O_2 / gm tissue / min); F = coronary blood flow (mL blood / gm tissue / min); Lo = a length along the capillary (cm); L = length of the capillary (cm).

Notably, this equation takes into account the effect of changing coronary blood flow. Under normal conditions, myocardial oxygen consumption (M) is the most important determinant of myocardial PO_2, followed by coronary blood flow (F) and the O_2 content of arteriolar blood (C) (Fig. 1.2). The radius of the Krogh tissue cylinder (R) has a significant influence on myocardial PO_2 only when its values exceeded normal. Changes in capillary radius (r) and oxygen conductivity (K) have little effect on myocardial PO_2, except in extreme non-physiological cases.

Rakusan (1971) also examined the consequences that pathological conditions would have on myocardial PO_2 by using realistic data reported in the literature as input values for the Krogh-Erlang equation. Myocardial PO_2 is markedly reduced in situations characterized by an increased radius of the Krogh cylinder (e.g. cardiac hypertrophy with decreased capillary numerical density) and increased myocardial oxygen consumption. Under such circumstances, subsequent small increases in the radius of the Krogh cylinder (e.g. subsequent decreases in capillary numerical density) lead to considerable reductions in myocardial PO_2 resulting in cellular hypoxia or even anoxia. Thus, in the case of pronounced cardiac hypertrophy the radius of the Krogh tissue cylinder becomes the most important determinant of myocardial oxygenation.

Another important myocardial O_2 determinant, which was later proposed, is the heterogeneity in capillary spacing (Turek and Rakusan, 1981). The Krogh model assumes that capillaries are homogeneously distributed throughout a muscle. However, this assumption is not valid for various tissues including the heart. Turek

Figure 1.2 Changes in myocardial PO_2 as a result of changes in individual oxygen determinants. 100% represents normal physiological conditions. The point of intersection of these curves indicates the PO_2 in the heart muscle under normal conditions. F = myocardial blood flow; C = oxygen content of arterial blood; r = capillary radius; K = Krogh's diffusion coefficient or oxygen conductivity; M = myocardial oxygen consumption; R = radius of the Krogh tissue cylinder. (Modified from Rakusan, 1971; Fig. 4).

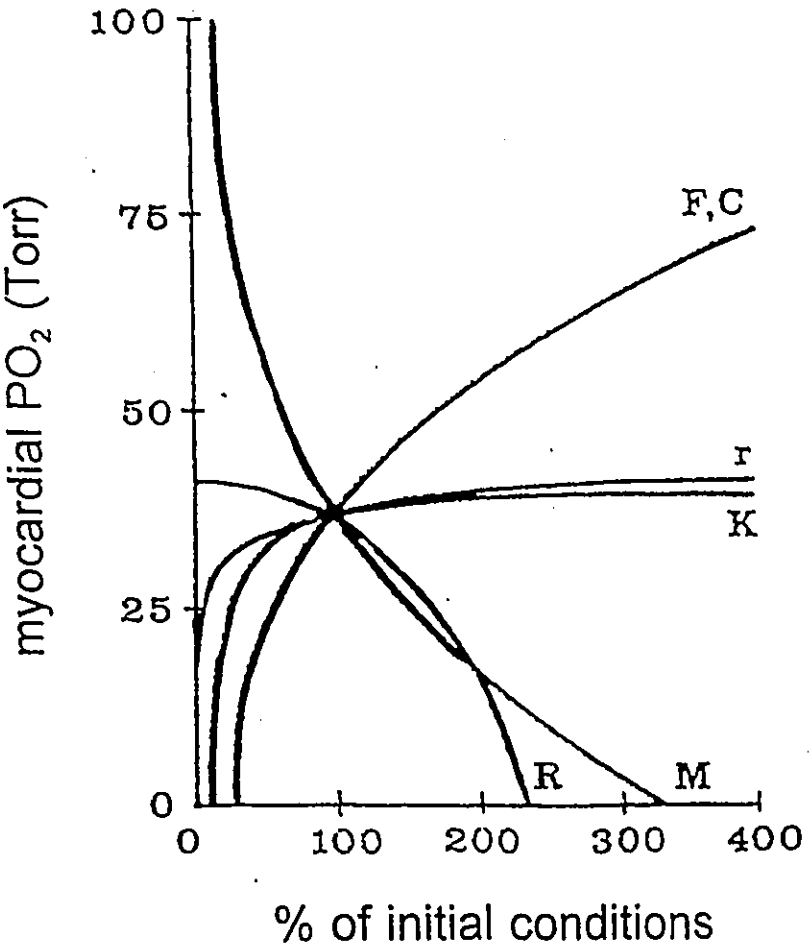
100
75
50
25
0
0
100
200
300
400
myocardial PO_2 (Torr)
% of initial conditions
F,C
r
K
R
M

and Rakusan (1981) determined that the distribution of intercapillary distances (distance between two adjacent capillaries in a tissue cross-section) was log-normal, indicating non-homogeneity in capillary spacing. An index of the heterogeneity in capillary spacing may be obtained from the standard deviation of this log-normal distribution (SD_{log}). Increasing heterogeneity in capillary spacing is associated with impaired myocardial oxygenation (Turek and Rakusan, 1981; Rakusan and Turek, 1985).

1.2.3 Advanced morphometric methods for assessing coronary capillary geometry

The following section outlines the advanced morphometric methods that were used in our research for the comprehensive assessment of coronary capillary network geometry. The relevance and advantages of these methods are discussed.

Method of Capillary Domains

The underlying principle of the domain method is to assign a region of tissue to each capillary within a cross-section by delineating equidistant borderlines between each capillary and all of its neighbouring capillaries (Hoofd et al., 1985). The resulting polygonal areas of tissue surrounding each individual capillary is referred to as the capillary domain and theoretically represents the region of myocardial tissue supplied by that capillary (Fig. 1.3). By converting each capillary domain into a circle of equivalent area the corresponding radius of the Krogh cylinder may be

Figure 1.3 Schematic representation of capillary domain computer print-out. Circles represent the location of capillary profiles within the tissue cross-section. Polygonal regions around the capillaries represent the capillary domain.

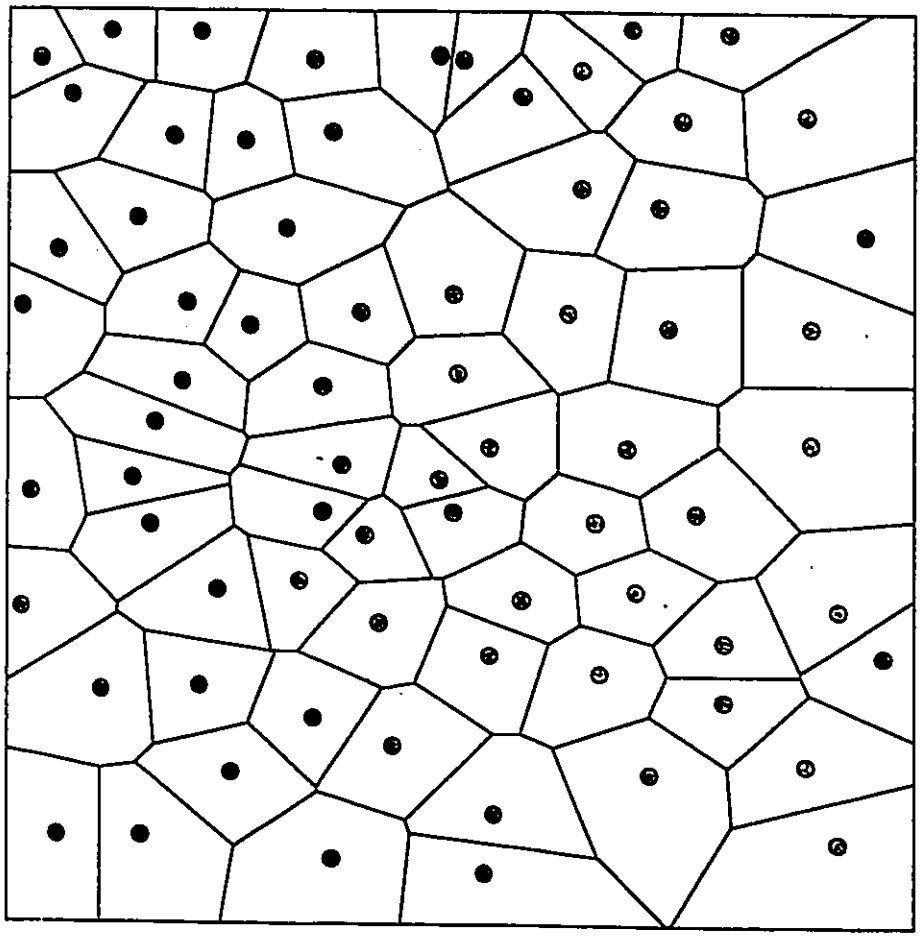

calculated. The distribution of these radii is log-normal and thus, the index of heterogeneity of capillary spacing (SD_{log}) may be determined. The capillary domain method is valuable as it enables determination of the heterogeneity index (SD_{log}), and can also be used as a morphometric measure of the geometrical conditions for myocardial oxygen supply at the level of an individual capillary. In contrast, capillary numerical density and the related average cross-sectional area of the Krogh cylinder, can only provide a global index of myocardial oxygen supply.

The development of a unique histochemical procedure, the Alkaline phosphatase/Dipeptidyl peptidase IV method (described later in section 1.7.1), which distinguishes capillaries located in proximal regions of the microvascular bed (i.e. proximal capillaries located close to their feeding arterioles) from capillaries located in distal regions (i.e. distal capillaries located close to their collecting venules), has enabled the examination of capillary geometry in two locations of the capillary network, having different oxygen supply conditions. When the capillary domain method is used in conjunction with the AP/DPP stain the area of tissue supplied by an individual capillary may be compared between proximal and distal regions of the capillary network.

According to the Krogh model a constant area of tissue is always supplied along the length of a capillary from arteriole to venule. However, in normal adult rats, proximal capillaries were found to have larger domain areas than distal capillaries (Batra et al., 1991; Batra and Rakusan, 1991, 1992). This configuration, which has

been described as a "truncated cone" (Batra et al., 1991), is more advantageous for oxygen supply than the classical Krogh model. With the "truncated cone" a smaller area of tissue is supported by capillaries in distal portions of the capillary bed where capillary PO_2 and O_2 content are lower. In comparison, a larger tissue area is supplied by capillaries in proximal regions as capillary PO_2 and O_2 content are higher.

Capillary segment length

Reconstruction of longitudinal capillary sets, which are comprised of all capillaries originating from a single arteriole and draining into a single venule (Batra et al., 1989), was facilitated by the AP/DPP method. Measurement of longitudinal capillary parameters (e.g. capillary set length, minimum capillary pathlength, etc.) can be made for different regions of the capillary network from these reconstructed sets (Batra and Rakusan, 1991; Batra et al., 1991). Even though the method of longitudinal reconstruction provides a lot of information regarding capillary geometry along the length of the capillary network, it has certain limitations. For instance, the number of capillary sets available within a section is very small and as such many sections have to be examined in order to find a sufficient number of reliable capillary sets. The tortuosity and intermingling of capillaries in and out of the plane of the section, occasionally results in the inability to trace an entire capillary from arteriole to venule. This discontinuity also presents problems in establishing whether all capillaries in a particular section belong to the same capillary set.

The simple, but practical "short cut" approach for evaluating capillary segment lengths, which are defined as the distance of a capillary portion located between two clearly visible successive branch points, provides an alternative reliable method for evaluating changes in geometry along the length of the capillary bed (Rakusan et al., 1994a). As capillary segment lengths can be determined for both proximal and distal capillaries, comparison may be made between these two regions of the capillary bed.

In normal adult rats, segment lengths are longer for capillaries located in proximal portions of the capillary bed than for capillaries located in distal portions (e.g. Batra et al., 1991). This differs from the Krogh model, which in fact does not describe capillary segments, but regards capillaries as being of constant length and running directly from arteriole to venule without branching (Krogh, 1919).

Capillary supply unit

Combining longitudinal and cross-sectional capillary data enabled conceptualization of a three dimensional volume of tissue supplied by an individual capillary segment (Rakusan et al., 1994a). This volume of tissue, called the capillary supply unit (Fig. 1.4), is defined as the product of the average capillary domain area and average capillary segment length. The capillary supply unit, which can be determined for both proximal and distal regions of the capillary network, represents the smallest three-dimensional supply volume which can be accurately modelled. In normal adult rats, the capillary supply unit is larger in proximal regions than in distal

Figure 1.4 Schematic representation of the Capillary Supply Unit and its possible relationship to a myocardial cell. (Modified from Rakusan et al., 1994a; Fig. 3).

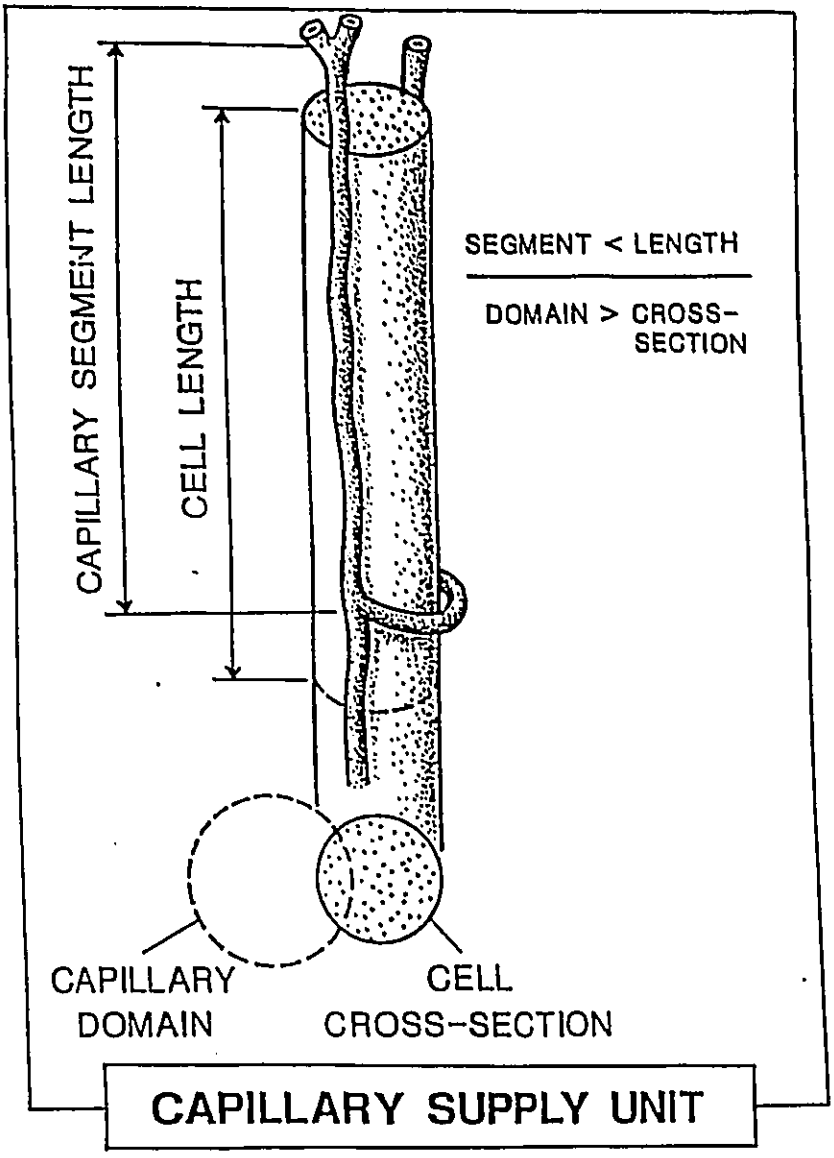
CAPILLARY SEGMENT LENGTH
CELL LENGTH
SEGMENT < LENGTH
DOMAIN > CROSS-SECTION
CAPILLARY DOMAIN
CELL CROSS-SECTION
CAPILLARY SUPPLY UNIT

regions of the capillary network (Rakusan et al., 1994b). Thus, proximal capillaries support a greater volume of tissue than distal capillaries in accordance with greater PO_2 in proximal portions and lower PO_2 in distal portions of the capillary network.

1.3 The coronary arteriolar network and regulation of oxygen supply

The total arteriolar cross-sectional area is an important factor in the regulation of maximal coronary blood flow and thus oxygen supply. Since maximal coronary blood flow is inversely proportional to the total arteriolar cross-sectional area, functional changes due to increased or decreased vasomotor tone, or morphometric changes due to arteriolar proliferation or rarefaction, or an altered wall thickness-to-lumen ratio, all of which affect the total arteriolar cross-sectional area, will impact on myocardial oxygenation.

Left ventricular hypertrophy in adult mammals is generally associated with an increase in minimal coronary vascular resistance and limitation in maximal coronary blood flow due either to inadequate growth of the coronary arterioles (decreased number of arterioles per unit area) or reduction in lumen radius as a consequence of medial hypertrophy (for reviews please see Chilian and Marcus, 1987; Tomanek, 1990). However, there are reports of left ventricular hypertrophy accompanied by proportional arteriolar growth and absence of medial hypertrophy, thereby preserving myocardial perfusion and likely oxygen delivery (for reviews please see Chilian and Marcus, 1987, and Tomanek, 1990; not included in reviews: Chen et al., 1994). One

can therefore appreciate that conditions such as cardiac hypertrophy, which can alter the morphometry of the microvascular network may adversely affect the geometrical conditions for oxygen diffusion and regulation of myocardial oxygen supply, thereby predisposing the heart to hypoxic events and potentially failure.

1.4 Normal postnatal growth of the coronary capillary network

In mammalian hearts, the establishment of definite morphological and biochemical characteristics of the vascular walls, as well as the orientation and spatial arrangement of capillaries within the myocardial layers, continues after birth (for review please see Rakusan, 1990).

Rat heart: In the rat, postnatal cardiac development can be described by four distinct stages (Rakusan et al., 1965). Stages 1 to 3 include the period from birth to adulthood, and stage 4, the period of senescence. The following discussion will focus only on the first three stages, as these pertain to the developmental periods which were examined in our studies.

The first stage, from birth until approximately the fourth postnatal week, is characterized by a substantial increase in the number of capillaries, as well as in the number and diameter of cardiac myocytes (Rakusan and Poupa, 1963). The increase in capillaries occurs at a faster rate than the increase in myocyte number as evidenced by a decrease in the ratio of cardiac myocytes to coronary capillaries during this stage

- from 4 to 1.5 (Rakusan et al., 1965). Similar changes have since been observed by Olivetti and co-workers (1980), and later by Anversa and co-workers (1986). As a consequence of the rapid capillary proliferation, irregularity in capillary spacing is observed during this period of cardiac development (Rakusan and Turek, 1985).

In the second stage, which includes the fourth to seventh postnatal week, myocyte proliferation has stopped and only their diameters continue to increase (Rakusan and Poupa, 1963). Capillary proliferation continues, though at a much slower rate, and consequently the ratio of myocytes to capillaries decreases from 1.5 to 1.0. In accordance with the increased myocyte diameter and decreased formation of new capillaries, capillary numerical density decreases (Rakusan and Poupa, 1963; Anversa et al., 1986, 1989; Batra and Rakusan, 1992) and the radius of the Krogh cylinder, which is the shortest at the start of this period, increases (Rakusan et al., 1965).

The third stage, which begins during the seventh postnatal week and continues into adulthood, is characterized by a constant ratio of myocytes-to-capillaries - 1:1. As myocyte diameter continues to increase, capillary numerical density continues to decrease (Rakusan and Poupa, 1963; Anversa et al., 1986, 1989; Batra and Rakusan, 1992) and consequently the radius of the Krogh cylinder increases. Despite decreasing capillary numerical density and increasing radius of the Krogh cylinder, capillary spacing becomes more homogeneous with age (Rakusan and Turek, 1985). Similar developmental changes in early postnatal capillary proliferation (Rakusan et

al., 1967) and in the myocyte-to-capillary ratio (Shipley et al., 1937) were observed in the hearts of rabbits.

Recently the domain and longitudinal reconstruction methods were used to analyze capillary network geometry, beginning at the post-weaning period of development (Batra and Rakusan, 1992). With age and increasing heart mass, capillary domain areas increased in both proximal and distal regions of the capillary bed; domain areas in proximal portions remained larger than in distal portions (Batra and Rakusan, 1992). Capillary segment lengths and capillary supply unit volumes also increase with age and heart mass (Rakusan et al., 1994b). Segment lengths and supply unit volumes were always greater in proximal than in distal portions of the capillary network under normal conditions.

Human heart: Changes in the developing coronary capillary network in human hearts are comparable to those described for the rat. Notably, only one further division of myocyte nuclei is believed to occur in human hearts between birth and the sixth postnatal month (for review please see Rakusan, 1984). As such, subsequent growth of the human heart occurs mainly by increases in the volume of individual myocytes. Roberts and Wearn (1941) observed a decrease in the myocyte-to-capillary ratio with age - from approximately 6 at birth, to 1 in adulthood. The ratio of one myocyte to one capillary remains constant in adult human hearts (Roberts and Wearn, 1941). Rakusan and co-workers (1992) reported a decrease in capillary numerical

density with age and increasing heart mass, during normal growth in early childhood. In adult human hearts, capillary numerical density remains relatively constant (Rakusan et al., 1992).

1.5 Normal postnatal growth of the coronary arteriolar network

While the quantitative changes in the capillary network during postnatal development are relatively well known, comparable data on early postnatal development of the arteriolar network in rats and humans are few.

Rat heart: It is known that growth of coronary arteries continues postnatally (Dbaly, 1973), however after approximately the 12th postnatal day, no new arterial stems or anastomoses are formed (Dbaly, 1973). Even though one cannot extrapolate directly, it may be hypothesized that development of the coronary arteriolar network follows a similar pattern - growth continues after birth, but gradually declines during the first few postnatal weeks, and thereafter no new arterioles are formed. Systematic morphometric assessment of the developing coronary arteriolar network is required.

Human heart: In human hearts, larger branches of the arteriolar tree are already formed at birth, while smaller vessels continue to proliferate postnatally. The magnitude of this proliferation is proportional to the increase in heart mass, as arteriolar numerical density is reportedly similar in hearts from infants, children, and

adults (Rakusan et al., 1994b).

To summarize, the early postnatal period of mammalian cardiac development is characterized by maturation and substantial proliferation of the coronary microvasculature, as well as establishment of capillary network geometry. With age and growth of the heart, proliferation of capillaries and possibly of arterioles, eventually stops. A relatively stable coronary vascular supply is a prominent feature of the adult period.

The adaptive expansion of the coronary microvascular network in the normally growing heart, can be separated from conditions in which inadequate growth of the microvascular network may lead to impaired myocardial oxygenation, as in the case of some forms of cardiac hypertrophy.

Many different factors play a role in the response of the coronary microvasculature to a hypertrophic stimulus. Among these is the developmental stage at which the stimulus is introduced. For example, in young mammals, volume and pressure overload-induced cardiac hypertrophy is generally accompanied by capillary growth, which results in either the maintenance or a smaller than expected decrease in capillary numerical density, and as such the geometrical conditions for oxygen supply are not impaired. In contrast, these same stimuli in adults induce cardiac hypertrophy without capillary growth, thus leading to decreased capillary numerical density and impaired geometrical conditions for oxygen supply (for review please see Rakusan, 1987; references not included in review: Batra et al., 1991; Batra and

Rakusan, 1991; Chen et al., 1994; Flanagan et al., 1994). Thyroid hormone-induced cardiac hypertrophy is characterized by biochemical and anatomical effects which separate it from other models of cardiac hypertrophy. The following section describes the unique aspects of thyroid hormone-induced cardiac hypertrophy, compares these with hypothyroid-induced cardiac atrophy, and reviews the current state of knowledge regarding the microvascular response to both hyper- and hypothyroidism, when induced in young and adult mammals.

1.6 Hyperthyroidism, hypothyroidism, and the coronary microvasculature

1.6.1 General background

Tetraiodothyronine or thyroxine (T_4), triiodothyronine (T_3), and reverse T_3 (rT_3) are the three known thyroid hormones produced and secreted by the thyroid gland. T_3 is the most biologically active of the three hormones, whereas rT_3 is secreted in very small amounts and has virtually none of the biological effects of the other two thyroid hormones (Haynes and Murad, 1980).

Thyroid hormones exert their effect on target tissues by binding to specific DNA-binding thyroid receptors (Sap et al., 1986; Weinberger et al., 1986; Izumo and Mahdavi, 1988; Koenig et al., 1988), and influencing gene transcription, and total RNA and protein synthesis (for reviews please see Samuels et al., 1989 and Brent et al., 1991; not included in reviews: Florini et al., 1973; Fagg-Sanford et al., 1978; Coleman et al., 1989; Ojamaa et al., 1992). A well-documented effect of thyroid

hormones on protein expression involves their regulation of myosin heavy chain isoforms (for reviews please see Morkin et al., 1983; Lompre et al., 1991). In adult rats thyroid ablation leads to predominant expression of the β-MHC isoform in ventricular tissue, while hormonal replacement therapy produces a reversion to a predominant α-MHC expression. Thyroid hormones also play a role in maintaining optimal levels of tissue metabolism, thermogenesis, and cardiac function in adult mammals, as well as in growth and maturation during the early postnatal period.

1.6.2 Cardiovascular manifestations of hyperthyroidism and hypothyroidism

The heart is a major target organ for the actions of thyroid hormones. Consequently, cardiac physiology can be influenced by sustained rises (i.e. hyperthyroidism) or falls (i.e. hypothyroidism) in plasma thyroid hormone levels (for reviews please see Morkin et al., 1983; Dillman, 1990; Woeber, 1992; Polikar et al., 1993; Klein and Ojamaa, 1995; not included in these reviews: Beznak, 1962, 1963; McCallister and Page, 1973; Craft-Cormney and Hansen, 1980; Talafih et al., 1983, 1984; Read et al., 1987; Coleman et al., 1989; Zimmer and Zierhut, 1990; Liu and Gerdes, 1990; Yao and Eghbali, 1992; Zimmer, 1993; Seppet et al., 1993; Weiss and Tse, 1995).

Adult-onset hyperthyroidism induces cardiac hypertrophy, that is characterized by a larger increase in myocyte cross-sectional area than in myocyte length (Campbell

and Gerdes, 1988; Campbell et al., 1991). Induction of cardiac hypertrophy by excess thyroid hormones occurs primarily in response to increased hemodynamic load and not from the direct actions of these hormones on the myocardium (Torres and Tucker, 1993; Rongish et al., 1995) - thyroxine treatment of recipient rats was not able to prevent atrophy of unloaded, heterotopically-transplanted hearts (Korecky et al., 1987).

Coronary capillary growth in proportion or in excess of the increase in myocardial mass, as well as the proportional growth of the arteriolar network, has been observed in rats (Craft-Cormney and Hansen, 1980; Chilian et al., 1985; Wachtlova et al., 1985; Mall et al., 1990; Tomanek et al., 1995) and pigs (Breisch et al., 1989). This growth resulted in the maintenance of capillary or arteriolar densities, or in some cases increased capillary numerical density, which in turn preserved or improved the geometrical conditions for myocardial oxygen supply. However, opposite changes in microvascular geometry have been reported. Gerdes and co-workers (1979) found that capillary growth in rats was not sufficient to compensate for the increase in myocardial mass. Similar observations were made by Weiss and Grover (1987) and Seiden and co-workers (1988) in adult hyperthyroid rabbits. The lack of agreement among studies is problematic for accurate theoretical modelling of myocardial oxygen supply and identification of possible mechanisms which may be involved in the microvascular response.

Most of these morphometric studies examined changes in the average capillary numerical density or average diffusion distance. As previously mentioned, these

indices can only provide a global estimate of myocardial capillarization, and no indication of the heterogeneity in capillary spacing or of geometrical changes along the length of the capillary bed. Furthermore, changes occurring predominantly in one region of the microvascular network may not be evident using parameters such as the average capillary numerical density. Comprehensive evaluation of capillary geometry in proximal and distal portions of the capillary network, using more advanced morphometric methods, is necessary for the accurate modelling of myocardial oxygen supply, as well as possibly helping to clarify the existing controversy.

Adult-onset hypothyroidism is generally considered to evoke the opposite effects on cardiac physiology, as hyperthyroidism (for reviews please see Morkin et al., 1983; Klein and Ojamaa, 1995). Hypothyroidism in adult mammals results in cardiac atrophy, owing primarily to a reduction in myocyte cross-sectional area (Liu and Gerdes, 1990). Decreased myocyte cross-sectional area effectively "draws" capillaries closer together, resulting in an increased number of capillaries per unit tissue area; this has been observed in adult hypothyroid rabbits (Tomanek et al., 1993). No appreciable effect on coronary arteriolar lumen diameter or arteriolar numerical density was observed. Interestingly, stimulation of capillary proliferation has also been postulated as contributing to the increased capillary numerical density found in adult-onset hypothyroidism (Wright and Hudlicka, 1981; Tomanek et al., 1993). To the best of our knowledge no other studies have examined the

microvascular response in this model.

In this model of adult hypothyroidism, it is unknown whether changes in capillary geometry occur uniformly throughout the network or whether these changes differentially influence the heterogeneity in capillary spacing in proximal and distal regions. Additionally, geometrical changes occurring along the length of the capillary network have not been reported.

Neonatal-onset hyperthyroidism and hypothyroidism: Many important processes which occur during normal postnatal cardiac growth and maturation are regulated by thyroid hormones. For example, proper development of the Ca^{2+}-handling mechanisms of the heart, depends on normal plasma thyroid hormone levels (Kolar et al., 1992; Wibo et al., 1995). Neonatal-onset hyperthyroidism accelerates the normal postnatal maturation of the sarcoplasmic reticulum leading to increased contractile function, whereas the opposite is true for neonatal-onset hypothyroidism (Kolar et al., 1992; Wibo et al., 1995).

Normal myocyte proliferation is also affected by altered neonatal thyroid status. Neonatal-onset hyperthyroidism reportedly inhibits normal postnatal myocyte proliferation and enhances myocyte hypertrophy, thus resulting in fewer cardiac myocytes within the left ventricle of young rats yet greater cardiac mass, as compared to normal age-matched euthyroid rats (Gerdes et al., 1983; Dubeck et al., 1989). It has been postulated that this decline in proliferation is due to a hastened transition

from hyperplastic to hypertrophic myocyte growth, induced by the hyperthyroid state. Conversely, neonatal-onset hypothyroidism has been shown to attenuate cardiac growth and maturation, possibly due to a reduction in myocyte growth and proliferation (Moussavi et al., 1985).

In comparison, very little is known about the involvement of thyroid hormones in the early postnatal development of the capillary and arteriolar networks. As normal postnatal growth and maturation of the microvascular network is essential for maintaining oxygen supply to the growing myocardium, abnormal formation of the microvascular bed may potentially impair normal cardiac development. Wachtlova and co-workers (1985) determined that 5 days of thyroxine treatment beginning on postnatal day 10, produced marked cardiac hypertrophy which was accompanied by proportional growth of the capillary network. However, the effect of thyroxine treatment on coronary arteriolar development was not examined, nor was the influence of neonatal hypothyroidism on development of the microvascular network.

It is generally accepted that early treatment of neonatal thyroid disorders in humans, results in normal intellectual development (e.g. Liu et al., 1994), however in rats, total body growth was still affected after return to euthyroidism (Meisami, 1984). Very few studies have determined however, whether abnormal cardiac development resulting from these neonatal thyroid conditions is normalized with re-establishment of euthyroidism (e.g. Moussavi et al., 1985). For a more complete understanding of long-term recovery from altered neonatal thyroid hormone status, the question of

whether changes in the normal development of the microvascular network induced by either neonatal hyper- or hypothyroidism, persist into adulthood after return to a euthyroid status also needs to be addressed.

1.7 Histochemical and immunohistochemical methods for assessment of coronary microvascular geometry and cell proliferation

Since the application of India ink/gelatin injections in the heart many different methodological approaches have been developed in an attempt to visualize the coronary microvascular network and facilitate accurate morphometric evaluation. The following discussion is divided into two main portions. The first portion, describes three histochemical techniques (Alkaline phosphatase/Dipeptidyl peptidase IV, *Bandeiraea simplicifolia I* lectin, and Silver-methenamine), which were used in this research. Even though these methods have previously been employed in morphometric studies of the coronary microvasculature, they are not routinely used and thus warrant discussion. The second portion describes an immunohistochemical method (detection of Proliferating Cell Nuclear Antigen), which has recently been modified for use in the heart, in order to detect cell proliferation.

1.7.1 Histochemical methods

Histochemical methods have traditionally been used to delineate the coronary microvascular network. Unlike injection techniques, these methods rely on the biochemical or enzymatic characteristics of endothelial cells and not on the perfusion

state of the vascular bed at the time of sacrifice. Histochemical methods generally require a small portion of cardiac tissue for processing, leaving the remaining tissue for biochemical or molecular assays.

Alkaline phosphatase (AP), an enzyme expressed on the surface of endothelial cells, has been widely used as a histochemical marker for capillaries in both skeletal and cardiac muscle (for review please see Hudlicka and Tyler, 1986). Similar techniques for staining capillary walls include the Periodic acid-Schiffs and ATPase methods (Sillau and Banchero, 1977; Rosenblatt et al., 1987; Hansen-Smith et al., 1992a; Erzen and Maravic, 1993).

Alkaline phosphatase and Dipeptidyl peptidase IV

Not all capillaries in the heart express the AP enzyme however. Lojda (1979) determined that another enzyme, Dipeptidyl (amino) peptidase IV (DPP), was present in distal parts of the capillary bed (i.e. in capillaries located close to their collecting venule) and in small venules, whereas AP was primarily localized in feeding arterioles and the proximal portion of the capillary bed (i.e. in capillaries located close to their feeding arteriole). The combined histochemical detection of both AP and DPP in myocardial tissue sections (Batra et al., 1989), has enabled morphometric evaluation of coronary capillaries, in both cross- and longitudinal sections, as a function of their location within the capillary bed (Batra et al., 1991; Batra and Rakusan, 1991, 1992).

Even though the AP/DPP method may be readily employed in many adult

animals (Grim and Carlson, 1990), its use is limited in immature hearts, as the enzymes are not fully expressed until approximately 21 days of age in rats (Batra and Rakusan, 1992). In addition, the expression of the AP enzyme is affected by some experimental conditions, such as hypoxia (Hansen-Smith et al., 1992b).

Bandeiraea simplicifolia I lectin

An alternative method, which uses a specific lectin, *Bandeiraea simplicifolia I* (BSI), to probe the terminal α-galactosyl saccharides associated with endothelial cell surfaces, has been introduced (Hansen-Smith et al., 1988; Hansen-Smith et al., 1992a). When lectins are combined with a visible marker, such as a peroxidase derivative or fluorochrome, they permit the localization of capillaries within tissue cross-sections. The BSI lectin method is more advantageous than dye injections or enzymatic methods, as it readily identifies capillaries in tissue cross-sections irrespective of perfusion state or degree of enzyme activity (Christie and Thomson, 1989). Furthermore, the sites for BSI lectin binding are present in the capillary bed of developing hearts, and are stable during hypoxia (Hansen-Smith et al., 1992a).

Silver-methenamine

The method of Silver-methenamine readily stains the basement membranes of both coronary capillaries and cardiac myocytes, thereby enabling morphometric analysis of myocytes and capillaries within cross-sections. The walls of coronary

arterioles are also clearly delineated using this procedure facilitating morphometric analysis of coronary arterioles.

It was necessary throughout the course of this research to employ these three different methods for the analysis of the coronary capillary network. Ideally, the AP/DPP method is the method of choice for comprehensive assessment of coronary capillaries in different regions of the capillary network. This method can only be used in frozen sections. However, for accurate morphometric evaluation of coronary arterioles, the Silver-methenamine method is generally used in thin plastic sections. Even though this method may also be used for the assessment of capillarization, in order to compare cross-sectional and longitudinal capillary data within the same hearts the BSI lectin method was used together with the AP/DPP method in frozen hearts. This lectin method enabled capillary numerical density estimates in the youngest rats examined (i.e. 12 days of age) - the AP/DPP method can not be used at this age.

1.7.2 Methods for the assessment of cell proliferation

Even though quantitative morphometric evaluation is probably the best method for examining microvascular geometry, one is not able to discern solely from these data whether geometrical changes may have resulted from microvascular proliferation, or from re-arrangement and expansion of existing material. Quantification of mitotic figures or labelling of proliferating cells with radioactive thymidine or non-radioactive bromodeoxyuridine, have been used to directly determine endothelial (e.g. Engerman

et al., 1967; Sholley et al., 1984; Wickline and Fischer, 1985) or cardiac myocyte proliferation (e.g. Sasaki et al., 1968; Kajstura et al., 1995).

Mitotic index

One of the simplest methods of estimating cell cycle activity is the quantitation of mitotic figures in histological sections. Mitotic rates are enumerated as mitotic figures per unit area or per determined number of cells. However, due to the extremely low number of mitotic figures and difficulty in identification, the use of this method for quantitative evaluation is limited (Linden et al., 1992).

Tritiated thymidine and Bromodeoxyuridine labelling

Newly synthesizing DNA incorporates labelled precursors, such as tritiated thymidine ([^{3}H]-thymidine) or its non-radioactive analogue, bromodeoxyuridine (BrdU), thereby enabling assessment of cell proliferation. To visualize the [^{3}H]-thymidine labelled nuclei a period of autoradiographic development, upwards of one week's exposure, is required. Alternatively, scintillation counters may be used to provide a measure of incorporated radioactivity, however identification of the specific cell types which are labelled would not be possible. In comparison, the development of an antibody to BrdU (Gratzner, 1982) enables demonstration by immunologic procedures, in a matter of hours. Other benefits of using BrdU-labelling include the elimination of radioisotope handling and need for autoradiography. Visualization

using standard immunological methods prevents the prolonged period of incubation and delay in obtaining results.

The primary limitation of both methods however, is the fact that [^{3}H]-thymidine and BrdU are only incorporated into viable cells actively synthesizing DNA, and thus these methods are not applicable in tissue which is already frozen or fixed. Additional limitations of these methods include variability in the timing of [^{3}H]-thymidine incubation and the concentration of BrdU during the incubation period, which can affect the quality of labelling and influence the labelling index (Linden et al., 1992).

Proliferating Cell Nuclear Antigen detection

The development of monoclonal antibodies to cell-cycle related antigens, has enabled the detection and quantitation of cell proliferation in routinely processed tissue sections. There are many antigens which may be used as markers for cell-cycle activity (e.g. Ki67, cyclins, etc), the one used in our research is the Proliferating Cell Nuclear Antigen (PCNA).

PCNA, a protein which functions as a cofactor to DNA polymerase δ (Miyachi et al., 1978; Mathews et al., 1984; Bravo and Macdonald-Bravo, 1987), has many characteristics which make it an effective marker for evaluating cell proliferation. It is a stable cell-cycle regulated nuclear protein with a half-life of approximately 20 hours (Bravo and Macdonald-Bravo, 1987), and is expressed maximally during the beginning of the synthesis phase of the cell cycle (Linden et al., 1992). PCNA is a

protein product of a late growth response gene and expression of this nuclear antigen characterizes cells oriented toward the proliferative process (Gadeau et al., 1991). Since PCNA is an endogenous cell proliferation marker that is preserved during tissue processing, immunohistochemical methods may be used to detect its presence in post-mortem fixed or frozen tissue.

Studies using PCNA immunostaining to examine cell proliferation in rat colon or human breast cancer cell lines correlate extremely well with measures of BrdU labelling or [^{3}H]-thymidine incorporation (for review see Dietrich, 1993; not included in review: van Dierendonck et al., 1991; Zeymer, et al., 1992; Lohr et al., 1995). Though primarily used in clinical testing, the PCNA method has recently been modified and applied to cardiac tissue for the detection of myocyte (Marino et al., 1991; Reiss et al., 1993; Quaini et al., 1994), smooth muscle (Gordon et al., 1990; Lawrence et al., 1995) and endothelial cell proliferation (Karimu and Burton, 1994; Rakusan et al., 1996) in both normal and pathological conditions.

One of the limitations of this method is that the PCNA protein is not only expressed during cell proliferation but also during the process of DNA repair (Yu et al., 1992; Li et al., 1995; Shivji et al., 1995). Thus, in experiments where DNA repair may occur, such as in myocardial infarction studies, PCNA labelling may be related to the repair process rather than cell proliferation. In our studies the PCNA method was used for the first time in conjunction with conventional morphometric techniques to provide comprehensive assessment of the coronary microvascular network response

to neonatal- and adult-onset hyperthyroidism and hypothyroidism.

BASIS FOR THE DISSERTATION

The work potential of the heart is dependent on an adequate supply of oxygen to the myocardial cells. The number (i.e. capillary numerical density) and spatial distribution of coronary capillaries throughout the myocardium (i.e. heterogeneity in capillary spacing) dictate the geometrical conditions for oxygen diffusion and supply. The number (i.e. arteriolar numerical density) and morphology (e.g. luminal diameter) of the coronary arterioles influence myocardial oxygen supply. The response of these two components of the vascular network to a pathological influence is therefore an important factor governing the maintenance of adequate myocardial oxygenation. Morphometric analysis of the coronary capillary and arteriolar response provides an indication of the adaptive capacity of the microvasculature to pathological growth. A greater understanding of the conditions that may induce coronary microvascular growth or rarefaction would further our knowledge of the potentially important mechanisms involved.

Adult-onset hyperthyroidism induces cardiac hypertrophy. Some studies report that this hypertrophy is accompanied by coronary capillary and arteriolar growth in proportion or in excess of the increase in cardiac mass. However, adequate growth of the coronary microvasculature in adult hyperthyroid in mammals has not been consistently observed. In contrast, there is a paucity of morphometric data regarding the response of the coronary microvasculature to adult-onset hypothyroidism. It has been shown that hypothyroidism in adult mammals leads to cardiac atrophy while

purportedly stimulating coronary capillary growth. The inconsistency among morphometric studies of adult-onset hyperthyroidism and paucity of morphometric data for adult-onset hypothyroidism is problematic not only for accurate modelling of myocardial oxygen supply, but also for a complete understanding of the microvascular networks adaptive potential of the microvasculature in adult hearts to altered thyroid hormone status.

During the early postnatal period of cardiac development the appropriate growth of the microvascular network is important in maintaining adequate myocardial oxygen supply to the growing myocardium. Thyroid hormones play an important role in the normal postnatal development of the heart. However, relatively little is known about the effect of neonatal-onset hyper- and hypothyroidism on the developing coronary arteriolar and capillary networks. Neonatal hyperthyroidism is known to enhance cardiac growth and maturation, whereas neonatal hypothyroidism slows these processes. Comparable effects of altered neonatal thyroid hormone status on the normal development of the coronary arteriolar and capillary networks have yet to be determined.

The spatial arrangement of the coronary microvascular network within the myocardium becomes established during postnatal development. Consequently, changes in the normal coronary microvascular growth induced during the neonatal period may persist into adulthood. Persistence of an abnormally formed microvasculature may affect myocardial oxygen supply and influence cardiac function.

The long-term effect of neonatal-onset hyper- or hypothyroidism on the coronary microvasculature or cardiac function is currently not known.

Sophisticated morphometric methods combined with unique histochemical and novel immunohistochemical techniques will be used to comprehensively examine the response of the coronary microvasculature to a hypertrophic (hyperthyroidism) or atrophic (hypothyroidism) influence introduced during the neonatal or adult stages. The results from this research will provide important morphometric data that may be used by others in the theoretical analysis of myocardial oxygen supply, will expand upon and perhaps lead to an unequivocal resolution of the discrepancies in reported effects of hyper- and hypothyroidism on coronary microvascular geometry, and further our knowledge concerning the ability of the coronary microvascular network to adapt to pathological influences.

STATEMENT OF THE PROBLEM

The response of the coronary microvasculature to hyperthyroidism or hypothyroidism induced during the neonatal or adult period, was morphometrically evaluated in an effort to test the following hypotheses:

1. Adult-onset hyperthyroidism and hypothyroidism elicit different responses in distal compared to proximal portions of the capillary network. The elicited responses serve to maintain the geometrical conditions for adequate myocardial oxygen supply in both regions of the capillary network.

2 There is evidence of endothelial cell proliferation (i.e. capillary angiogenesis) with adult-onset hyperthyroidism and hypothyroidism.

3. Neonatal-onset hyperthyroidism and hypothyroidism influence development of the coronary capillary and arteriolar networks.

4. Changes in microvascular geometry, induced by altered neonatal thyroid status, persist into adulthood after re-establishment of a euthyroid status.

CHAPTER 2

EFFECT OF ADULT-ONSET HYPO- AND HYPERTHYROIDISM ON CORONARY CAPILLARY GEOMETRY

2.1 Introduction

A considerable body of literature regarding thyroid hormone-induced cardiac hypertrophy in adult mammals and the many unique characteristics which separate it from other hypertrophic models has been accumulated in recent years; some of these features were discussed in the introduction of this dissertation (for review please see Morkin et al., 1983; Woeber, 1992; Polikar et al., 1993; Klein and Ojamaa, 1995). However, data regarding the effect of thyroid hormone-induced cardiac hypertrophy on the coronary capillary network remains controversial. Morphometric studies have reported inadequate growth of the coronary microvasculature (Gerdes et al., 1979; Weiss and Grover, 1987), growth that is proportional to (Craft-Cornney and Hansen, 1980; Wachtlova et al., 1985; Breisch et al., 1989; Tomanek et al., 1993), or growth that exceeds (Chilian et al., 1985) the cardiomegaly induced by adult-onset hyperthyroidism. The lack of consensus among such studies makes it difficult to accurately model the coronary capillary network and the changes it undergoes when exposed to excess thyroid hormone. In contrast, data describing changes to coronary capillary geometry induced by adult-onset hypothyroidism are limited (Tomanek et al., 1993).

The purpose of this study was to: (1) resolve the conflict in previous reports

regarding the response of the coronary capillary network to adult-onset hyperthyroidism, and (2) to extend previous morphometric studies of adult-onset hyper- and hypothyroidism that have focused primarily on changes in capillary numerical density. The use of novel histochemical and immunohistochemical techniques, combined with more comprehensive morphometric methods will enable characterization of changes in capillary geometry that result from an excess or deficiency of circulating thyroid hormone. Localization of these changes within the capillary bed will also be determined. In this manner, a more complete understanding of the geometrical conditions for oxygen supply to the hypertrophied and atrophied myocardium will be attained.

2.2 Materials and Methods

2.2.1 Animals and Treatment

Adult male Sprague-Dawley rats (250-300 g; Charles River) were used for this study. Rats were randomly divided into four groups: control (n=15), hyperthyroid (n=7), hypothyroid (n=11), and hypothyroid/hyperthyroid (n=13). The hypo-hyperthyroid group was included in this study in order to assess the plasticity of the coronary capillary network in adult rats when an hypertrophic stimulus is introduced immediately following an atrophic influence. All rats were maintained on standard rat diet *ad libitum*.

Treatment of the rats was as follows: rats in the hyperthyroid group received

daily subcutaneous (s.c.) injections of 3,3',5-triiodo-L-thyronine (T_3; 20 µg/100 g body mass); rats in the hypothyroid and hypo-hyperthyroid groups received 0.05% 6-n-propyl-2-thiouracil (PTU) daily in their drinking water and daily s.c. injections of 0.9 % physiological saline (0.1 ml/100 g body mass); and control rats received daily s.c. injections of 0.9 % physiological saline (0.1 ml/100 g body mass). All treatments were continued for 28 days. On the 29th day, only rats in the hypo-hyperthyroid group were given daily s.c. injections of T_3 (20 µg/100 g BW) for a period of 6 days. Body mass in all groups was measured every other day for the entire treatment period.

At the end of the respective treatment periods rats were anaesthetized with sodium pentobarbital (52 mg/100 g body mass). The right carotid artery was cannulated and a Grass polygraph recorder (Model 7B) was used to record mean arterial pressure and heart rate. Hearts were arrested in diastole following a bolus injection of saturated KCl. After excision, all surrounding fat and connective tissue were removed and the atria and ventricles were separated. Ventricles were then divided by removal of the right ventricular free-wall, leaving the septum and left ventricle intact; both right ventricle and left ventricle plus septum were weighed. Only the left ventricular free-wall was used for morphometric and immunohistochemical analysis.

2.2.2 Histology

The left ventricle plus septum was sectioned into three equal portions

transverse to the base-apex axis of the heart. The apical portion was used to determine the percent dry weight of the tissue (ratio of dry weight to wet weight), whereas the remaining two portions were rapidly frozen in liquid nitrogen and stored at -80^0 C until further processing.

Frozen tissue sections were prepared for Silver-methenamine and Alkaline phosphatase/Dipeptidyl peptidase IV (AP/DPP) staining, as well as Proliferating Cell Nuclear Antigen (PCNA) immunohistochemical processing. The Silver-methenamine procedure was used to facilitate identification of both capillaries and muscle fibres within tissue cross-sections. Fibre diameters, capillary and myocyte numerical density, and myocyte-to-capillary ratios were calculated. The method of AP/DPP enables visualization of the capillary network in both cross and longitudinal sections, as a function of location within the capillary bed (i.e. proximal versus distal). Capillary numerical density and various other indices of capillarization (e.g. capillary domain area and segment length, minimum capillary pathlength, number of segments per path, etc.) were examined. Determination of an index of cell-cycle activity was enabled by the method of PCNA immunohistochemistry. Estimation of PCNA labelling in endothelial cells provided corroborating evidence for capillary angiogenesis.

Unless otherwise stated, all staining procedures were performed at room temperature (23 - 25^{0}C).

Avalone's modification of the Jones Silver-methenamine stain

Midmyocardial cross-sections (5 μm) were processed using Avalone's modification of the Jones Silver-methenamine stain for basement membranes (Du Pont Co., 1979). Tissue sections were incubated in 1% Periodic acid (11 min) and rinsed in distilled water (5 min). Sections were then incubated in a Silver-methenamine solution (10 min) maintained at 60^{0}C. Sections were subsequently rinsed in warmed distilled water (60^{0}C) and cover-slipped using glycerol-gelatin. An example of a silver stained section including arteriole is shown in Plate 1.

Alkaline Phosphatase/Dipeptidyl Peptidase IV staining

Cross and longitudinal midmyocardial sections (16 μm) were stained according to the AP/DPP method. Frozen sections were fixed (5 min) in a solution of cooled (4^{0}C) chloroform:acetone (1:1) then incubated in a medium containing a substrate for the DPP IV enzyme (90 min). Sections were rinsed in distilled water (10 min) and then incubated in a medium containing a substrate for the AP enzyme (25 min). Sections were rinsed in distilled water (10 min) and cover-slipped using glycerol-gelatin.

Colour distinction was made between capillaries located in proximal regions (i.e. capillaries located close to their feeding arteriole) and capillaries located in distal regions of the capillary network (i.e. capillaries located close to their collecting venule). Capillaries in proximal regions stain blue and capillaries in distal regions

Plate 1 Photomicrograph illustrating a Silver-methenamine stained coronary arteriole within a section of adult rat left ventricular myocardium. Scale bar = 30 μm.

stain red (Plate 2). An intermediate or transition zone, in which individual capillaries contain both AP and DPP IV enzymes, was observed between proximal and distal portions. Capillaries in this transition zone stain blue-red or purple; this zone is more obvious in longitudinal than in cross-section. Thus, based on their histochemical properties, capillaries were identified as: proximal (blue), distal (red), or mixed (blue-red or purple)

Proliferating Cell Nuclear Antigen (PCNA) immunohistochemistry

Midmyocardial cross-sections (6 µm) were processed using an indirect method of PCNA immunohistochemical detection. Frozen sections were initially fixed in acetone (10 min) and then incubated in a 3% hydrogen peroxide/methanol solution (30 min). This latter step served to inhibit endogenous peroxidase activity and preserve optimal anti-PCNA immunoreactivity (Casasco et al., 1993). Sections were next rinsed in phosphate buffered saline (PBS; pH 7.4) for 10 minutes and incubated with a primary mouse monoclonal anti-PCNA antibody, diluted 1:10 in PBS (DAKO-PCNA, PC10; Dimension Laboratories Inc.). During antibody incubation sections were placed in a wet chamber for one hour. After rinsing in PBS (10 min), a secondary goat anti-mouse IgG_{2a} (gamma specific) peroxidase-conjugated antibody (Cedarlane) was applied (diluted 1:100 in PBS). Sections were again placed in a wet chamber and left for one hour. Next, sections were incubated in a 3'-diaminobenzidine (DAB) solution (DAB Kit; Dimension Laboratories Inc.) and placed

Plate 2 Photomicrographs showing Alkaline phosphatase/Dipeptidyl peptidase IV stained cross- (upper) and longitudinal sections (lower) of adult rat left ventricular midmyocardium. Proximal capillaries (capillaries located closer to their feeding arterioles) stain blue (open arrows). Venular capillaries (capillaries located closer to their collecting venule) stain red (closed arrows). Scale bar = 30 μm.

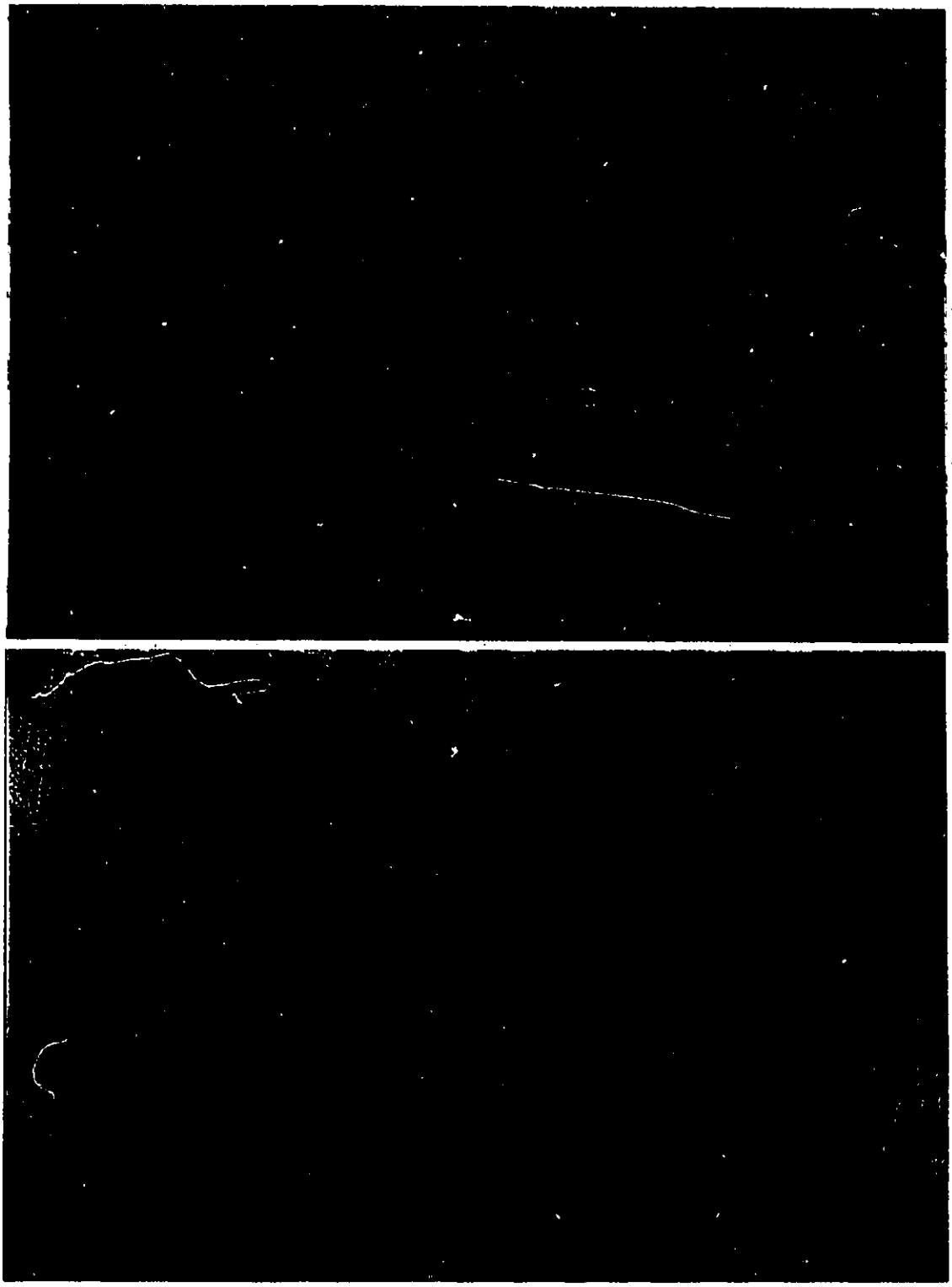

in a wet chamber for 30 minutes. DAB functions as the substrate for the peroxidase enzyme, forming a coloured end-product that precipitates at the site of the antigen, thereby enabling localization of the antigen within the tissue. Sections were stained with haematoxylin and eosin and cover-slipped using Permount. The haematoxylin and eosin stain enhanced the contrast between PCNA immunoreactive and non-immunoreactive nuclei. Sections of rat small intestine or 2 day old rat heart served as positive tissue controls, while an excess of secondary antibody applied to sections of myocardium provided an indication of antibody specificity.

Nuclei demonstrating intense brown (diffuse or granular) nuclear staining were considered positive for PCNA expression (PCNA+), whereas nuclei having very faint, diffuse brown staining were not considered positive (Plate 3). Though the criteria for classifying PCNA labelled nuclei are prone to interobserver variation due to its subjective nature, these criteria have been used by other investigators (e.g. Linden et al., 1992; Suzuki et al., 1992; Casasco et al., 1993). To minimize this variability the same person, in blind fashion, performed the evaluation for the duration of the study.

2.2.3 Morphometric Analysis

Silver-stained cross-sections

Five photomicrographs of midmyocardial cross-sections, each covering approximately 28,500 μm^2, were taken per heart. In each picture the number of capillaries and myocytes was determined using the "correction of edge effect". These

Plate 3 Photomicrograph showing Proliferating Cell Nuclear Angtigen (PCNA) labelled nuclei (arrows) in a section of two day old rat heart. Section was stained with haematoxylin. Scale bar = 30 μm.

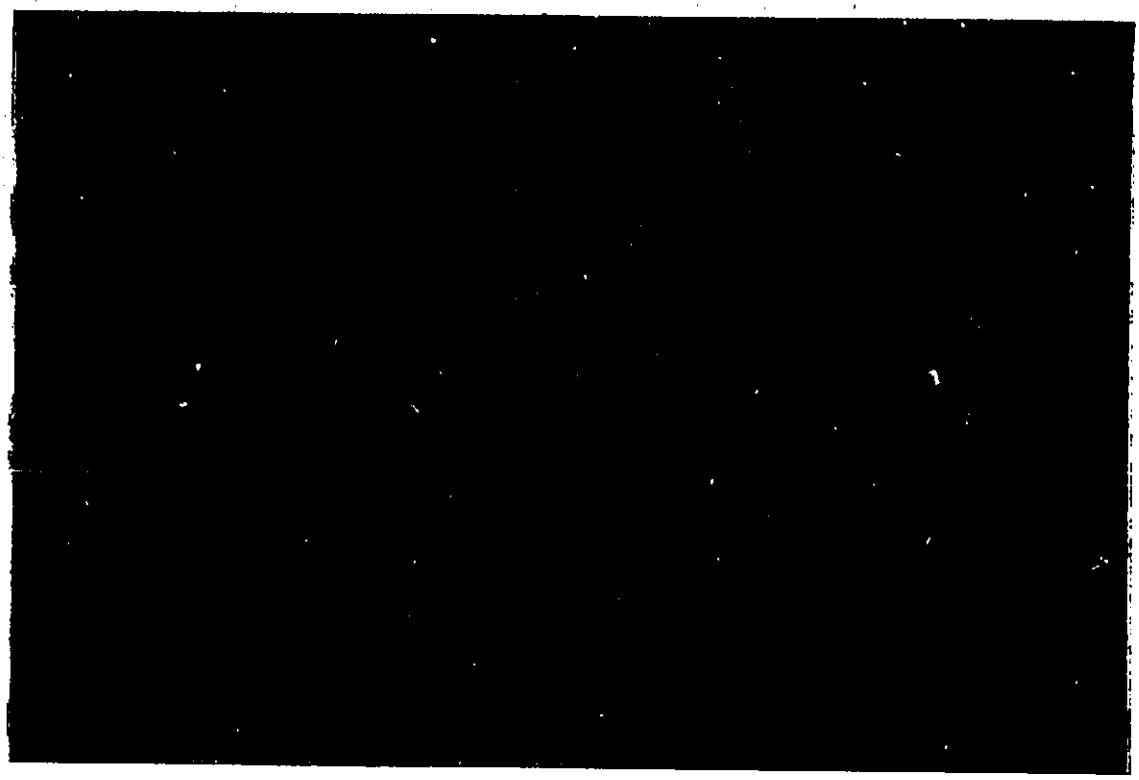

counts were used to calculate the capillary and myocyte numerical densities as well as myocyte-to-capillary ratios for hearts in each group.

Myocyte diameters were measured from these sections with the aid of an Olympus microscope and digitizing tablet linked to an IBM computer-based image analysis program (Bioquant, R&M Biometrics, Inc.). Diameters were measured from one fibre edge to the other fibre edge at the shortest distance spanning the myocyte cross-section. Approximately 150 myocyte diameters were measured per heart.

AP/DPP cross-sections: Capillary domains

Representative drawings of capillary profiles within cross-sections were made for each heart with the use of a drawing tube attached to an Olympus microscope. Five drawings were made per heart, each drawing covered approximately 36, 400 μm^2, and contained approximately 75 to 125 capillary profiles. Each capillary profile was identified as either blue (proximal) or red (distal). These drawings were then digitized using a Summagraphics digitizing tablet linked to an IBM computer. The digitized data were entered into the computer-based domain program (Hoofd et al., 1985). The domain program calculated the polygonal area of tissue surrounding an individual capillary, the capillary domain. Capillary domain areas were determined for both proximal and distal capillaries within each heart. By converting each capillary domain into a circle of equivalent area the corresponding radius of the Krogh cylinder was determined. The index of heterogeneity in capillary spacing (SD_{log}) was estimated

from the log-normal radii distribution. Capillary numerical densities for each heart were also estimated from AP/DPP stained cross-sections and compared to those from silver-stained sections.

AP/DPP longitudinal sections

Capillary set reconstruction: Approximately 3 to 4 capillary sets, which are comprised of all capillaries originating from a single feeding arteriole and draining into a single collecting venule, were reconstructed for each heart. The following parameters, which have been defined elsewhere (Batra et al., 1991), were measured: (a) minimum capillary pathlength - the minimum path along a capillary from feeding arteriole to collecting venule; (b) mean capillary pathlength - the average capillary path from feeding arteriole to collecting venule; (c) capillary set length - the total length of all capillaries from one feeding arteriole to one collecting venule; (d) proximal, distal, and mixed capillary segment lengths - a segment length being defined as the distance along a capillary between two consecutive branching points; (e) the number of segments per path, (f) the number of proximal, distal and mixed segments per set, and (g) the total number of segments per set. Capillary set reconstruction was performed for hearts in the control, hyperthyroid, and hypothyroid groups only.

Capillary segment length: The short-cut approach of measuring capillary segments lengths was also used. Comparison was made between capillary segment

length data obtained from set reconstruction and from the short-cut method. Capillary segment lengths were measured as a function of capillary type (i.e. proximal, distal, mixed) in all experimental groups. A total of 150 segments were measured per heart using an IBM computer-based image analysis program (Bioquant, R&M Biometrics, Inc.). Only segments which could be traced in their entirety from one branching point to another successive branching point were measured. "H" segments, which are defined as short perpendicular segments joining two adjacent parallel capillaries, were not included in the longitudinal analysis. As these "H" segments are abundant and easily detected within sections their inclusion would skew the data and serve to lower the average segment length.

Capillary supply unit: Average values of proximal and distal capillary domain areas and of proximal and distal segment lengths were used to calculate the capillary supply unit volume (i.e. product of the capillary domain area and capillary segment length) for proximal and distal regions of the capillary network.

PCNA/Haematoxylin and eosin cross-sections

Approximately 600 nuclei were counted per heart and categorized as either endothelial (ENDO), myocyte (MYO), or 'other' nuclei (OTHER). The OTHER category included those nuclei that could not be identified as either endothelial or myocyte (eg. smooth muscle cell nuclei, fibroblast nuclei, mast cell nuclei,

lymphocyte nuclei, etc.). From these counts the overall nuclei density (total number of nuclei per mm^2) and the nuclei density for each category (ENDO, MYO, OTHER) were determined. Differences in the proportion of ENDO, MYO, and OTHER nuclei within hearts were examined.

PCNA immunoreactive nuclei were identified and categorized as PCNA-positive endothelial (ENDO+), PCNA-positive myocyte (MYO+), or PCNA-positive other (OTHER+) nuclei. The number of ENDO+, MYO+, and OTHER+ nuclei was expressed as a percentage of the total number of nuclei counted.

2.2.4 Statistical Analysis

All results are expressed as mean ± SEM. Data from the myocyte-to-capillary ratios, myocyte diameters, capillary and myocyte numerical densities, and nuclei density estimates were analyzed using a one-way Analysis of Variance (ANOVA). Differences between group means were examined using the Tukey HSD post hoc test. The Tukey HSD post hoc test provides similar results, with respect to significance of differences, as the Bonferroni post hoc test (Wallenstein et al., 1980).

Data from capillary domain areas, capillary segment lengths, and capillary set reconstruction, all of which demonstrated a log-normal distribution, were logarithmically transformed prior to statistical analysis. The logarithmically transformed domain data were analyzed using a two-way ANOVA - Nested design model. The variable "hearts" was considered the nested factor within the treatment

groups. The logarithmically transformed segment length and reconstruction data were analyzed using a one-way ANOVA; differences between group means were examined using the Tukey HSD post hoc test. Interaction terms were assessed using least-square pairwise contrasts.

Chi-square (χ^2) analysis was used to examine differences in the nuclei proportions among the groups. PCNA data were transformed, using an arcsin transformation, prior to statistical analysis. This transformation, which was determined to be the most appropriate (residual analysis), was used in order to stabilize the variances of the error terms and because the proportions were based on different numbers of cases (Neter et al., 1990). The transformed data were analyzed using a two-way ANOVA and Tukey HSD post hoc test. For all of the above analyses differences were considered statistically significant at $P<0.05$.

2.3 Results

2.3.1 Body mass, heart rate, and mean arterial pressure (MAP)

T_3, PTU, and PTU/T_3 treatment effectiveness was assessed by examination of overall change in body mass, heart rate, and mean arterial pressure (MAP) (Table 2.1). The increase in body mass over the treatment period was significantly less than in control rats for all experimental groups. This reduced growth response agreed with observations from other thyroid hormone studies. Changes in heart rate served as an index of thyroid hormone status. For hypothyroid rats the significant ($P<0.01$)

Table 2.1 Body mass, heart rate, and mean arterial pressure data

Groups	BM (g)	Heart rate (bpm)	MAP (mmHg)
CON	461 ± 9	350 ± 11	96 ± 6
HYPER	384 ± 6[1]	514 ± 22[1]	98 ± 16
HYPO	344 ± 7[1,2]	225 ± 5[1,2]	95 ± 22
HYPO/HYPER	312 ± 7[1,2]	498 ± 9[1,3]	76 ± 6

Values are mean ± SEM. BM: body mass; bpm: heart beats per minute; MAP: mean arterial pressure; CON, control; HYPER, hyperthyroid; HYPO, hypothyroid; HYPO/HYPER, hypothyroid/hyperthyroid. [1] $P<0.01$ v. CON; [2] $P<0.01$ v. HYPER; [3] $P<0.01$ v. HYPO.

decrease in heart rate indicated that these animals were in a hypothyroid state. Hyperthyroid and hypo-hyperthyroid rats showed a significant increase ($P<0.01$) in heart rate indicating a hyperthyroid state. Mean arterial pressures did not differ significantly among the groups.

2.3.2 Heart mass

Myocardial hypertrophy was indicated in hyperthyroid rats by the significant increase in absolute left (LV) and right ventricular (RV) mass ($P<0.01$) and relative heart mass (HM:BM; $P<0.01$) compared to control (Table 2.2). In hypothyroid rats a decrease in the absolute (both RV and LV; $P<0.01$) and relative heart mass ($P<0.05$) indicated myocardial atrophy. A significant increase in the relative heart mass ($P<0.01$) of hypo-hyperthyroid rats was observed, however absolute LV and RV mass was similar to control. When compared to hypothyroid, the hypo-hyperthyroid rats showed a 43% increase in ventricular mass ($P<0.01$) indicating that 6 days of T_3 administration could stimulate an increase in the ventricular mass of previously hypothyroid animals. The percent tissue dry weight were comparable among the four groups, indicating that the resultant hypertrophy in the hyperthyroid group was due to an increase in cardiac muscle mass and not to an increase in the water content of the heart. Similarly, the atrophy seen in the hypothyroid group resulted from decreased myocardial mass and not decreased water content in these hearts.

Table 2.2 **Left ventricular mass, heart-to-body mass ratio, and percent tissue dry weight data**

Groups	RV mass (mg)	LV + S mass (mg)	HM:BM ratio (mg/g)	% tissue dry weight
CON	232 ± 6	868 ± 17	2.40 ± 0.06	25.5 ± 0.4
HYPER	373 ± 18[1]	1329 ± 57[1]	4.38 ± 0.14[1]	25.2 ± 1.0
HYPO	151 ± 5[1,3]	552 ± 13[1,3]	2.06 ± 0.03[2,3]	22.6 ± 1.1
HYPO/ HYPER	239 ± 10[3,4]	770 ± 19[3,4]	3.18 ± 0.06[1,3,4]	23.5 ± 1.0

Values are mean ± SEM. RV: right ventricle; LV + S: left ventricle plus septum; HM: heart mass; BM: body mass; CON, control; HYPER, hyperthyroid; HYPO, hypothyroid; HYPO/HYPER, hypothyroid/hyperthyroid. [1] P<0.01 v. CON; [2] P<0.05 v. CON; [3] P<0.01 v. HYPER; [4] P<0.01 v. HYPO.

2.3.3 *Myocyte diameters, myocyte-to-capillary ratios, and capillary numerical density*

Myocyte diameters and myocyte-to-capillary ratios were similar (Figure 2.1), among all groups. Myocyte diameters were similar between hypothyroid and hypo-hyperthyroid rats, suggesting that the increased LV mass in hypo-hyperthyroid rats likely resulted from an increase in myocyte length.

A difference of less than 10% was found between capillary numerical density estimates from silver-stained and AP/DPP stained sections. We decided to present the capillary numerical density data based on AP/DPP staining only (Fig. 2.2), in order to compare these to longitudinal measurements. Capillary numerical density was similar among the control, hyperthyroid, and hypo-hyperthyroid groups despite the increase in LV mass in hyperthyroid and hypo-hyperthyroid relative to hypothyroid rats. Capillary numerical density was significantly increased in hypothyroid compared to control ($P<0.01$).

2.3.4 *Capillary domain area and SD_{log}*

Approximately 66% of the capillaries sampled from control sections stained blue (proximal) and 34% stained red (distal). Similar proportions were observed in the hypothyroid group: 63% blue and 37% red, and hyperthyroid group: 72% blue and 28% red.

Proximal capillary domain areas were significantly larger than distal capillary domain areas in control, hypothyroid, and hypo-hyperthyroid ($P<0.01$) but not in

Figure 2.1 Myocyte diameter measurements (upper) and myocyte-to-capillary ratio results (lower) for control (CON), hyperthyroid (HYPER), hypothyroid (HYPO), and hypo/hyperthyroid (HYPO/HYPER) rats. * $P<0.01$ v. HYPER. Results are presented as mean + SEM.

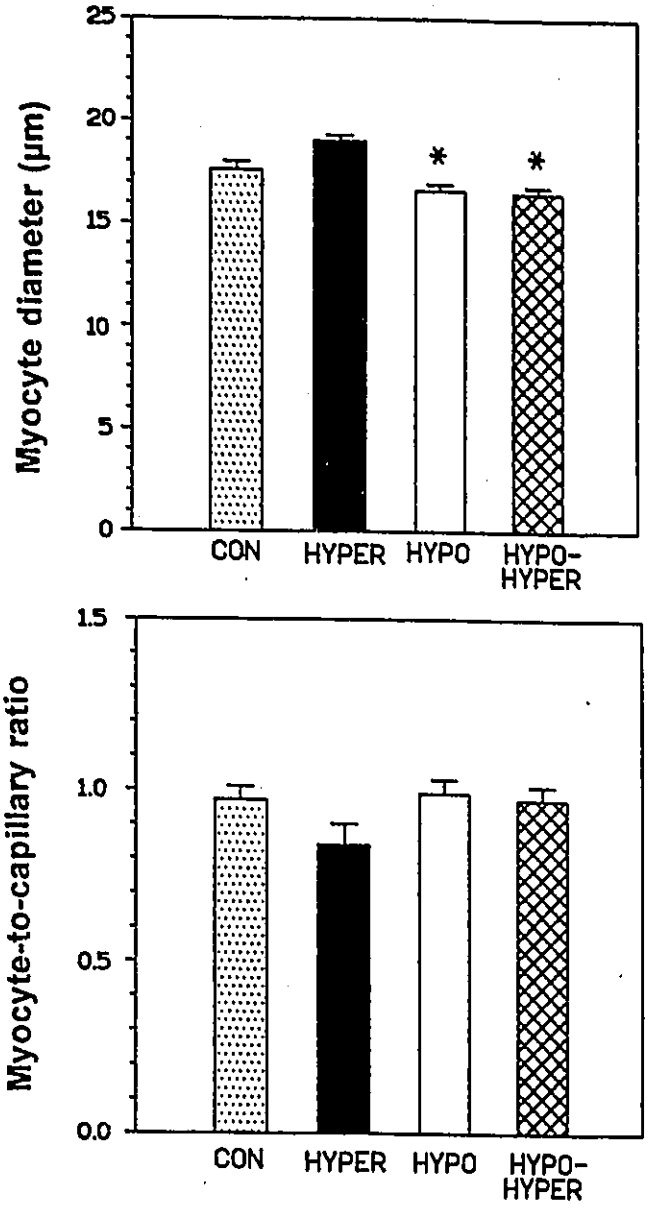
Myocyte diameter (μm)
25
20
15
10
5
0
*
*
CON
HYPER
HYPO
HYPO-HYPER
Myocyte-to-capillary ratio
1.5
1.0
0.5
0.0
CON
HYPER
HYPO
HYPO-HYPER

Figure 2.2 Capillary numerical density data, from AP/DPP stained sections, for control (CON), hyperthyroid (HYPER), hypothyroid (HYPO) and hypothyroid/hyperthyroid (HYPO/HYPER) rats. * $P<0.01$ v. CON. Results are presented as mean + SEM.

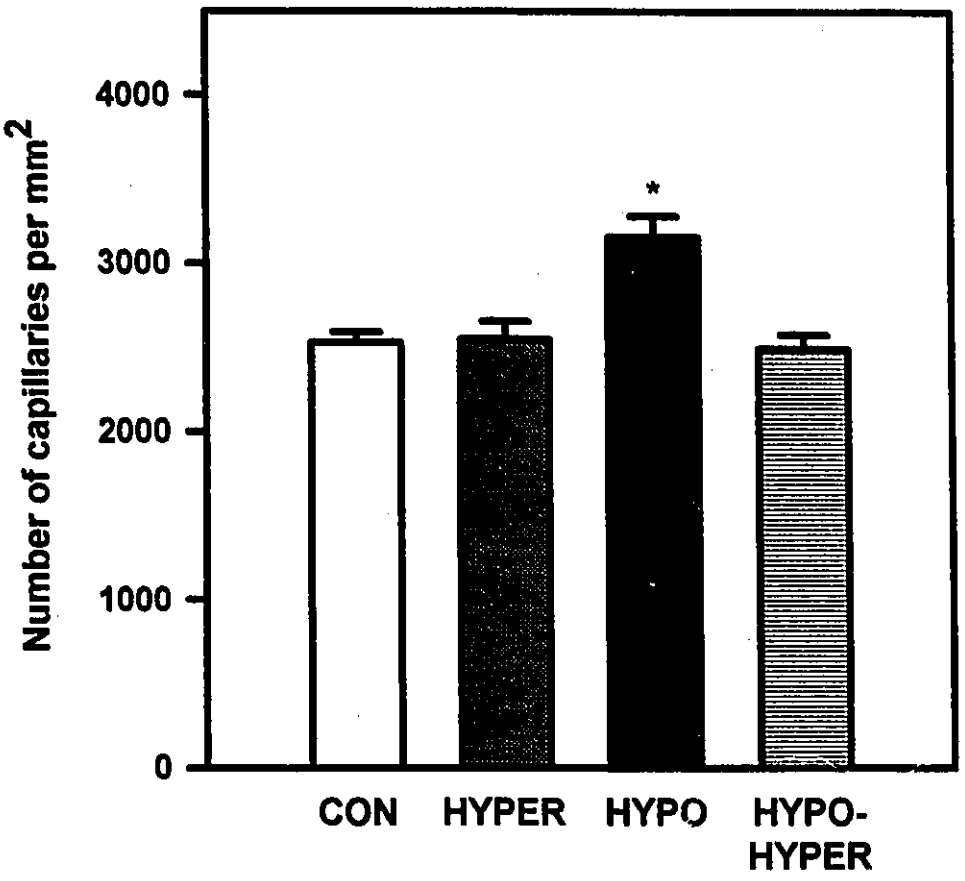
Number of capillaries per mm2
4000
3000
2000
1000
0
*
CON
HYPER
HYPO
HYPO-
HYPER

hyperthyroid hearts (Table 2.3). Proximal domain areas were significantly smaller ($P<0.01$) in hyperthyroid and hypothyroid hearts as compared to control. Only the hypothyroid group demonstrated a significant decrease in distal domain area compared to control ($P<0.01$). The index of heterogeneity in capillary spacing (SD_{log}), calculated for both proximal and distal regions of the capillary network within each group, was similar among the four groups and between the proximal and distal regions within individual groups.

2.3.5 Capillary set reconstruction

Analysis of capillary set reconstruction parameters (Table 2.4) revealed that the mean and minimum capillary pathlength in hypothyroid rats were significantly shorter ($P<0.01$) than in control. All other parameters were similar among the groups.

2.3.6 Capillary segment length

A significant correlation between segment lengths estimated by the capillary set reconstruction method and the "short-cut" method was found: $r = 0.896$, $r^2 = 0.80$ ($P<0.01$). The difference between segment length estimates made by the capillary set reconstruction and "short-cut" method was less than 15%. The average capillary segment lengths determined by the "short-cut" method are outlined in Table 2.5. These average segment lengths were the ones used in the calculation of the capillary supply unit volumes. In all groups, mixed segment lengths were consistently longer

Table 2.3 Capillary domain area and SD_{log} measurement data for all groups

Groups	Capillary domain area (μm^2)		SD_{log}	
	Proximal	**Distal**	**Proximal**	**Distal**
CON	388 ± 2	373 ± 3[4]	0.059 ± 0.002	0.056 ± 0.001
HYPER	381 ± 3[1]	380 ± 5	0.058 ± 0.002	0.059 ± 0.003
HYPO	325 ± 2[1,2]	305 ± 2[1,2,4]	0.060 ± 0.002	0.056 ± 0.001
HYPER/ HYPO	390 ± 2[3]	369 ± 3[3,4]	0.061 ± 0.002	0.059 ± 0.002

Values are mean ± SEM. SD_{log}: standard deviation of the logarithmic distribution of Krogh radii; CON: control; HYPER: hyperthyroid; HYPO: hypothyroid; HYPO/HYPER: hypothyroid/hyperthyroid. [1] P<0.01 v. CON; [2] P<0.01 v. HYPER; [3] P<0.01 v. HYPO; [4] P<0.01 v. proximal domain area.

Table 2.4 Data from longitudinal capillary set reconstruction

Group	MCL	MCP	CSL	# of segments per path	# of segments per capillary set			
					Prox	Dist	Mixed	Total
CON	375 ± 34	476 ± 8	1933 ± 129	7 ± 1	8 ± 1	7 ± 1	5 ± 1	20 ± 2
HYPER	371 ± 31	498 ± 7	1886 ± 129	9 ± 1	12 ± 3	7 ± 1	6 ± 1	25 ± 2
HYPO	299 ± 29[1]	410 ± 6[1]	1590 ± 103	8 ± 1	10 ± 1	8 ± 1	5 ± 1	22 ± 2

Values are mean ± SEM. MCL: minimum capillary pathlength; MCP: mean capillary pathlength; CSL: capillary set length; Prox: proximal capillary; Dist: distal capillary; Mixed: "transitional" capillary segment; Total: total number of segments per capillary set; CON, control; HYPER, hyperthyroid; HYPO, hypothyroid. [1] $P<0.01$ v. CON.

Table 2.5 Capillary segment length data for proximal, distal, and mixed capillary segments

Group	Segment length (μm)		
	Proximal	Distal	Mixed
CON	94 ± 1	87 ± 2	137 ± 2
HYPER	79 ± 1[1]	68 ± 3[1]	120 ± 4[1]
HYPO	79 ± 1[1]	61 ± 2[1,2]	125 ± 2[1]
HYPO/HYPER	90 ± 1[1,2,3]	74 ± 2[1,2,3]	127 ± 1[1]

Values are mean ± SEM. CON: control; HYPER: hyperthyroid; HYPO: hypothyroid; HYPO/HYPER: hypothyroid/hyperthyroid; Mixed: "transitional" capillary segment; Mixed > proximal > distal segments in all groups at $P<0.01$. [1] $P<0.01$ v. CON; [2] $P<0.01$ v. HYPER; [3] $P<0.01$ v. HYPO.

than proximal ($P<0.001$), which in turn were longer than distal segment lengths ($P<0.01$). Proximal, distal, and mixed capillary segments were significantly shorter in hyperthyroid, hypothyroid, and hypo-hyperthyroid hearts ($P<0.01$) than in control.

2.3.7 Capillary supply unit (CSU)

Capillary supply unit volumes for proximal segments were significantly larger than CSU volumes for distal segments ($P<0.01$) in all groups except the hyperthyroid group (Fig. 2.3). Capillary supply unit volumes for both proximal and distal capillaries were significantly lower in hypothyroid compared to control rats. A significant increase in CSU volumes for both proximal ($P<0.001$) and distal capillaries ($P<0.01$) was observed in the hypo-hyperthyroid compared to the hypothyroid group. Capillary supply unit volumes for proximal and distal capillaries were comparable between hyperthyroid and control groups.

2.3.8 Nuclei density counts

The nuclear density estimates (total number of nuclei per mm^2) for the different groups are shown in Figure 2.4. Only the hypo-hyperthyroid group demonstrated a significant increase in overall nuclear density compared to control ($P<0.01$). When the nuclear density estimates were analyzed based on the different nuclei types (Table 2.6), a 56% increase in endothelial ($P<0.01$) and 34% increase in "other" ($P<0.05$) nuclei was noted in the hypo-hyperthyroid as compared to control. No significant

Figure 2.3 Proximal (solid bars) and distal (hatched bars) capillary supply unit (CSU) volumes for control (CON), hyperthyroid (HYPER), hypothyroid (HYPO), and hypothyroid/hyperthyroid (HYPO/HYPER) rats. * $P<0.01$ v. proximal CSU. Results are presented as mean + SEM.

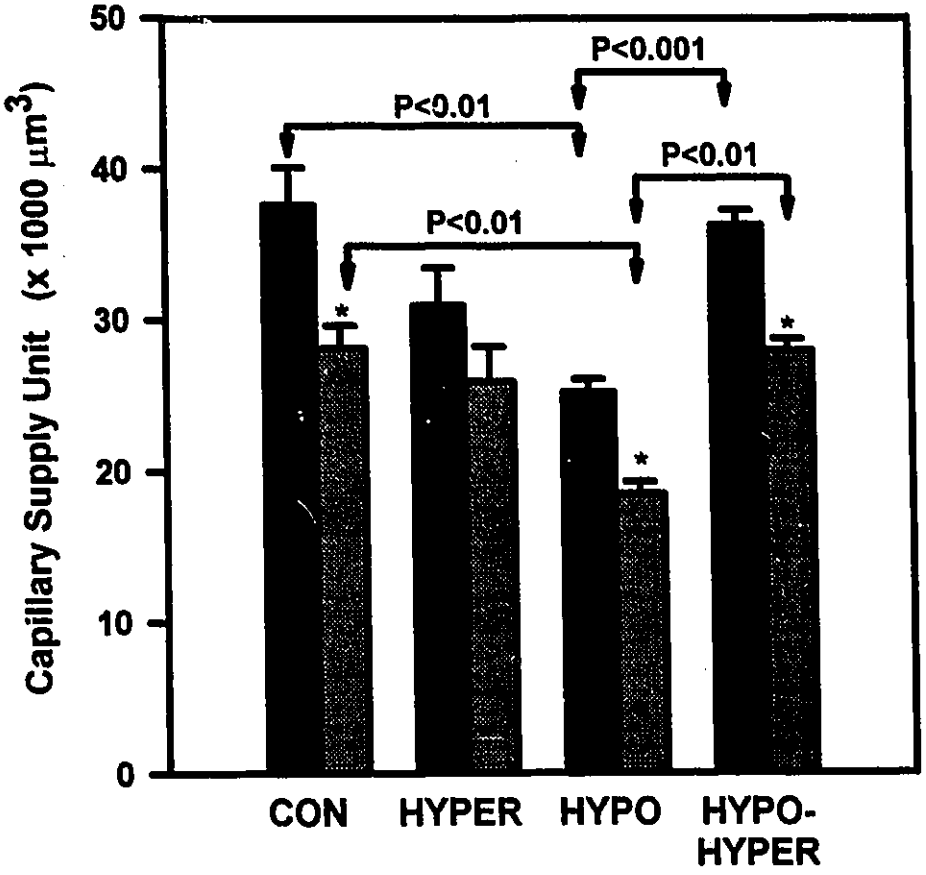
Capillary Supply Unit (x 1000 μm³)
50
40
30
20
10
0
P<0.001
P<0.01
P<0.01
P<0.01
*
*
*
CON
HYPER
HYPO
HYPO-HYPER

Figure 2.4 Total nuclei density (number of nuclei per mm^2) in left ventricular myocardium of control (CON), hyperthyroid (HYPER), hypothyroid (HYPO), and hypothyroid/hyperthyroid (HYPO-HYPER) adult rats. * $P<0.01$ v. CON and HYPER. Results are presented as mean ± SEM.

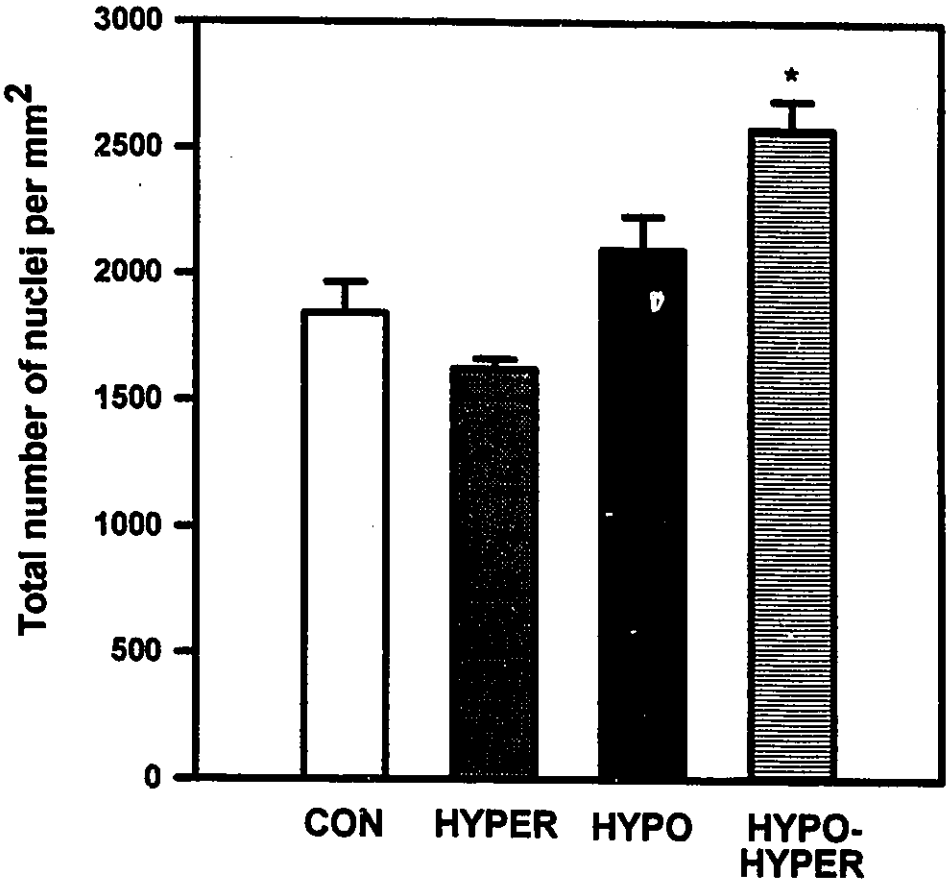
Total number of nuclei per mm2
3000
2500
2000
1500
1000
500
0
*
CON
HYPER
HYPO
HYPO-
HYPER

Table 2.6 Number of endothelial, myocyte, and "other" nuclei per mm^2

Group	Nuclei Type		
	Endo	Myo	Other
CON	641 ± 43	462 ± 43	740 ± 60
HYPER	508 ± 61	330 ± 23	786 ± 32
HYPO	612 ± 57	531 ± 48	956 ± 74
HYPO/HYPER	1000 ± 90[1,2,3]	585 ± 54[4]	993 ± 45[5]

Values are mean ± SEM; CON, control; HYPER, hyperthyroid; HYPO, hypothyroid; HYPO/HYPER, hypothyroid/hyperthyroid; ENDO, endothelial nuclei; MYO, myocyte nuclei; OTHER, other remaining nuclei. [1] $P<0.01$ v. CON; [2] $P<0.01$ v. HYPER; [3] $P<0.01$ v. HYPO; [4] $P<0.05$ v. HYPER; [5] $P<0.05$ v. CON.

change in these same two parameters were found in the hyperthyroid or hypothyroid groups. It should be noted however that the 28% decrease in hyperthyroid and the 15% increase in hypothyroid myocyte nuclear density was in accordance with the resultant myocyte hypertrophy with hyperthyroidism and myocyte atrophy with hypothyroidism.

2.3.9 Distribution of nuclei types

The hyper- and hypothyroid groups demonstrated a significant difference ($P<0.01$ and $P<0.05$ respectively) in the percentage distribution of nuclei types compared to control (Fig. 2.5). A decrease in per cent of ENDO and MYO nuclei versus an increase in per cent of OTHER nuclei was observed in the hyperthyroid group. Similarly, a decrease in ENDO and an increase in OTHER nuclei was noted in the hypothyroid group; no difference in the per cent of myocyte nuclei was found.

2.3.10 PCNA labelling

Results from the analysis of PCNA labelling indices among the groups is presented in Figure 2.6. Only the hypo-hyperthyroid group demonstrated a significant increase in ENDO+ (550%) and OTHER+ (463%) nuclei compared to the control ($P<0.01$) and hypothyroid groups (2500% and 2150% respectively; $P<0.01$). Notably, no MYO+ nuclei were detected in hearts from any group.

Figure 2.5 Relative percentage of endothelial (ENDO), myocyte (MYO), and "other" (OTHER) nuclei in left ventricular midmyocardium of control (CON), hyperthyroid (HYPER), hypothyroid (HYPO), and hypothyroid/hyperthyroid (HYPO-HYPER) adult rats. A significant difference in nuclei proportions was found between CON versus HYPER ($P<0.01$) and CON versus HYPO ($P<0.05$). Results are presented as percentages.

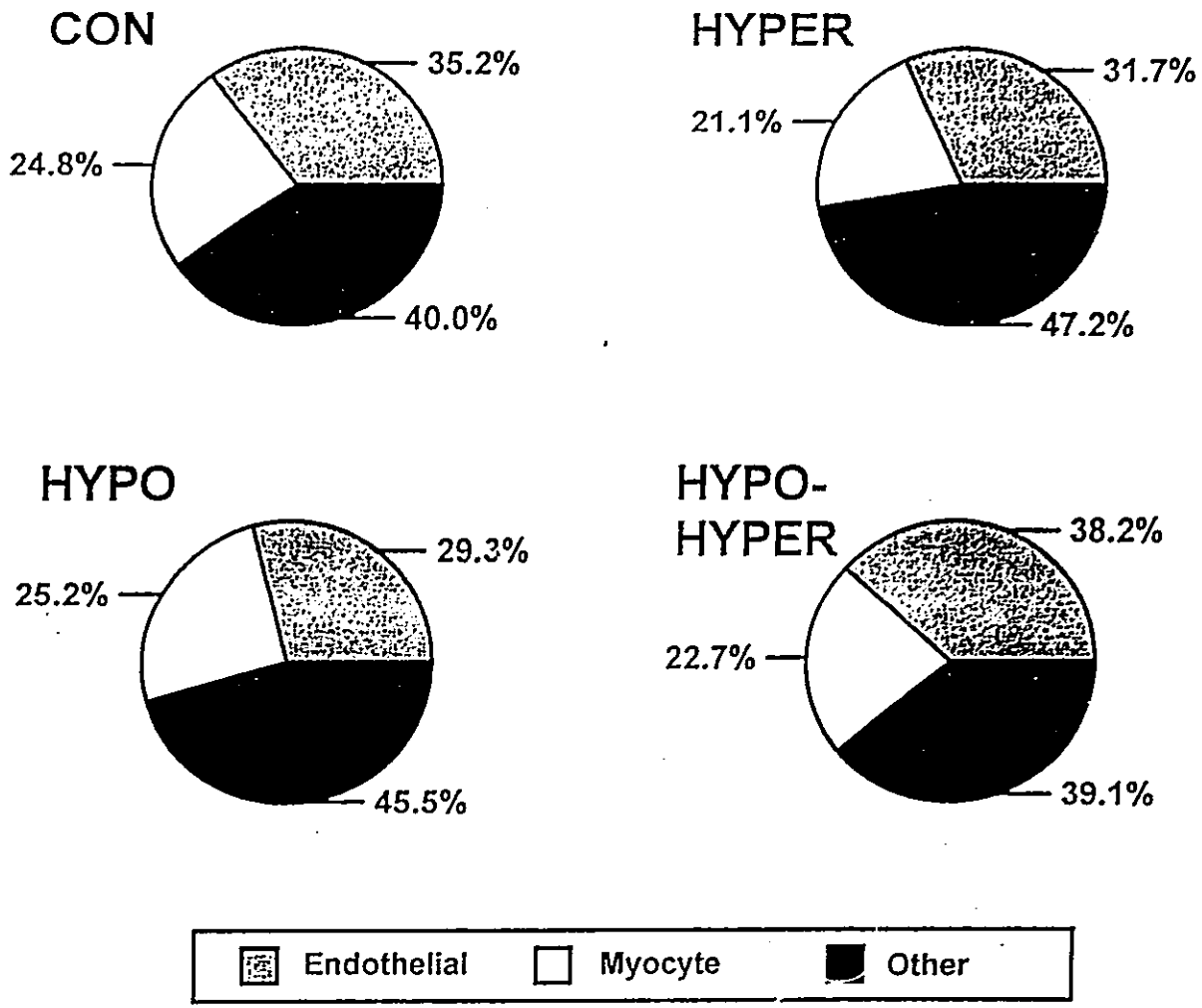
CON
35.2%
24.8%
40.0%
HYPER
31.7%
21.1%
47.2%
HYPO
29.3%
25.2%
45.5%
HYPO-
HYPER
38.2%
22.7%
39.1%
Endothelial
Myocyte
Other

Figure 2.6 Proportion of PCNA labelled endothelial (ENDO) and "other" (OTHER) nuclei per 1000 nuclei in left ventricular myocardium of control (CON), hyperthyroid (HYPER), hypothyroid (HYPO), and hypothyroid/hyperthyroid (HYPO-HYPER) adult rats. * $P<0.01$ v. CON; $^{\delta}$ $P<0.01$ v. HYPO. No PCNA labelled myocyte nuclei were found in any of the adult hearts. Results are presented as mean ± SEM.

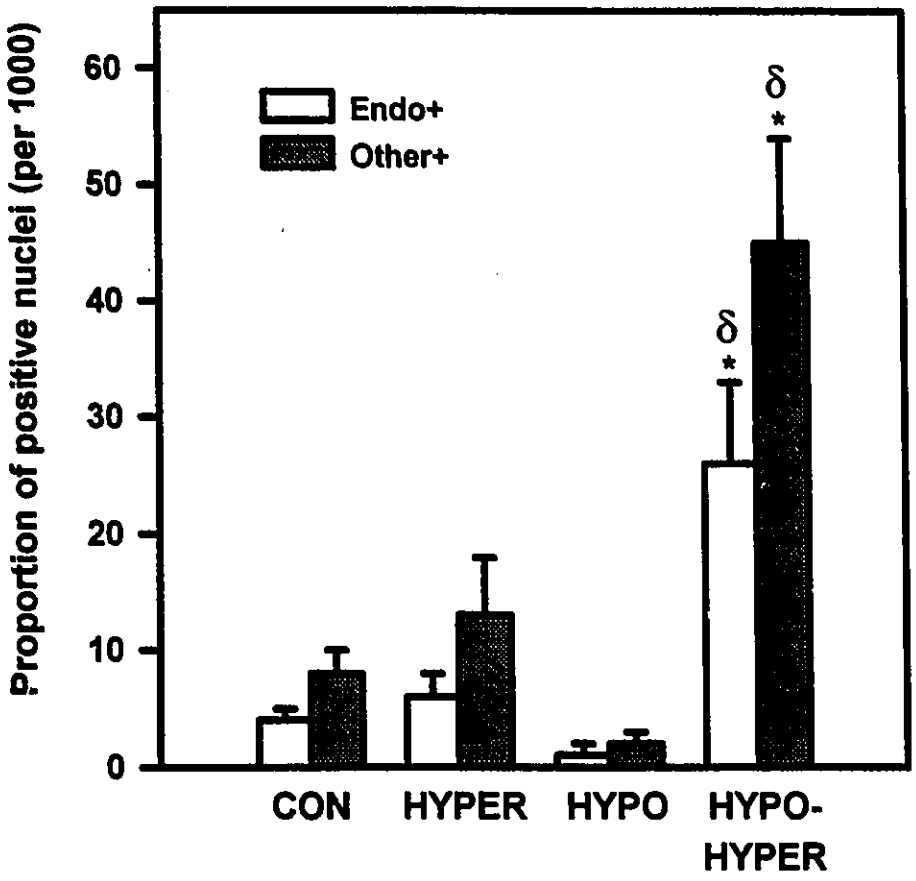
Proportion of positive nuclei (per 1000)
60
50
40
30
20
10
0
Endo+
Other+
δ
*
δ
*
CON
HYPER
HYPO
HYPO-
HYPER

2.4 Discussion

It is generally accepted that the response of the myocardium to an excess of circulating thyroid hormone is additional growth in mass. Normally, thyroid hormones play a role in the maintenance of an optimal level of cardiac function and oxygen consumption by the tissue. However, in clinical disorders such as hyperthyroidism the increase in cardiac work and tissue metabolism usually result in a concomitant increase in tissue oxygen consumption and myocardial mass.

Effect of adult-onset hyper- and hypothyroidism on cardiac mass

The induced cardiac hypertrophy in hyperthyroid, and cardiac atrophy in hypothyroid rats was in accordance with previous findings (Liu and Gerdes, 1990; Tomanek et al., 1993). The 82% increase in relative heart mass in hyperthyroid rats in this study was larger than in a similar study that used the same species and a similar period of treatment (Campbell et al., 1991). The increased cardiac mass was due to an increase in tissue mass.

Effect of hyper- and hypothyroidism on nuclei density and nuclei proportions

The significant change in proportion of nuclei types, induced by adult-onset hyper- and hypothyroidism, was due to an increase in "other" cell types. As this "other" category includes every cell type (e.g. smooth muscle, fibroblast, lymphocyte, etc.), that are not identified as endothelial or myocyte, the increased proportion may

reflect increases in any of these cell populations. An increased number of fibroblasts may be the most plausible explanation in hyperthyroid rat, as T_3 treatment has been shown to stimulate fibroblast proliferation in culture (Yao and Eghbali, 1992).

Cardiac myocyte diameters

The absence of significant changes in cardiac myocyte diameters with hyper- and hypothyroidism is in contrast to other studies (hyperthyroidism: McAllister and Page, 1973; Gerdes et al., 1979; Campbell et al., 1991; hypothyroidism: Liu and Gerdes, 1990). In light of the significant changes in heart mass noted in the hyper- and hypothyroid groups in this study, it is likely that marked changes in cardiac myocyte length occurred. In addition, for hyperthyroid rats the possibility may also be advanced that myocyte hypertrophy does not account entirely for the increased ventricular mass but that myocyte hyperplasia may be a potential contributing factor. The maintenance of the myocyte-to-capillary ratio supports this possibility. Notably, the lack of PCNA-labelled cardiac myocytes does not preclude the likelihood of myocyte hyperplasia since myocyte proliferation may have occurred during the early stages of hyperthyroidism and thus would not be detected at the time of sacrifice. However, because myocyte number, cell length or cell volume were not measured in this study it cannot be directly concluded which process (myocyte hypertrophy or hyperplasia) was the major contributor to the increase in ventricular mass.

Coronary capillary numerical density

Analysis of capillary numerical density measurements suggested the occurrence of capillary angiogenesis in thyroid hormone-induced hypertrophic hearts and possibly in hypothyroid-induced atrophic hearts. Capillary numerical density was almost identical in control and hyperthyroid rat hearts despite the presence of myocardial hypertrophy. Using capillary numerical density values from control (2559 capillaries/mm^2) and the estimated 16% increase in myocyte cross-sectional area from the hyperthyroid group, an average expected capillary numerical density (2206 capillaries/mm^2) can be calculated for hyperthyroid rats. According to these estimates, if capillary proliferation had not occurred the increase in myocyte diameter would have resulted in decreased capillary numerical density, as is reported in other forms of adult hypertrophy (reviewed in Rakusan, 1987 and in Anversa and Sonnenblick, 1990). A decrease in capillary numerical density was not found in hyperthyroid rats thus, indicating capillary angiogenesis. No significant increase in the number of PCNA labelled endothelial nuclei was found however in the hyperthyroid group, likely due to the fact that the majority of capillary angiogenesis may have already occurred.

Increased capillary numerical density with adult-onset hypothyroidism was in accordance with the only other morphometric study of adult-onset hypothyroidism (Tomanek et al., 1993). This increase may have resulted from the reduction in myocyte diameter, which would bring capillaries closer together, thus increasing the number of capillaries per unit area of tissue. However, an alternative explanation may

be that capillary proliferation also occurred in these hearts. It has been proposed that the capillary response to hypothyroidism mimics that of bradycardially-paced hearts in which capillary numerical density increases (Wright and Hudlicka, 1981; Hudlicka et al., 1988; Tomanek et al., 1993). Calculation and comparison of the expected (2,875 capillaries/mm^2) and observed capillary numerical density (3152 capillaries/mm^2) in the hypothyroid group provides support for angiogenesis. The postulated mechanism responsible for promoting capillary angiogenesis under these conditions will be discussed in Chapter 5 (General Discussion).

Geometry of the coronary capillary network

In hyperthyroid rats, domain areas for proximal and distal capillaries were of approximately equal size - a geometrical configuration resembling the Krogh tissue cylinder. This is different to the control situation in which proximal capillaries supply larger areas of tissue than distal capillaries, and to that observed for pressure overload induced hypertrophy where the difference between proximal and distal domains is even more pronounced (Batra and Rakusan, 1991). In the hypertrophic hearts, the observed decrease in the domain areas in proximal regions and maintenance of the domain area in distal regions of the capillary bed suggests either an increase in the number of myocardial capillaries or a decrease in myocyte cross-sectional area. Since thyroid hormone induced hypertrophy did not result in decreased myocyte cross-sectional area, smaller domains are likely due to an increased number of capillaries -

capillary angiogenesis. Results from capillary segment length and set reconstruction analysis also support capillary proliferation. The decrease in domain area of proximal capillaries and shorter proximal capillary segment lengths suggests that capillary proliferation was greater in proximal regions of the capillary bed.

Capillary geometry as described by capillary domain area and segment length analysis was similar in the hypo-hyperthyroid group as in control. Longer capillary segment lengths in the hypo-hyperthyroid group relative to the hypothyroid suggests longitudinal growth of capillaries. An increased number of PCNA labelled endothelial nuclei supports this hypothesis. In hypothyroid rats, the smaller domain areas and capillary segment lengths in proximal and distal regions of the capillary bed agree with the occurrence of myocardial atrophy and possible capillary proliferation.

It is important to note that interpreting capillary segment length data without any other longitudinal parameters (e.g. number of segments per path) can be complicated. For instance, an increased segment length likely reflects capillary elongation (growth in the longitudinal axis). However, whether capillary elongation results from enlargement of existing endothelial cells or from endothelial cell proliferation is hard to discern based on segment length data alone. Shorter segment lengths likely reflect an increase in capillary branching as capillary rarefaction is generally believed to involve the entire capillary and not small portions of capillaries. Finally, the maintenance of capillary segment length despite changes in heart size, may result from either: (1) lack of changes in the capillary bed, or (2) capillary

growth (elongation and formation of additional capillary branches or connections). Capillary numerical density estimates and PCNA data may help to discern which of these two scenarios is more plausible.

Capillary supply unit volumes

Capillary supply unit (CSU) volumes were reduced for proximal and distal capillaries in atrophic hearts but were maintained in hypertrophic hearts. The maintenance of CSU volume in the hyperthyroid group, despite the resultant cardiomegaly, resulted from capillary growth and an increase in capillary ramifications. Considering the increased myocardial oxygen demand, which is characteristic of this model (Talafih et al., 1983, 1984; Weiss and Tse, 1995), maintaining the CSU volume together with an increased blood flow, likely preserved the conditions for adequate myocardial oxygen supply. The reduced myocardial mass and possibility of capillary proliferation in the hypothyroid group translated into a smaller tissue volume supplied by a capillary segment in both regions of the capillary bed. In the hypo/hyperthyroid group, return of the CSU to control values demonstrates the ability of capillaries to adapt to changes in heart mass within a relatively short period of time (6 days).

A very interesting relationship between CSU volumes estimated in this study and myocyte volumes estimated in other studies was observed. Results from studies that have determined myocyte volume during hypothyroidism - 21 000 μm^3 (Liu and

Gerdes, 1993) and hyperthyroidism - 30 000 μm^3 (Campbell et al., 1991) show a great deal of similarity to the CSU values in this study. Notably, these myocyte volume values lie in between the proximal and distal CSU estimates for hypothyroid (Prox: 25 249 μm^3; Dist: 18 516 μm^3) and hyperthyroid rats (Prox: 30 886 μm^3; Dist: 25 865 μm^3). If an average CSU volume was estimated for the hypothyroid (21 883 μm^3) and the hyperthyroid group (28 376 μm^3) it can be observed how remarkably close these values are to the respective myocyte volumes (21 000 μm^3 and 30 000 μm^3). Notably, this relationship has also been observed during postnatal cardiac development in the rat (Rakusan et al., 1994b). The importance of the relationship between CSU and myocyte volume is unknown. However, it suggests that the regulation of oxygen supply may be at the level of individual myocytes.

Summary

The foregoing results demonstrate that thyroid hormone induced hypertrophy can stimulate coronary capillary growth without changing the heterogeneity in capillary spacing. Thus normal myocardial capillarization and geometrical conditions for oxygen supply were maintained in adult animals in spite of the resultant hypertrophy. In hypothyroidism, cardiac atrophy was accompanied by capillary growth and improved geometrical conditions for myocardial oxygen supply. The new three-dimensional parameter, the capillary supply unit, which was shown to be closely related to myocyte size, reflected the geometrical changes in cross- and longitudinal

sections. Capillary supply unit analysis indicated that geometrical conditions for myocardial oxygen supply were maintained under both hypertrophic and atrophic influences. The plasticity of the capillary bed in adult hearts was also evident in the hypo/hyperthyroid group, suggesting that despite the fact that capillary proliferation in adult mammalian hearts is rare under normal conditions, the capacity for capillary proliferation is not absent.

CHAPTER 3

EFFECT OF NEONATAL HYPO- AND HYPERTHYROIDISM ON CORONARY CAPILLARY GEOMETRY

3.1 Introduction

A close relationship between thyroid status, heart mass, and coronary capillary growth has been found in adult mammals. The preceding study (Chapter 2) extended our knowledge of this relationship to the regional changes that occur within the capillary network. Adult-onset hyperthyroidism induced cardiac hypertrophy and coronary capillary proliferation in both regions of the capillary network. In comparison, adult-onset hypothyroidism induced cardiac atrophy and possibly coronary capillary proliferation. Thyroid hormones have been shown to play an important role in normal postnatal growth and maturation of the heart (e.g. Moussavi et al., 1985; Torres and Tucker, 1993). Based on this premise and the findings in adult hearts, we examined the effect of altered plasma thyroid hormone levels on the developing coronary capillary network during the neonatal period. As the capillary network is undergoing sizeable growth and maturation during this period (Rakusan et al., 1965; Rakusan and Turek, 1985), one may expect that any effect would be more pronounced. In fact, studies comparing the effect of pressure overload on coronary adaptations in neonatal and adult mammals have reported that the cardiac response elicited in neonates is different to the response in adults (Rakusan et al., 1992; Flanagan et al., 1994). Few studies have examined the response of the developing

coronary capillary network to altered neonatal thyroid status.

In the rat heart, neonatal hypothyroidism leads to delayed maturation (Meisami, 1984) and attenuated cardiac growth, whereas accelerated maturation and enhanced cardiac growth are induced by neonatal hyperthyroidism (Kolar et al., 1992). Thus, alterations in plasma thyroid hormone levels during the neonatal period may also affect the normal formation and maturation of the coronary capillary network. Since the geometrical arrangement of the capillary network determines the diffusion conditions for oxygen transfer to myocardial tissue, irregular or insufficient formation of the microvascular bed may result in inadequate myocardial oxygenation possibly leading to compromised cardiac development. As the work capacity of the heart depends on an adequate supply of oxygen, abnormal development of the coronary capillary network during the neonatal period may possibly have a long-term effect on cardiac function.

The aim of this study was to: (1) morphometrically examine the effect of early neonatal-onset hypo- and hyperthyroidism on the growth and development of coronary capillaries, and (2) determine in adult rats whether long-term changes in capillary geometry or cardiac function were induced by either neonatal thyroid condition. Furthermore, as altered neonatal thyroid status influences the rate of maturation, this model and the results of this study may be useful in determining if the early rapid formation of new capillaries and subsequent decline is dependent on the rate of cardiac growth or on tissue maturation.

3.2 Materials and Methods

3.2.1 Animals and Treatment

Newborn male and female Sprague-Dawley rats (Charles River) were used in this study. On the first postnatal day all newborn rats were removed, mixed, and randomly redistributed to the dams in order to minimize any confounding effect of genetics or litter size on early postnatal development. Each litter, now consisting of approximately 10 rats per dam, was randomly assigned to one of three treatment groups: control, hyperthyroid, or hypothyroid. Treatment began on the second postnatal day, according to the following schedule: control rats received subcutaneous (s.c.) injections of 0.9% saline (0.1 ml/100 g body mass) every second day; rats in the hyperthyroid group received s.c. injections of 3,3',5-triiodo-L-thyronine (T_3; 20 μg/100 g body mass) every second day; and rats in the hypothyroid group had 0.05% 6-n-propylthiouracil (PTU) added daily to the drinking water of the mothers; PTU is effectively transferred to nursing rats through the mothers' milk (Moussavi et al., 1985). The preceding treatment protocol is similar to that used by Kolar and co-workers (1992).

On postnatal day 12 rats in one third of the litters from each of the three treatment groups were sacrificed (12 day old: control, n=11; hyperthyroid, n=8; hypothyroid, n=9). In remaining litters, treatment continued until postnatal day 28. At this time, rats in half of the remaining litters from each treatment group were sacrificed (28 day old: control, n=7; hyperthyroid, n=10; hypothyroid, n=9), while

remaining rats were weaned and allowed to grow until approximately 80 days of age (control, n=8; previously hyperthyroid, n=9; previously hypothyroid, n=9). Body mass was monitored in neonatal rats during the treatment period. Mothers and weaned rats were maintained on standard rat diet *ad libitum*. Though both male and female rats were treated, only the hearts from male rats were used for morphometric analysis; female rats were used to obtain blood samples for serum T_3 analysis. The gender of the rat was not believed to influence the results of serum T_3 analysis, as free serum T_3 levels are comparable between male and female rats until 3 months of age (Segal et al., 1982) - the oldest rats in our study are approximately 1½ months of age.

3.2.2 Total serum T_3 determination

In addition to examining the changes in heart rate, development of hypo- and hyperthyroidism was also verified by radioimmunoassay analysis of total serum T_3 levels (Diagnostic Veterinary Service, Ontario, Canada). Blood samples were collected from halothane-anaesthetized female rats by either decapitation and bleeding (12 day old rats) or by cardiac puncture (28 and 80 day old rats). Samples were pooled within experimental groups to obtain a sufficient volume of serum for testing.

3.2.3 Measurement of cardiac function

Heart rates were determined in 12 and 28 day old halothane-anaesthetized male rats from ECG recordings on a Grass 1P1F Polygraph. Blood pressure in the left

(LV) and right (RV) ventricles of 80 day old male rats, anaesthetized with pentobarbital sodium (52mg/100 g body mass, i.p.), was measured using a Millar catheter-tip transducer connected to the Polygraph and a PC computer. The catheter was inserted into the left ventricular cavity via the right carotid artery under continuous pressure monitoring. Measurements were recorded after a stabilization period of 10-15 minutes; recordings were made every 5 minutes over a 15-20 minute interval and the mean was calculated. Similarly, the catheter was introduced into the RV via the right jugular vein.

The analog pressure signal was digitized with a sampling frequency of 1 KHz and stored on computer for later processing. The following parameters were derived: left and right ventricular systolic pressure (LVSP, RVSP), left ventricular end-diastolic pressure (LVEDP), developed pressure (LVDevP), and the maximal rates of pressure development (+dP/dt)max and fall (-dP/dt)max. In addition, the time constant of relaxation (τ) was calculated, based on an experimental model of isovolumic pressure decay, as the time required for the pressure at (-dP/dt)max to be reduced by 1/e (Mirsky and Pasipoularides, 1990). The maximum rate of pressure development and fall, and the constant of relaxation, provide an indication of the contractile characteristics of the heart. The inotropic state of the heart is determined by the maximal rate of pressure development. Left and right ventricular pressure, left ventricular developed and end-diastolic pressure, provide an indication of heart function. Heart rate for 80 day old rats was calculated from the LV pressure signal.

The preceding functional measurements were accomplished with the kind collaboration of Drs. Frank Kolar and Frank Papousek.

3.2.4 Histology

Under anaesthesia, hearts from male rats were arrested in diastole using a bolus injection of concentrated KCl. After being excised surrounding fat and fibrous tissue was trimmed away and the atria were separated from the ventricles. The right ventricular free-wall was dissected free and weighed. The intact left ventricle and septum were also weighed and sectioned into two (12 day old) or three (28 and 80 day old) portions perpendicular to the base-apex axis of the heart. Apical portions were used for percent tissue dry weight estimations, while remaining portions were snap frozen in liquid nitrogen and stored at -80^{0}C until further analysis. Only the midmyocardium of the left ventricular free-wall was used for morphometric analysis.

Frozen tissue sections were processed using three different histological methods: *Bandeiraea simplicifolia I* (BSI) lectin, Alkaline phosphatase/Dipeptidyl peptidase IV (AP/DPP), or Proliferating Cell Nuclear Antigen (PCNA) immunohistochemistry. The BSI lectin staining method was employed in this study to identify capillaries within tissue cross-sections as the AP/DPP method could not be used in hearts from rats younger than 21 days of age (Batra and Rakusan, 1992). BSI lectin staining, performed in all age groups, was used for capillary numerical density determination. AP/DPP staining was performed in longitudinal sections from 28 and

80 day old rats for all groups - capillary segment lengths were measured in these sections. PCNA immunohistochemistry was used to provide a measure of cell-cycle activity and consequently cell proliferation.

Unless otherwise indicated, all histochemical procedures were performed at room temperature.

Bandeiraea simplicifolia I (BSI) lectin staining

Midmyocardial cross-sections (12 μm) from 12, 28 and 80 day old hearts were pre-incubated in phosphate-buffered saline (PBS; pH 7.4) (10 min) before exposure to peroxidase-conjugated BSI lectin (25 μg/ml in PBS; Sigma) for 30 minutes. BSI lectin binds to the terminal α-galactosyl saccharides associated with endothelial cell surfaces. Sections were next incubated with a 3'-diaminobenzidine (DAB) solution (DAB Kit; Dimension Laboratories Inc.; 30 minutes), after which they were rinsed with PBS (10 min) and cover-slipped using Permount. Capillary profiles were identified in cross-sections by their brown colour.

Alkaline Phosphatase/Dipeptidyl Peptidase IV staining

Longitudinal midmyocardial sections from 28 and 80 day old hearts were subject to AP/DPP staining. A detailed description of this histochemical procedure may be found in the preceding chapter.

PCNA/Haematoxylin and eosin staining

Cross-sections of left ventricular midmyocardium from 12, 28, and 80 day old hearts were processed according to the method of PCNA detection. PCNA data was used to corroborate morphometric data. A detailed description of this immunohistochemical procedure may be found in the preceding chapter.

3.2.5 Morphometric Analysis

BSI Lectin stained cross-sections

Five or six representative drawings of capillary profiles within tissue cross-sections were made for each heart using an Olympus microscope and drawing arm attachment. From these drawings - each drawing covering an area of approximately 36, 400 μm^2 - the average capillary numerical density was calculated for each heart.

PCNA/H&E stained cross-sections

The reader is referred to the method section of the preceding chapter for a complete description of the sampling procedure and parameters measured.

AP/DPP stained longitudinal sections

Due to the convenience and reliability of the "short-cut" method, it was used for longitudinal analysis instead of the capillary reconstruction set method. The reader is referred to the method section of the previous chapter for a complete description

of the sampling procedure and parameters measured.

3.2.6 Statistical Analysis

Results are presented as mean ± SEM. Body and heart mass data, capillary numerical density, and segment length data were analyzed using a two-way Analysis of Variance (ANOVA) with differences among group means determined using the Tukey HSD post hoc test. It should be noted that segment length data demonstrated a log-normal distribution and were thus logarithmically-transformed prior to statistical analysis. Chi-square (χ^2) analysis was used to determine an overall significant difference in nuclei proportions among the groups. PCNA data were transformed using an arcsin transformation and the transformed data were analyzed using a two-way ANOVA and Tukey HSD post hoc test. All results were considered statistically significant at $P<0.05$.

3.3 Results

3.3.1 Serum T_3 levels and heart rate measurements

Serum T_3 analysis confirmed the development of hypothyroidism (12 day old control: 0.7 nmol/L; hypothyroid: <0.2 nmol/L) and possibly hyperthyroidism (1.3 nmol/L) at 12 and 28 days of age (28 day old control: 0.4 nmol/L; hyperthyroid: 23.0 nmol/L; hypothyroid: <0.2 nmol/L). Corresponding changes to heart rate in the hyper- or hypothyroid group agreed with the results of the serum T_3 analysis (Fig. 3.1). Rats

Figure 3.1 Heart rates in 12 and 28 day old control (CON), hyperthyroid (HYPER), and hypothyroid (HYPO) rats, and in rats 52 days after treatment was stopped (80 days old). Heart rate increased significantly between 12 and 28 days in CON and HYPER rats, and between 28 day old HYPO and 80 day old previously HYPO rats, at $P<0.01$. * $P<0.01$ v. CON; $^{\delta}$ $P<0.01$ v. HYPER; $^{\Psi}$ $P<0.05$ v. CON. Results are presented as mean + SEM.

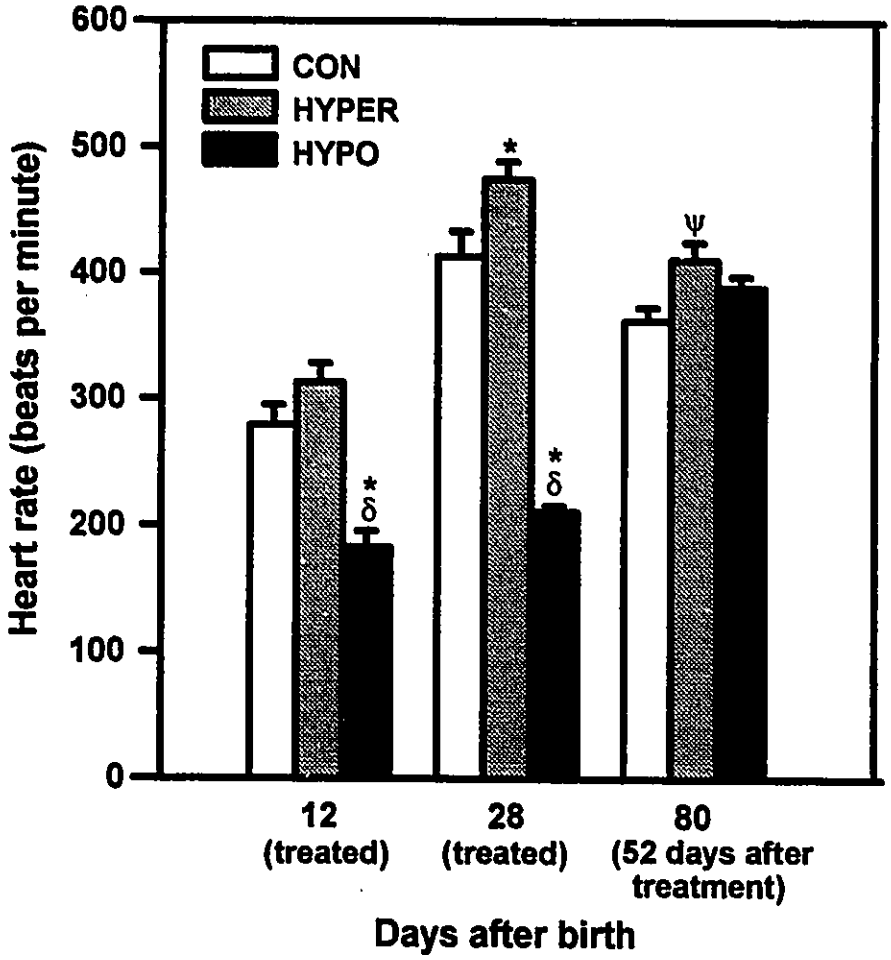
600
500
400
300
200
100
0
CON
HYPER
HYPO
Heart rate (beats per minute)
*
δ
*
δ
Ψ
12
(treated)
28
(treated)
80
(52 days after
treatment)
Days after birth

in the hyperthyroid groups had a higher heart rate, which only reached statistical significance at 28 days ($P<0.05$), whereas hypothyroid rats had significantly lower heart rates at both 12 and 28 days ($P<0.01$), compared to age-matched controls.

At 80 days of age, 52 days after treatment had stopped, serum T_3 levels were comparable among the groups (approximately 1.0 nmol/L), suggesting that euthyroidism had been re-established in neonatally hyper- and hypothyroid rats. Heart rates were similar between 80 day old control and previously hypothyroid rats in accordance with T_3 levels. However, the heart rate in previously hyperthyroid rats remained significantly higher than control ($P<0.05$) in spite of normal T_3 levels. This finding may reflect a lasting influence of hyperthyroidism on heart rate, a sensitivity of this group to the anaesthetic or surgical procedure.

3.3.2 Maturational indices

Maturation was accelerated in hyperthyroid rats, as evident from by observations made during the treatment period - early eye opening (day 10 versus day 12 in control rats), facilitated fur and ear growth, and better neuromuscular coordination. Conversely, hypothyroidism delayed eye opening (day 14), slowed fur and ear growth, and resulted in poorer neuromuscular coordination.

3.3.3 Functional data

Left and right ventricular functional parameters from 80 day old rats, 52 days

after treatment was stopped, are summarized in Table 3.1. RV and LV systolic pressure, LV end-diastolic and developed pressure, as well as the maximal rates of pressure development were all significantly greater in previously hyperthyroid rats ($P<0.05$) compared to age-matched control. No lasting effects of neonatal hypothyroidism on cardiac function were detected.

3.3.4 Body mass and heart mass data

Body mass in hyperthyroid rats was comparable to control at both 12 and 28 days, but was significantly lower ($P<0.01$) 52 days after treatment was discontinued (Table 3.2). Body mass in 12 day old hypothyroid rats was similar to age-matched controls, but was significantly lower in 28 day old hypothyroid and remained lower 52 days after treatment was stopped ($P<0.01$). These results indicate that both neonatal thyroid conditions induced long-term deficits in body growth.

Heart mass increased with age in control and hyperthyroid groups ($P<0.01$). Compared to age-matched controls, hyperthyroidism induced a sizeable increase in right (RV) and left ventricular (LV) mass and relative heart mass (HM:BM) at 12 ($P<0.05$ and $P<0.01$ respectively) and 28 days of age ($P<0.01$). Interestingly, the increase in RV and LV mass was of similar proportion. It thus appears that hyperthyroidism equally enhanced the rate of right and left ventricular growth. In hypothyroid rats, significantly lower RV and LV mass ($P<0.01$), as well as lower relative heart mass ($P<0.01$) were detected at 12 and 28 days compared to age-

Table 3.1 **Left and right ventricular functional data 52 days after treatment was stopped in Control, previously Hyperthyroid, and previously Hypothyroid rats**

Group	RVSP (mmHg)	LVSP (mmHg)	LVEDP (mmHg)	LVDevP (mmHg)	$(+dP/dt)_{max}$ (mmHg/s)	$(-dP/dt)_{max}$ (mmHg/s)	τ (ms)
CON-80	27 ± 2	124 ± 6	3.4 ± 0.6	120 ± 6	6917 ± 342	6028 ± 339	6.4 ± 0.8
HYPER-EU-80	35 ± 3[1]	154 ± 3[1]	5.8 ± 0.6[1]	149 ± 2[1]	8361 ± 165[1]	6697 ± 669	7.4 ± 0.3
HYPO-EU-80	24 ± 1[2]	128 ± 5[2]	3.7 ± 0.6	126 ± 5[2]	7551 ± 292	6738 ± 271	6.0 ± 0.2

Values are means ± SEM. RVSP: right ventricular systolic pressure; LVSP: left ventricular systolic pressure; LVEDP: left ventricular end-diastolic pressure; LVDevP: left ventricular developed pressure; (+dP/dt)max: maximum rate of pressure development; (-dP/dt)max: maximum rate of pressure fall; τ: time constant of relaxation. CON-80: 80 day old control rats; HYPER-EU-80: 80 day old previously hyperthyroid rat (52 days after treatment was stopped); HYPO-EU-80: 80 day old previously hypothyroid rats (52 days after treatment was stopped). [1] $P<0.05$ v. CON; [2] $P<0.01$ v. HYPER.

Table 3.2 **Body and heart mass data for 12 and 28 day old Control, Hyperthyroid, and Hypothyroid rats, and for rats 52 days after treatment was stopped (80 day old)**

Group	BM (g)	RV mass (mg)	LV + S mass (mg)	HM/BM ratio (mg/g)	RV/LV ratio	% tissue dry weight
CON-12	24 ± 1	36 ± 2	91 ± 4	5.4 ± 0.2	0.40 ± 0.03	21 ± 2
HYPER-12	22 ± 2	46 ± 6 [3]	112 ± 8[3]	7.0 ± 0.3[1]	0.41 ± 0.03	20 ± 2
HYPO-12	21 ± 1	26 ± 2[2]	62 ± 4[1,2]	4.2 ± 0.2[1,2]	0.43 ± 0.03	28 ± 3
CON-28	78 ± 2[4]	64 ± 3[4]	221 ± 7[4]	3.6 ± 0.1	0.29 ± 0.01	32 ± 2[4]
HYPER-28	70 ± 3[4]	85 ± 5[1,4]	272 ± 14[1,4]	5.1 ± 0.2[1]	0.31 ± 0.01[4]	20 ± 2[3]
HYPO-28	32 ± 1[1,2,4]	18 ± 1[1,2]	79 ± 5[1,2]	3.0 ± 0.1[1,2]	0.24 ± 0.02[2,3]	24 ± 4
CON-80	442 ± 8[1,5]	217 ± 10[5]	836 ± 35[5]	2.4 ± 0.1	0.26 ± 0.01	27 ± 1
HYPER-EU-80	324 ± 6[1,5]	203 ± 17[5]	638 ± 45[1,5]	2.6 ± 0.1	0.32 ± 0.01[1]	27 ± 1
HYPO-EU-80	303 ± 9[1,5]	175 ± 5[3,5]	591 ± 12[1,5]	2.5 ± 0.1	0.30 ± 0.01[3]	27 ± 1

Values are mean ± SEM. BM: body mass; RV: right ventricle; LV + S: left ventricle and septum; HM/BM: heart mass/body mass. CON-12, CON-28, CON-80: 12, 28, and 80 day old control rats; HYPER-12 and HYPER-28: 12 and 28 day old hyperthyroid rats; HYPER-EU-80: 80 day old previously hyperthyroid rats (52 days after treatment stopped); HYPO-12 and HYPO-28: 12 and 28 day old hypothyroid rats; HYPO-EU-80: 80 day old previously hypothyroid rats (52 days after treatment was stopped). HM/BM ratios decreased significantly with age in all groups, at $P<0.01$. RV/LV ratios decreased significantly between 12 and 28 days in all groups, at $P<0.05$. [1] $P<0.01$ v. CON; [2] $P<0.01$ v. HYPER; [3] $P<0.05$ v. CON; [4] $P<0.05$ v. 12 day old; [5] $P<0.01$ v. 28 day old.

matched controls. A lower RV/LV ratio in 28 day old hypothyroid rats ($P<0.05$) versus age-matched controls indicated that hypothyroidism attenuated the rate of RV growth more than LV growth.

After discontinuing treatment, both previously hyper- and hypothyroid rats demonstrated an increase in RV and LV mass over 28 day old values ($P<0.01$). Despite the increases, ventricular mass remained lower than control in previously hypothyroid rats ($P<0.05$), whereas only LV mass was lower in previously hyperthyroid rats ($P<0.01$). These results indicate an inhibitory or attenuating effect of both neonatal thyroid conditions on subsequent left ventricular growth. Relative heart mass was similar among the groups, however RV/LV ratio was significantly greater in both previously hyper- and hypothyroid rats ($P<0.01$ and $P<0.05$, respectively) indicating a larger increase in RV compared to LV mass after treatment was discontinued.

Percent tissue dry weight was similar among the groups with the exception of the 28 day old hyperthyroid group, which had a lower percent tissue dry weight than age-matched control ($P<0.05$) suggesting the possibility of edema (Table 3.2). Notably, the percent tissue dry weight of 28 day old control was significantly higher than at 12 day of age ($P<0.05$).

3.3.5 Morphometric data

Capillary numerical density

The number of capillaries per mm^2 decreased with increasing age in control rats (Fig. 3.2); neonatal hyperthyroidism did not affect this developmental pattern. However, no appreciable decrease in capillary numerical density between 12 and 28 days was noted with neonatal hypothyroidism. Greater capillary numerical density ($P<0.05$) was observed in the 12 day old hyperthyroid group compared to age-matched control, however this difference was absent at 28 days of age in the hyperthyroid group. Considering the induced LV hypertrophy in 28 day old hyperthyroid rats these results suggest that hyperthyroidism stimulated marked capillary proliferation. Capillary numerical density in 12 and 28 day old hypothyroid rats was not significantly different from age-matched controls suggesting slowing of capillary proliferation in proportion to the diminished LV growth. After return to euthyroidism, capillary numerical density was similar among all groups.

Capillary segment lengths

In control and hypothyroid rats proximal capillary segments were always longer than distal segments at 28 and 80 days of age ($P<0.01$) (Table 3.3). No significant difference in proximal and distal segments was found in the 28 day old hyperthyroid group suggesting possibly greater longitudinal growth or alternatively less branching in distal capillary segments of this group.

Figure 3.2 Coronary capillary numerical density (number of capillaries per mm^2) in 12 and 28 day old control (CON), hyperthyroid (HYPER), and hypothyroid (HYPO) rats, and in rats 52 days after treatment was stopped (80 days old). Capillary numerical density decreased significantly with age in HYPER and previously HYPER rats ($P<0.01$); between 28 and 80 day old CON rats ($P<0.05$); and between 28 day old HYPO and 80 day old previously HYPO rats ($P<0.01$). * $P<0.05$ v. CON; $^{\delta}$ $P<0.01$ v. HYPER. Results are presented as mean + SEM.

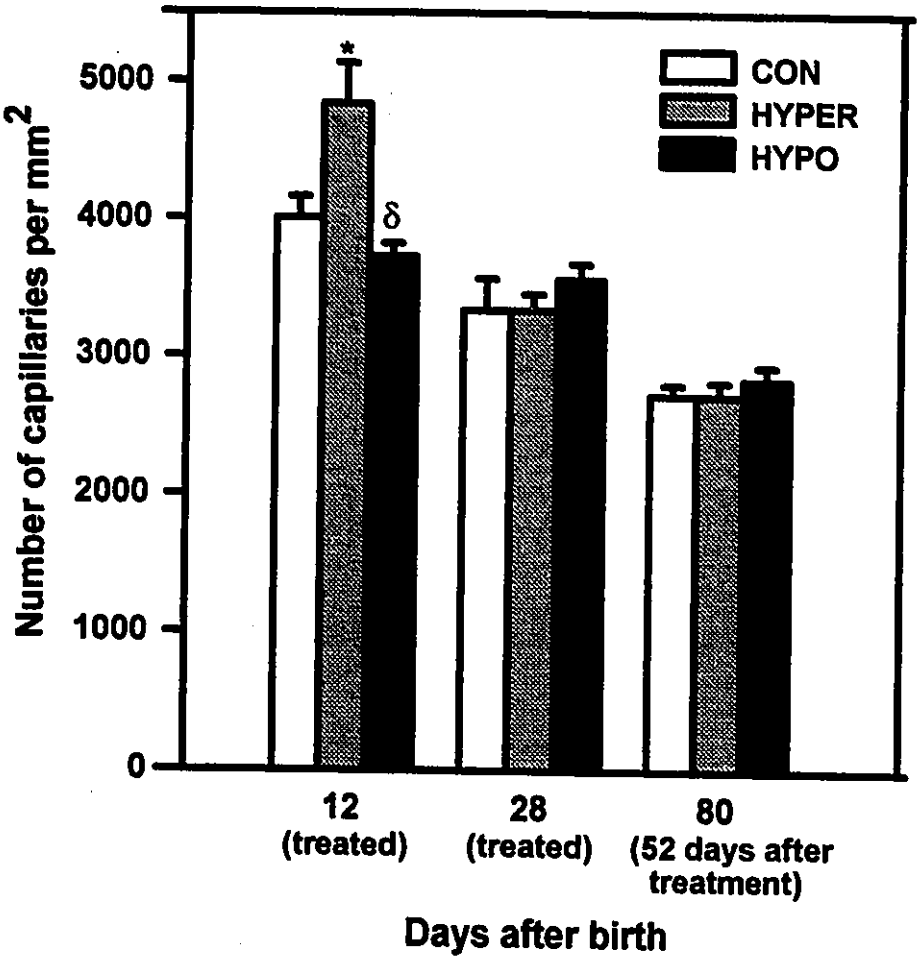
Number of capillaries per mm2
5000
4000
3000
2000
1000
0
*
δ
CON
HYPER
HYPO
12
(treated)
28
(treated)
80
(52 days after
treatment)
Days after birth

Table 3.3 **Capillary segment length data for 28 day old Control, Hyperthyroid and Hypothyroid rats, and for rats 52 days after treatment was stopped (80 day old)**

Group	Capillary segment lengths (μm)	
	Proximal	Distal
CON-28	68 ± 3	54 ± 2[2]
HYPER-28	71 ± 2	66 ± 4
HYPO-28	63 ± 2	52 ± 2[1,2]
CON-80	99 ± 3[4]	74 ± 3[2,4]
HYPER-EU-80	90 ± 3[4]	61 ± 1[2,3]
HYPO-EU-80	97 ± 4[4]	68 ± 2[2,4]

Values are mean ± SEM. CON-28: 28 day old control rats; CON-80: 80 day old control rats; HYPER-28: 28 day old hyperthyroid rats; HYPER-EU-80: 80 day old previously hyperthyroid rats (52 days after treatment stopped); HYPO-28: 28 day old hypothyroid rats; HYPO-EU-80: 80 day old previously hypothyroid rats (52 days after treatment stopped). [1] $P<0.05$ v. HYPER; [2] $P<0.01$ v. proximal; [3] $P<0.01$ v. CON; [4] $P<0.01$ v. 28 day old.

With age and greater heart mass, capillary segment lengths increased significantly in control and previously hypothyroid rats ($P<0.01$); proximal capillary segment lengths increased in hyperthyroid rats ($P<0.01$). However, in 80 day old previously hyperthyroid rats, distal capillary segments were not only similar to 28 day old lengths, but were significantly smaller than those in 80 day old control rats ($P<0.01$). These results suggest either an inhibition of subsequent distal segment growth once euthyroidism was re-established, or increased branching in the distal portions of the capillary bed.

Total nuclei density

In control rats the number of nuclei per mm^2 decreased between 12 and 28 days of age ($P<0.05$) but not thereafter (Fig. 3.3). On the other hand, neonatal hyper- and hypothyroidism showed no initial decrease in nuclei density between 12 and 28 days, but did show a decrease between 28 and 80 days ($P<0.05$). At 12 days of age, hypothyroid rats had a lower nuclei density compared to age-matched control ($P<0.05$).

Relative nuclei proportions

The relative proportions of endothelial (ENDO), myocyte (MYO), and "other" (OTHER) nuclei changed between 12 and 28 days in control and hyperthyroid rats ($P<0.01$) - decreased percentage of MYO and increased percentage of ENDO and

Figure 3.3 Total nuclei density (number of nuclei per mm^2) in 12 and 28 day old control (CON), hyperthyroid (HYPER), and hypothyroid (HYPO) rats, and in rats 52 days after treatment was stopped (80 days old). * $P<0.05$ v. CON; $^{\delta}$ $P<0.05$ v. 12 day old; $^{\Psi}$ $P<0.05$ v. 28 day old. Results are presented as mean + SEM.

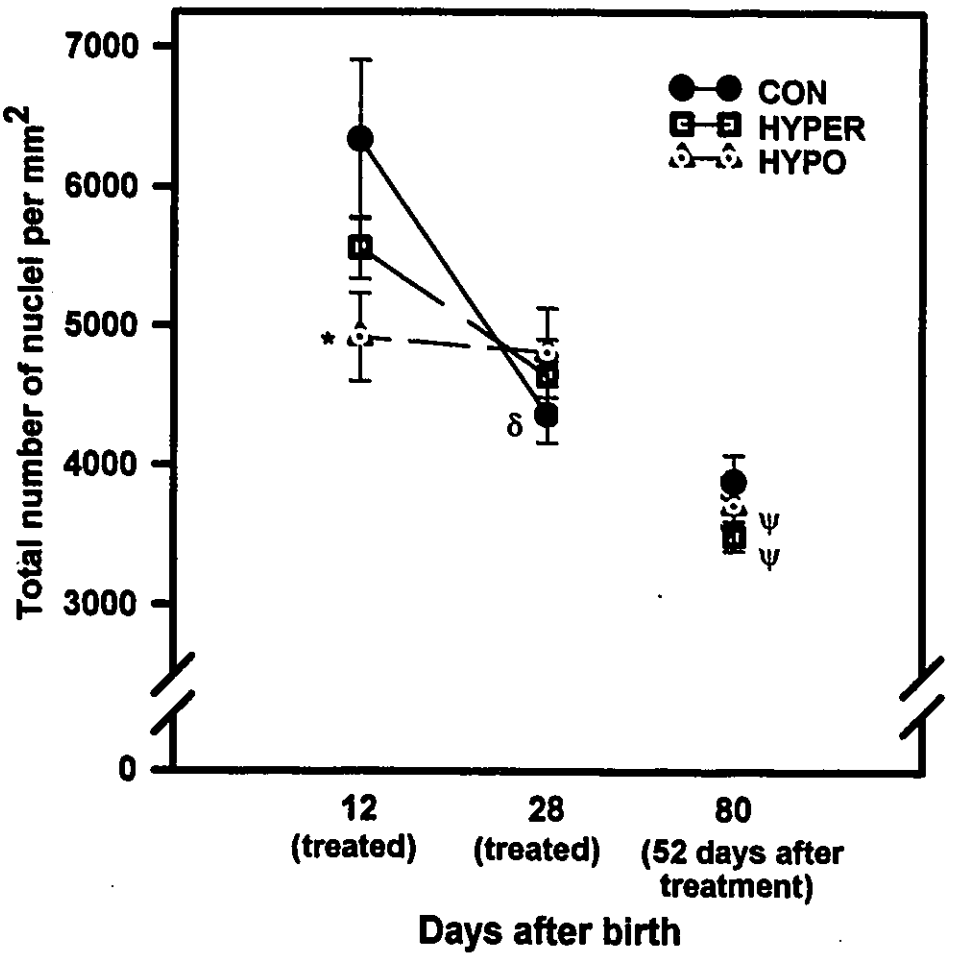
7000
6000
5000
4000
3000
0
Total number of nuclei per mm2
CON
HYPER
HYPO
*
δ
ψ
ψ
12
(treated)
28
(treated)
80
(52 days after
treatment)
Days after birth

OTHER (Fig. 3.4). This redistribution was delayed in hypothyroid rats. Both neonatal hypo- and hyperthyroidism induced significant changes in nuclei proportions in 12 and 28 day old rats as compared to age-matched controls ($P<0.05$) - hyperthyroidism induced a greater proportion of OTHER nuclei, whereas hypothyroidism induced a greater proportion of MYO nuclei. Fifty-two days after treatment was discontinued, nuclei proportions were comparable among the groups suggesting no lasting effect of either neonatal thyroid condition on the relative proportions of nuclei types.

PCNA labelling

An increase in the number of PCNA-positive endothelial (ENDO+) nuclei between 12 and 28 day old control hearts indicated endothelial cell proliferation, which likely reflects the occurrence of extensive capillary growth (Fig. 3.5). At 12 days of age, hyperthyroid rats had a higher percentage of ENDO+ nuclei than control ($P<0.05$). The largest percentage of ENDO+ nuclei occurred at 12 days of age in hyperthyroid rats but at 28 days of age in control rats. By day 28, the previously higher percentage of ENDO+ nuclei in hyperthyroid rats had decreased to a similar level as 28 day old controls. After treatment was stopped, the number of ENDO+ nuclei was comparable among the groups.

The number of PCNA-positive myocyte nuclei (MYO+) decreased with age in all groups. No statistical difference in MYO+ nuclei among the groups was detected

Figure 3.4 Relative percentage of endothelial (ENDO), myocyte (MYO), and "other" (OTHER) nuclei in 12 and 28 day old control (CON), hyperthyroid (HYPER), and hypothyroid (HYPO) rats, and in rats 52 days after treatment was stopped (80 days old). Overall relative proportions are significantly different among 12 and 28 day old HYPER and 80 day old previously HYPER rats (HYPER-EU), between CON-12 and CON-28, and between HYPO-28 and 80 day old previously HYPO rats (HYPO-EU), at $P<0.05$. * $P<0.01$ v. CON. Results are presented as percentages.

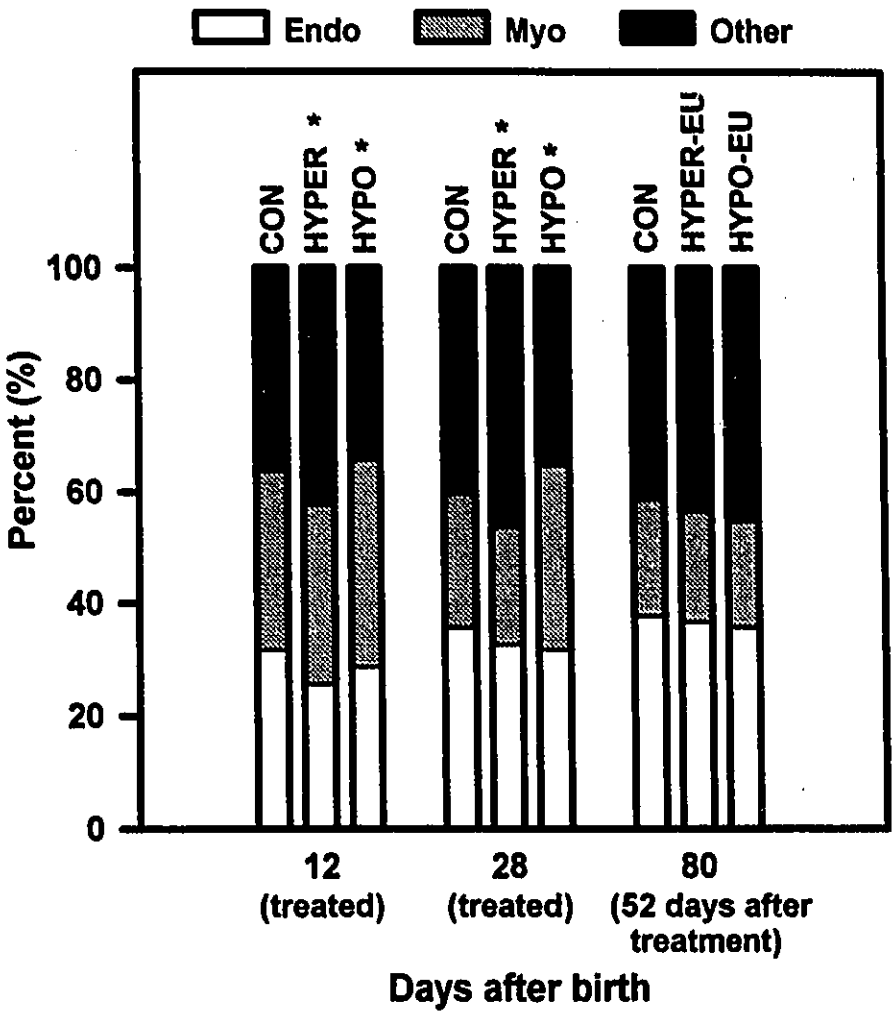
Endo
Myo
Other
CON
HYPER *
HYPO *
CON
HYPER *
HYPO *
CON
HYPER-EU
HYPO-EU
Percent (%)
100
80
60
40
20
0
12
(treated)
28
(treated)
80
(52 days after
treatment)
Days after birth

Figure 3.5 Number of PCNA labelled endothelial (ENDO), myocyte (MYO), and "other" (OTHER) nuclei per 1000 nuclei in 12 and 28 day old control (CON), hyperthyroid (HYPER), and hypothyroid (HYPO) rats, and in rats 52 days after treatment was stopped (80 days old). * $P<0.05$ v. CON; $^{\delta}$ $P<0.05$ v. HYPER. Please note that ordinate scales are different among the three graphs. Results are presented as mean + SEM.

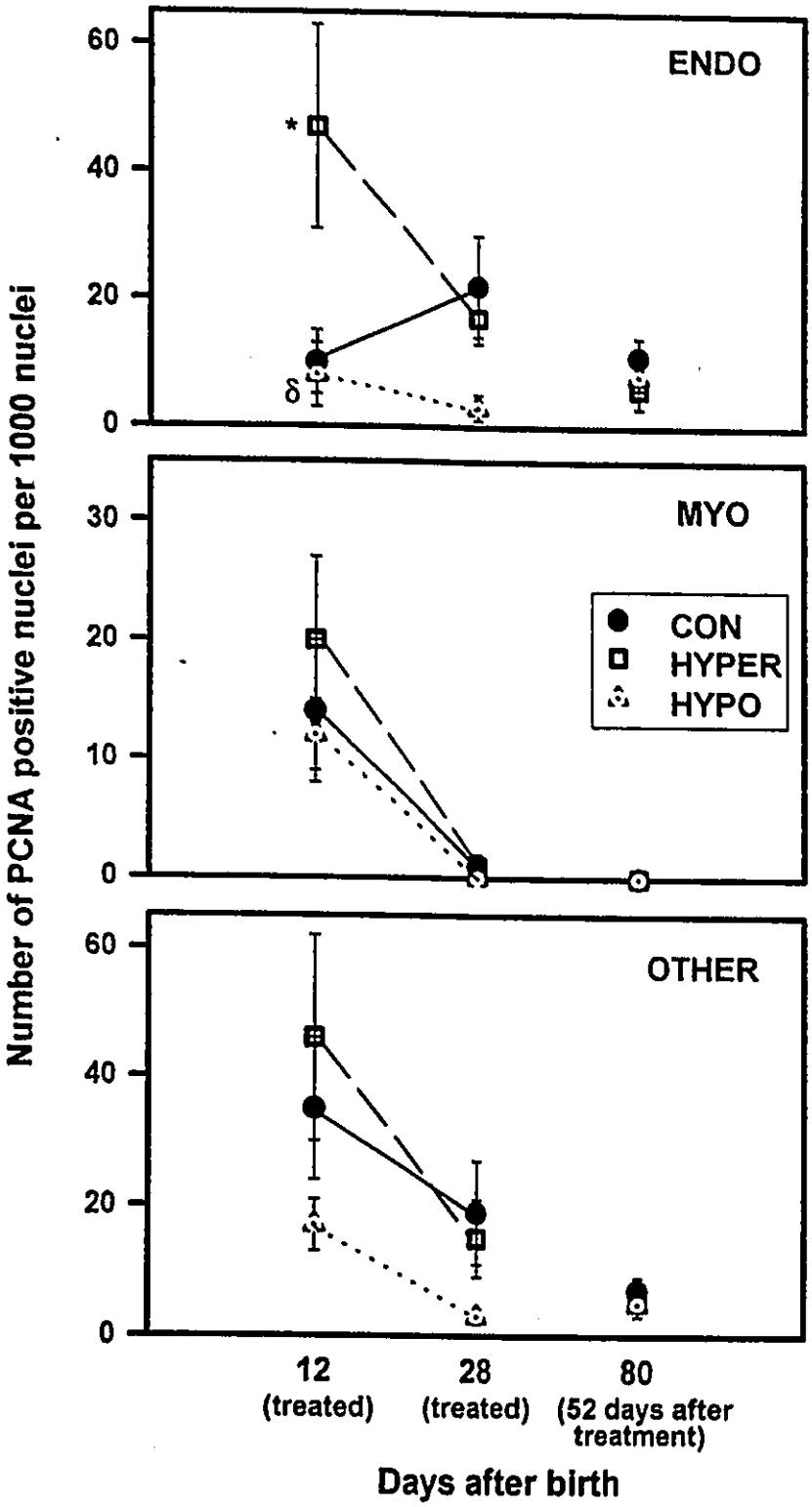
ENDO
MYO
OTHER
CON
HYPER
HYPO
Number of PCNA positive nuclei per 1000 nuclei
60
40
20
0
30
20
10
0
60
40
20
0
*
δ
12
(treated)
28
(treated)
80
(52 days after
treatment)
Days after birth

at any age. The lack of MYO+ nuclei in 80 day old control rats agrees with the idea that myocyte proliferation is rare in adult animals; this phenomenon was not changed by either neonatal hyper- or hypothyroidism. The occurrence of PCNA-positive "other" (OTHER+) nuclei decreased with age in control and hyperthyroid groups and between 12 and 28 days in the hypothyroid group.

3.4 Discussion

Cardiac hypertrophy and accelerated maturation were produced in neonatal rats treated with excess triiodothyronine (T_3), whereas attenuated cardiac growth and delayed maturation were induced in neonatal rats treated for a similar period with the anti-thyroid goitrogen propylthiouracil. These results agree with other studies (Meisami, 1984; Moussavi et al., 1985; Kolar et al., 1992).

The proportional increase in right and left ventricular mass was different from the predominant right ventricular hypertrophy reported in a similar neonatal study (Kolar et al., 1992). It is possible that treatment every second day may not produce the same degree of increased hemodynamic load as daily treatment and this in part, may account for the discrepancy. The predominant attenuation of right ventricular growth relative to left in hypothyroid rats differs from the report of proportionally lower right and left ventricular mass in neonatal hypothyroid rats (Kolar et al., 1992).

A reduction in cell proliferation with early neonatal hypothyroidism has been previously described for other body organs (Brasel and Winick, 1970) and is

supported in the present study by the smaller number of PCNA-positive endothelial nuclei and the similarity in overall nuclei density between 12 and 28 day old hypothyroid rats. Thus, alterations in thyroid status during the neonatal period not only accelerate or delay maturation, but also influence the degree of cell proliferation and the rate of cardiac growth.

Coronary capillary morphometry

Commensurate with the enhanced cardiac growth induced by hyperthyroidism, enhanced capillary proliferation was also observed in these rats. After 12 days of T_3 treatment the significantly larger capillary numerical density in spite of increased cardiac mass, together with a significantly greater number of PCNA-positive endothelial nuclei, provides evidence indicative of capillary proliferation. After 28 days of T_3 treatment, capillary proliferation declined to a level which was proportional to the increase in left ventricular mass as indicated by the similarity in capillary numerical density between 28 day old control and hyperthyroid rats. The decrease in number of PCNA-positive endothelial nuclei between 12 and 28 days of age in hyperthyroid rats supports this finding. The induction of capillary proliferation in response to hyperthyroidism has previously been observed in adult (Chapter 2; Chilian et al., 1985; Wachtlova et al., 1985; Mall et al., 1990) and senescent hyperthyroid rats (Tomanek et al., 1995), as well as in adult hyperthyroid pigs (Breisch et al., 1989). The similarity in length between proximal and distal capillary segments in 28 day old

hyperthyroid rats, which contrasts findings in control hearts, suggests that growth of segments along the longitudinal axis (i.e. capillary elongation) was more pronounced in distal regions of the capillary bed than in proximal. Alternatively, the formation of capillary branches may also have decreased in distal regions. One possible explanation for this finding may be based on the increased metabolism and myocardial oxygen consumption produced by hyperthyroidism (Talafih et al., 1983, 1984; Weiss and Tse, 1995). These increases may exacerbate the low PO_2 found in distal portions of the capillary bed, which in turn may stimulate distal capillary growth.

In contrast, neonatal hypothyroidism appeared to slow the formation of new capillaries in proportion to the reduction in cardiac growth, thus maintaining capillary numerical density. These findings are different to the increased capillary numerical density previously reported in adult hypothyroid rabbits (Tomanek et al., 1993) and in adult hypothyroid rats (Chapter 2). Data from capillary segment length analysis indicated that even though formation of new capillaries may have been slowed, growth in length of existing capillaries may not have been appreciably affected. Growth of the capillary network can occur by formation of new capillary connections or by elongation of existing capillaries. If neonatal hypothyroidism had attenuated both of these processes, then for the smaller heart mass noted in these rats one would have expected shorter capillary segments; this was not the case. The similarity in number of PCNA-positive endothelial nuclei at 12 days of age in the hypothyroid and control groups suggests normal endothelial cell proliferation that may correspond to

elongation of capillaries. Subsequently, the decline in number of PCNA-positive endothelial nuclei between 12 and 28 days in hypothyroid rats supports the postulated attenuation in formation of new capillary branches or connections.

Based on the results of this study one may speculate that the decline in capillary proliferation that occurs during normal postnatal development depends more on tissue maturation than on the rate of cardiac growth. For instance, the rate of cardiac growth (the increase in heart mass over a period of time) was similar in both control and hyperthyroid rats between 12 and 28 days, yet tissue maturation was accelerated in hyperthyroid rats. During this same time the decline in capillary numerical density was greater in hyperthyroid compared to control (decrease of ~17% in control versus ~34% in hyperthyroid rats) despite the fact that the increase in heart mass was similar between the two groups (an increase in LV mass of ~142% in both groups). The decline in capillary proliferation, which results in decreased capillary numerical density, thus appears to be consistent with a dependence on tissue maturation rather than on the rate of cardiac growth. Also in support of this hypothesis is the finding in hyperthyroid rats that the number of PCNA labelled endothelial cells decreased earlier than in control. An analysis of the similarities and differences in microvascular response between neonatal- and adult-onset hyper- and hypothyroidism, will be presented in Chapter 5 (General Discussion).

Long-term effects of altered neonatal thyroid status

Both neonatal hyper- and hypothyroidism resulted in long-term body and cardiac growth deficits, albeit likely by different mechanisms - hypothyroidism affected both right and left ventricular growth whereas neonatal hyperthyroidism only affected left ventricular growth. It has been proposed that neonatal hyperthyroidism leads to a reduction in myocyte number by hastening the transition from hyperplastic to hypertrophic growth (Gerdes et al., 1983). Thus, it may be that the smaller number of myocytes in these hearts are not able to produce the same increase in cardiac mass with age as in normal hearts. In neonatal hypothyroidism despite the fact that the number of cardiac myocytes may not be affected by a delay in transition from hyperplastic to hypertrophic growth, reduction in other hormones (e.g. growth hormone) that play an important role in cardiac development may compromise cardiac growth subsequent to re-establishment of euthyroidism (Moussavi et al., 1985).

No long-term changes in capillarization were observed with neonatal hypothyroidism. However, the similarity of distal segment lengths between 28 day old hyperthyroid and 80 day old previously hyperthyroid rats together with increasing left ventricular mass during this period, may possibly be explained either by an inhibition of the growth of distal segments or by elongation and formation of new capillary connections, thereby maintaining segment lengths. PCNA data indicates that there is some cell-cycle activity in endothelial nuclei, however without other longitudinal parameters (i.e. number of distal segments per capillary set; total capillary

length, etc.) it is difficult to discern which mechanism is responsible for these changes or lack of change.

Neonatal hyperthyroidism appeared to induce lasting positive effects on heart rate and on indices of systolic function of the heart. The explanation of these observations is unclear and many possible mechanisms may be taken into account; these mechanisms will be discussed in Chapter 5 (General Discussion).

Summary

Results from this study provide evidence of increased cardiac growth accompanied by substantial capillary proliferation in neonatal hyperthyroidism and attenuation of cardiac growth with reduced capillary proliferation in neonatal hypothyroidism. Both neonatal thyroid conditions resulted in long-term deficits to body and cardiac growth, but only neonatal hyperthyroid rats demonstrated maintenance of distal segment length, 52 days after treatment stopped. Additionally, neonatal hyperthyroidism produced a lasting positive influence on the inotropic and chronotropic characteristics of heart function, though a plausible explanation or physiological relevance has yet to be determined. One other interesting finding based on our results is that the decline in capillary proliferation observed during the neonatal period of development appears to depend more on maturation than on the rate of cardiac growth.

CHAPTER 4

EFFECT OF NEONATAL HYPER- AND HYPOTHYROIDISM ON CORONARY ARTERIOLES

4.1 Introduction

The previous two chapters focused on the response of the coronary capillary network to hyper- or hypothyroidism induced either during the neonatal period or in adulthood. The current chapter concentrates on the response of the developing coronary arteriolar network to neonatal-onset hyper- or hypothyroidism.

The profound effects of altered thyroid hormone levels on the coronary microvasculature have been extensively examined in adult mammals (Chapter 2; Chilian et al., 1985; Tomanek et al., 1993; Wachtlova et al., 1985) and more recently in senescent rats (Tomanek et al., 1995). In both adult and senescent rats, cardiac hypertrophy induced by either excess triiodothyronine or thyroxine was shown to stimulate coronary capillary (Chapter 2) and arteriolar growth (Chilian et al., 1985; Tomanek et al., 1995). However, despite the important role that thyroid hormones play in normal cardiac growth and maturation during the neonatal period the effect of hypo- and hyperthyroidism on the development of the coronary arteriolar network in neonatal animals has not been fully examined. To the best of our knowledge, mammalian studies that have documented neonatal arteriolar growth are presently limited to normal human hearts (Rakusan et al., 1994b).

In the mammalian heart, the neonatal period of cardiac development is

characterized not only by changes in tissue morphology and composition but also by significant growth and expansion of the microvascular network (reviewed in Rakusan and Heron, 1996). The normal formation and maturation of arteriolar and capillary networks during this developmental period is essential for the maintenance of adequate oxygen supply to the rapidly growing myocardium. The coronary arteriolar network is important in regulating resistance and consequently nutritive blood flow and oxygen supply. Irregular formation of the coronary arteriolar network could lead to inadequate myocardial oxygenation and nutritive supply with the possibility of compromised cardiac development. In addition, since the microvascular network, under normal conditions becomes more stable as the animal enters adulthood, changes in vascularization occurring in the neonatal period may be irreversible.

The aim of this study was two-fold: (1) to morphometrically examine the effect of neonatal-onset hypo- and hyperthyroidism on the developing arteriolar networks, and (2) to determine whether changes in arteriolar geometry resulting from either neonatal condition, persist into adulthood once euthyroidism is re-established.

Notably, this study is very similar to the study in Chapter 3 however, because Silver-methenamine staining of very thin plastic sections (1 μm) is the method of choice for accurate morphometric evaluation of coronary arterioles, the frozen hearts from the previous study could not be used. If only Silver-methenamine stained plastic sections were used for both arteriolar and capillary examination, analysis of capillary geometry in two different regions of the capillary network would not be possible

(recall AP/DPP has to be used in frozen sections). Moreover, determination of a PCNA labelling index would not be feasible in plastic sections due to the fixation and embedding processes.

4.2 Materials and Methods

4.2.1 Animals and Treatment

The handling of animals and the treatment schedule have been detailed in the previous chapter (please see section 3.2.1). The exact same procedures were followed in this study. The experimental groups and number of animals studied in each group were as follows: 12 day old: control, n=11; hyperthyroid, n=12; hypothyroid, n=9; 28 day old: control, n=8; hyperthyroid, n=8; hypothyroid, n=8; 80 day old: control, n=8; previously hyperthyroid, n=8; previously hypothyroid, n=8. The body mass of the newborn rats was monitored for the entire treatment period. Mothers and weaned rats were maintained on standard rat diet *ad libitum*. Even though both male and female newborns were treated, only the hearts from male rats were used for morphometric analysis; female rats were used for obtaining blood samples, which were used in determination of total serum T_3 levels. Halothane anaesthetized male rats were connected, using needle electrodes, to a Grass polygraph recorder (Model 7B) on which heart rate recordings were made. Heart rate and serum T_3 analysis served as indices of thyroid hormone status.

4.2.2 Total serum T_3 determination

Blood sampling was performed as previously described (please see Chapter 3).

4.2.3 Histology

Hearts were stopped in diastole following a bolus injection of saturated KCl. The hearts were then excised and any remaining fat or fibrous tissue was trimmed away. The right ventricular free-wall was dissected free and weighed, leaving the left ventricle and septum intact. The left ventricle and septum were weighed and sectioned into either two (12 day old) or three (28 and 80 day old) portions, perpendicular to the base-apex axis. Hearts from 12 day old rats were sectioned into two portions due to their small size. The apical portion, in 28 and 80 day old rats, was used to determine the percent dry weight. However, due to the small amount of tissue available, the percent tissue dry weight was not determined in the 12 day old groups. The remaining upper and middle portions were fixed by immersion in 1.5% glutaraldehyde, buffered to pH 7.4 with phosphate buffer; both portions from 12 day old hearts were immersion fixed. After fixation and alcohol dehydration, samples were embedded in historesin and prepared for microtome sectioning. Only the left ventricular free wall was used for morphometric analysis.

Avalone's modification of the Jones Silver-methenamine stain

Midmyocardial cross-sections (1 μm thick) were cut and stained using

Avalone's modification of the Jones silver methenamine method for staining basement membranes. This staining procedure was used to facilitate identification of arterioles, capillaries, and myocyte within tissue cross-sections. A complete description of the Silver-methenamine staining procedure may be found in Chapter 2. Notably, the time of incubation in the Silver-methenamine solution was longer for plastic sections (20-25 min), and had to further be adjusted for staining of 12 and 28 day old hearts (45 min to 1 h).

4.2.4 Morphometric Analysis

Capillary numerical density, myocyte density and myocyte-to-capillary ratio

The reader is referred to the method section of Chapter 2 for a complete description of the sampling procedures and morphometric parameters measured.

Arteriolar measurements

Entire tissue sections of the left ventricle (subepi-, mid-, and subendomyocardium) were evaluated for arterioles using an Olympus microscope (magnification 1820x) linked to an image analyzer (Bioquant, R&M Biometrics). The total area of the section was measured. All arteries and arterioles encountered within this section were measured and recorded, irrespective of the sectioning angle. A minimum of 100 arteriolar profiles were measured in each heart.

For every arteriolar profile observed the shortest (minimum) external diameter,

the longest (maximum) external diameter perpendicular to the short axis, and the minimum internal diameter were measured. All arterioles having a maximum-to-minimum diameter ratio ≤ 5 were used for morphometric analysis. It has been shown that over 96% of the vessel profiles within a section meet this criterion (Rakusan and Wicker, 1990); a similar phenomenon was observed in the present study (~ 95%).

The maximum external diameter was measured strictly for determination of the ratio which is used as our inclusion/exclusion criterion. The minimum external diameter represents the true diameter of the arteriole as this parameter remains constant despite changes in the cutting angle. The minimum internal diameter together with the minimum external diameter, was used in the calculation of arteriolar wall thickness. It was sometimes difficult to distinguish the smallest arterioles from venules or expanded capillaries. In these cases, the structure was checked using a higher magnification. Arteriolar walls are always relatively thicker than the walls of these other vessels of the same size, usually layers of smooth muscle cells are seen in arteries and arterioles (venules had only occasional smooth muscle cells and larger veins had only a few small bundles of muscle cells), and the shape of the cross-sectional profile of arterioles was fairly round, oval, or ellipsoidal, indicating a relatively rigid wall.

Vessels were categorized as a function of their minimum external diameter. The categorization of arterioles enables later analysis of relative arteriolar frequency as a function of arteriolar size. The average arteriolar wall thickness, average

minimum external diameter, average internal diameter, and frequency of each arteriolar size were determined. Arteriolar length density (average length of arterioles per volume of tissue), Lc, was also calculated using an equation developed for the analysis of vessels arranged in any orientation (Anversa and Capasso, 1991; Chen et al., 1994). To obtain an accurate estimate of length density the angle at which the vessel is oriented within the plane of the section must be taken into account. For instance, the length of a vessel sectioned (L) sectioned at an oblique angle (θ) in a given volume of tissue, may be represented by the following equation, $L = H/\cos\theta$, where H is the thickness of the volume of tissue. In comparison, the length of a vessel (Ln) sectioned transversely ($\theta = 0$) would be represented by the equation $Ln = H$ (recall $\cos 0 = 1$). Thus, the contribution of an arteriole sectioned at an oblique angle would vary depending on the size of that angle.

For each arteriolar profile a ratio (R) of long axis (maximum external diameter) to short axis (minimum external diameter) was calculated; this ratio accounts for the orientation angle of the arteriole. The quotient of the sum of these ratios to the area examined (A) provided the arteriolar length density.

$$Lc = (R_1 + R_2 + R_3 \ldots R_n)/A$$

Total arteriolar length in the left ventricles of each heart was determined using left ventricular volume estimates (LV mass/1.06 g/mm^3) and the corresponding average arteriolar length density.

4.2.5 Statistical Analysis

Data were analyzed using a two-way ANOVA with differences between group means determined using a Tukey HSD post hoc test. Differences in the frequency distribution graph were determined using Chi-square (χ^2) analysis. All differences between group means were considered statistically significant at $P<0.05$.

4.3 Results

4.3.1 Serum T_3 levels

Serum T_3 levels increased 18-fold in 12 day old (control: 0.8 nmol/L; hyperthyroid: 18.6 nmol/L) and 40-fold in 28 day old hyperthyroid rats (control: 1.4 nmol/L; hyperthyroid: 46.0 nmol/L) compared to age-matched controls indicating that these rats were hyperthyroid at the time of sacrifice. Serum T_3 levels were lower in 12 day old hypothyroid (0.5 nmol/L) compared to age-matched control rats, and almost undetectable in 28 day old hypothyroid (<0.01 nmol/L). According to these measurements, 28 day old rats exhibited definite hypothyroid levels of T_3 at the time of sacrifice. At 80 days of age (52 days after treatment was stopped), serum T_3 levels were comparable among the three groups (~ 1.0 nmol/L), indicating that neonatal hyper- and hypothyroid rats had returned to a euthyroid state. Similar changes in serum T_3 levels were noted in the previous study (Chapter 3).

4.3.2 Heart rate measurements

Changes in heart rate (Fig. 4.1) are comparable to those already described in Chapter 3 with one exception - 80 day old previously hyperthyroid rats in the present study did not have a significantly greater heart rate than 80 day old controls.

4.3.3 Day of eye opening

Notably, the day of eye opening differed among control (day 12), hyperthyroid (day 10), and hypothyroid rats (day 14). Since eye opening is considered an index of maturation, these results suggest that early neonatal hyperthyroidism hastens maturation, whereas the opposite was true for early neonatal hypothyroidism.

4.3.4 Body mass data

Disruption in thyroid hormone levels during the neonatal period appear to affect the normal increase in body mass associated with development (Fig. 4.2). The effect of altered neonatal thyroid conditions was most noticeable between day 28 and day 80, the period after treatment had stopped.

Body mass data for all groups are reported in Table 4.1. Both 12 day old hyper- and hypothyroid rats exhibited significantly lower body mass than age-matched controls ($P<0.05$) however, only 28 day old hypothyroid rats maintained significantly lower ($P<0.01$) body mass. The lower body mass in 12 day old hyperthyroid rats differs from the preceding study. This discrepancy may be due to biological variation,

Figure 4.1 Heart rate measurements in control (CON), hyperthyroid (HYPER), and hypothyroid (HYPO) rats after 12 and 28 days of treatment, and 52 days after treatment was stopped (day 80).There was a significant difference at $P<0.01$ between 12 and 28 days in both CON and HYPER, and between 28 day old HYPO and 80 day old previously HYPO. * $P<0.05$ *v.* CON; $^{\delta}$ $P<0.01$ *v.* HYPER. Results are presented as mean + SEM.

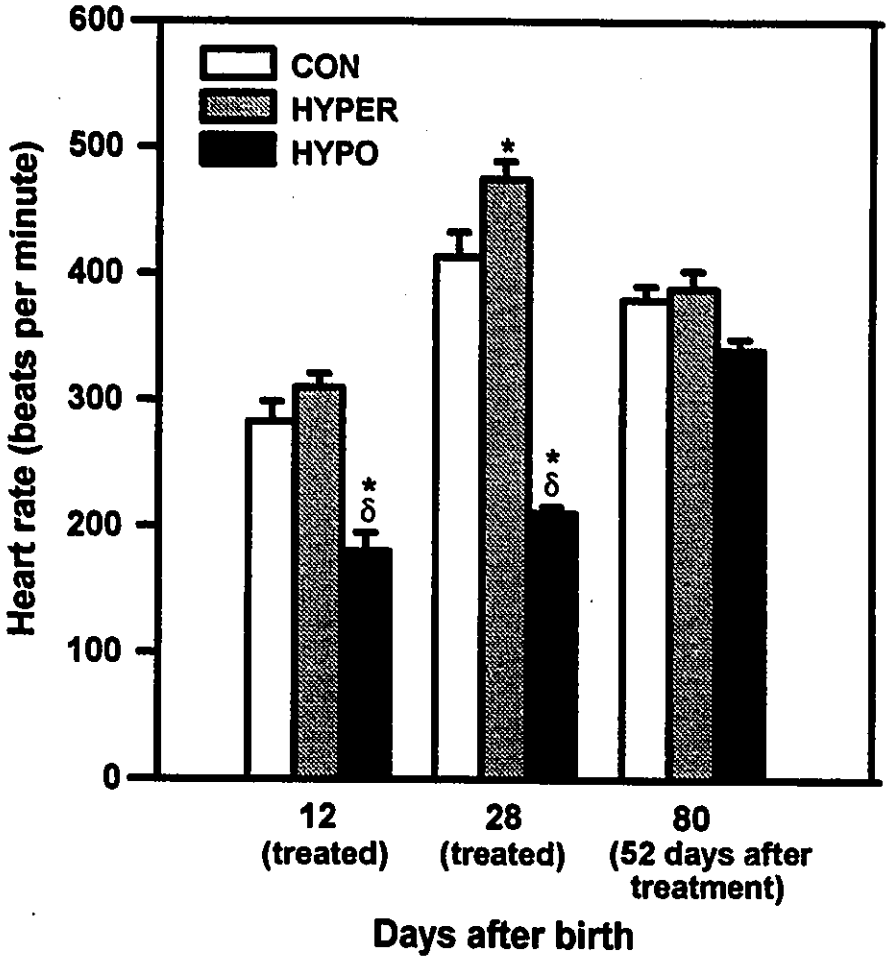
600
500
400
300
200
100
0
CON
HYPER
HYPO
Heart rate (beats per minute)
*
δ
*
δ
12
(treated)
28
(treated)
80
(52 days after
treatment)
Days after birth

Figure 4.2 Body mass changes associated with age in control (CON), hyperthyroid (HYPER), and hypothyroid (HYPO) from 1 to 80 days of age. Day of eye opening for each group: CON - day 12, HYPER - day 10, HYPO - day 14. The period of treatment is indicated at the bottom of the graph. Results are presented as mean ± SEM.

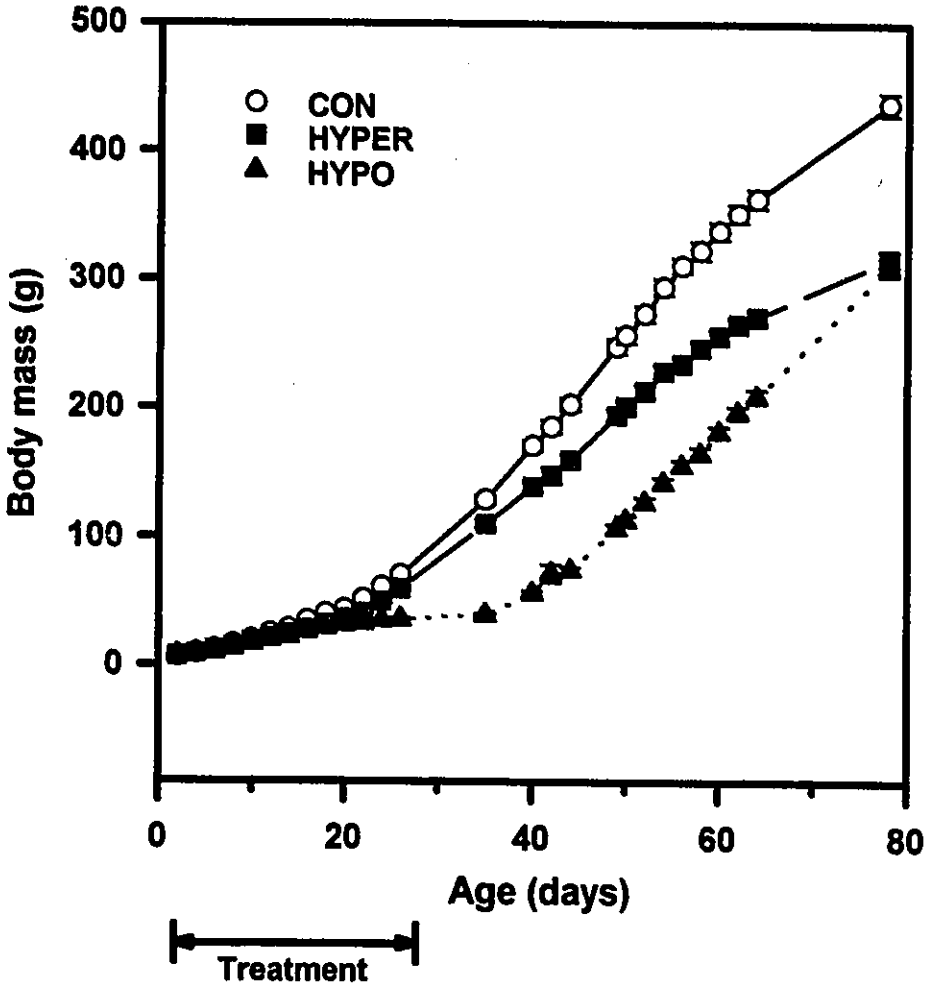
500
400
300
200
100
0
Body mass (g)
CON
HYPER
HYPO
0
20
40
60
80
Age (days)
Treatment

Table 4.1 **Body mass and heart mass data for 12 and 28 day old Control, Hyperthyroid, and Hypothyroid rats, and for rats 52 days after treatment was stopped (80 day old)**

Group	BM (g)	RV mass (mg)	LV + S mass (mg)	RV/LV ratio	HM:BM ratio (mg/g)
CON-12	27 ± 1	27 ± 1	104 ± 4	0.26 ± 0.02	4.8 ± 0.1
HYPER-12	22 ± 1[3]	32 ± 2	88 ± 4[3]	0.36 ± 0.01[5]	5.4 ± 0.1[3]
HYPO-12	22 ± 1[3]	21 ± 1[2]	68 ± 3[2,5]	0.31 ± 0.01	4.0 ± 0.2[5]
CON-28	90 ± 2	66 ± 2	262 ± 6	0.25 ± 0.01	3.6 ± 0.1
HYPER-28	87 ± 1	88 ± 5[1]	341 ± 10[1]	0.26 ± 0.02	4.9 ± 0.2
HYPO-28	34 ± 1[1,2]	18 ± 1[1,2]	90 ± 2[1,2]	0.20 ± 0.01[3,4]	3.1 ± 0.1[1,2]
CON-80	452 ± 10	205 ± 7	895 ± 30	0.23 ± 0.01	2.5 ± 0.1[5]
HYPER-EU-80	330 ± 10[1]	165 ± 7[1]	721 ± 22[1]	0.23 ± 0.01	2.7 ± 0.1[5]
HYPO-EU-80	243 ± 19[1,2]	140 ± 9[1]	548 ± 41[1,2]	0.26 ± 0.01[5]	2.9 ± 0.1

Values are mean ± SEM. CON-12, -28, -80: control at 12, 28, and 80 days; HYPER-12, -28: 12 and 28 day hyperthyroid; HYPO-12, -28: 12 and 28 day hypothyroid; (HYPER-EU)-80: previously hyperthyroid, 52 days after treatment stopped; (HYPO-EU)-80: previously hypothyroid, 52 days after treatment stopped; RV: right ventricle; LV: left ventricle; HM: heart mass; BM: body mass. All groups are significantly difference among 12, 28, and 80 day old rats for body mass, RV and LV mass data at $P<0.01$. [1] $P<0.01$ *v.* CON; [2] $P<0.01$ *v.* HYPER; [3] $P<0.05$ *v.* CON; [4] $P<0.05$ *v.* HYPER; [5] $P<0.01$ *v.* 12 and 28 day old.

as a different group of rats was used in the preceding chapter. Between day 12 and 28, body mass increased ($P<0.01$) 233% in control, 295% in hyperthyroid, and 50% in hypothyroid rats suggesting that hyperthyroidism hastened the rate of body growth during this period, while hypothyroidism slowed the rate. After cessation of treatment, the rate of body mass increase in 80 day old previously hyper- and previously hypothyroid rats was slower than control resulting in significantly lower BM at 80 days ($P<0.01$).

4.3.5 Heart mass data

Changes in heart mass for all groups are reported in Table 4.1. Neonatal hyperthyroidism resulted in significantly lower left ventricular (LV) mass at 12 days of age ($P<0.05$), but significantly greater LV mass at 28 days ($P<0.01$) compared to age-matched controls. Based on these observations it would appear that 11 days of T_3 treatment did not induced LV hypertrophy in the hyperthyroid group, but 27 days of T_3 treatment did. No difference was noted in right ventricular (RV) mass between 12 day old hyperthyroid and control rats, however in 28 day old hyperthyroid rats RV mass was markedly greater than age-matched ($P<0.01$). This differs from the preceding study in which both RV and LV mass were significantly greater in 12 day old hyperthyroid compared to control rats. These ventricular mass changes are also reflected in the RV/LV ratios. Twelve day old hyperthyroid rats had a significantly greater RV/LV ratio ($P<0.01$) than age-matched controls indicating a slower rate of

LV growth relative to right. Heart mass/body mass (HM/BM) ratios were significantly greater in 12 ($P<0.05$) but not 28 day old hyperthyroid rats relative to controls.

Changes in the RV and LV mass with hypothyroidism are comparable to those described previously (Chapter 3), though the magnitude of these changes are not identical between studies. Similarly, the changes in ventricular mass, observed 52 days after treatment was stopped, are comparable to those in the preceding study. Percent dry weight of the tissue was not significantly different among the 28 and 80 day old groups (data not shown).

4.3.6 Capillary numerical density, myocyte numerical density, and myocyte-to-capillary ratios

In control, capillary numerical density increased markedly ($P<0.01$) between day 12 and 28, then decreased significantly ($P<0.01$) after day 28 (Fig. 4.3). Notably, this differs from the changes in capillary numerical density described previously (Chapter 3) - capillary numerical density decreased between 12 and 28 days of age. Myocyte densities decreased significantly ($P<0.01$) with increasing age. These relative density changes are reflected in the corresponding myocyte-to-capillary ratios. A significant decrease ($P<0.01$) in this ratio is observed postnatally as the rate of capillary proliferation surpasses that of myocyte proliferation, reaching approximately adult values around day 28. Similar developmental changes were observed in the capillary and myocyte numerical densities, and myocyte-to-capillary ratio for both hyper- and hypothyroid rats, and after return to euthyroidism. Twenty-eight day old

Figure 4.3 (A) Capillary numerical density (number of capillaries per mm^2), (B) Myocyte numerical density (number of myocytes per mm^2) and (C) Myocyte-to-capillary ratios in the left ventricular myocardium of control (CON), hyperthyroid (HYPER), and hypothyroid (HYPO) rats at 12 and 28 days of age, and 52 days after treatment was stopped (80 days of age). All groups show a significant difference among 12, 28 and 80 day old rats for both capillary and myocyte numerical density data, at $P<0.01$. A significant difference was noted between 12 and 28 day old rats for the myocyte-to-capillary ratio data, at $P<0.01$. * $P<0.05$ v. CON and HYPER; $^{\delta}$ $P<0.01$ v. CON and HYPER. Results are presented as mean + SEM.

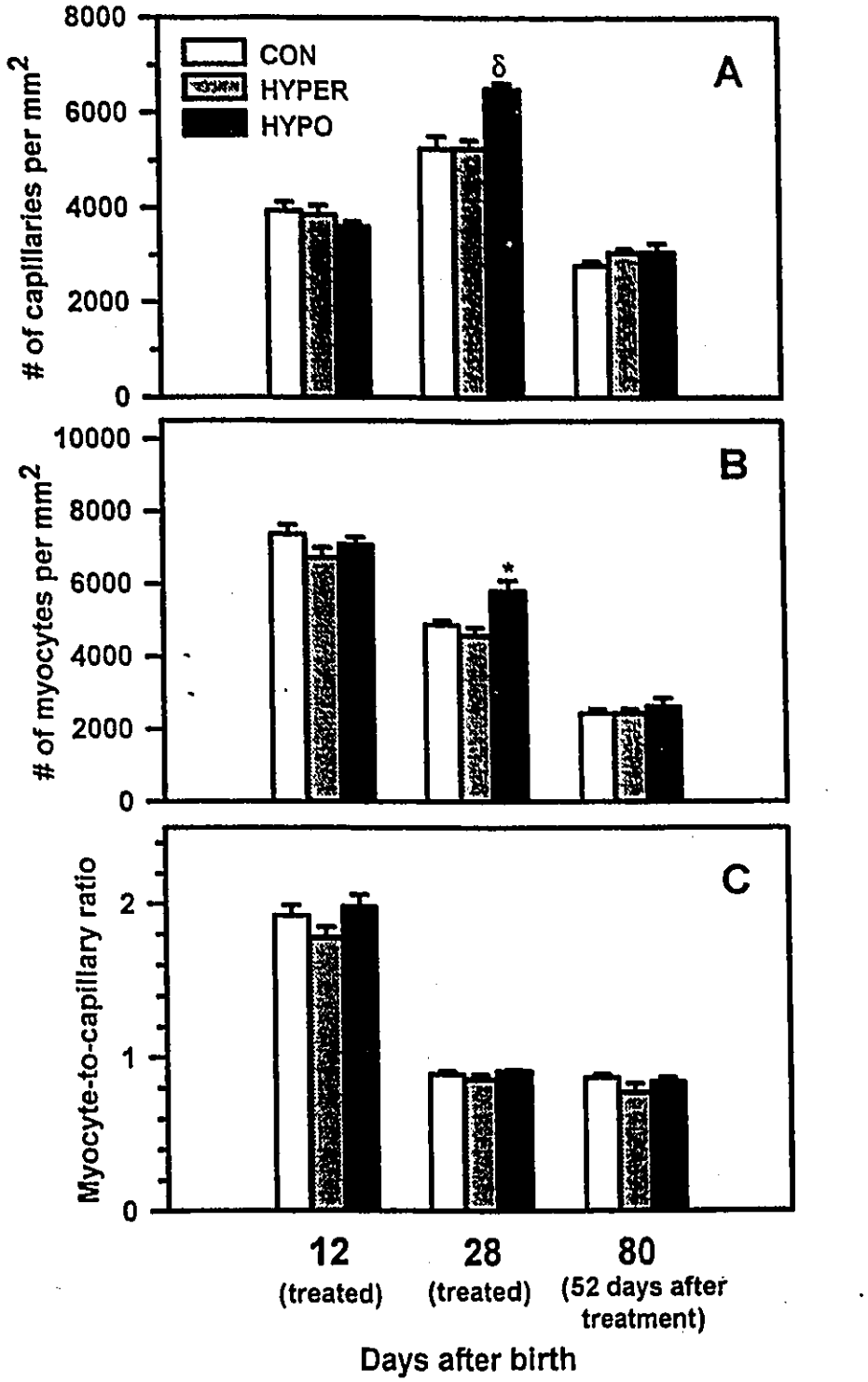
8000
6000
4000
2000
0
# of capillaries per mm2
CON
HYPER
HYPO
δ
A
10000
8000
6000
4000
2000
0
# of myocytes per mm2
*
B
2
1
0
Myocyte-to-capillary ratio
C
12
(treated)
28
(treated)
80
(52 days after treatment)
Days after birth

hypothyroid rats demonstrated a significant increase in capillary ($P<0.01$) and myocyte numerical densities ($P<0.05$) compared to age-matched controls suggesting the possible occurrence of both capillary and myocyte proliferation. This is different to the preceding study in which capillary numerical density in 28 day old hypothyroid rats was similar to control.

4.3.7 Arteriolar numerical density and total arteriolar length

Arteriolar numerical density increased postnatally ($P<0.01$) between 12 and 28 days of age in control, then subsequently decreased ($P<0.01$) between 28 and 80 days of age (Fig. 4.4). Neonatal hyper- and hypothyroidism did not dramatically alter this normal developmental pattern, but did affect absolute numerical density values. hypothyroid rats had a significantly lower arteriolar numerical density at 12 days of age compared to age-matched controls ($P<0.05$). In hyperthyroid rats, arteriolar numerical densities at 12 and 28 days of age were similar to age-matched control. At 80 days of age (52 days after treatment stopped), arteriolar numerical densities were comparable among the three groups.

In control rats, total arteriolar length increased ($P<0.01$) with increasing age (Fig. 4.5). However, in neonatal hyperthyroidism this developmental pattern was not maintained - large increase during the hyperthyroid period but no change in total arteriolar length was found between 28 and 80 days. Total arteriolar length in the left ventricle was significantly greater in 28 day old hyperthyroid ($P<0.05$), but was

Figure 4.4 Arteriolar numerical density (number of arterioles per mm^2) in the left ventricle of control (CON), hyperthyroid (HYPER) and hypothyroid (HYPO) at 12, 28, and 80 days of age (52 days after treatment was stopped). All groups show a significant difference among 12, 28 and 80 days for arteriolar numerical density, at $P<0.01$. * $P<0.05$ v. CON and HYPER. Results are presented as mean + SEM.

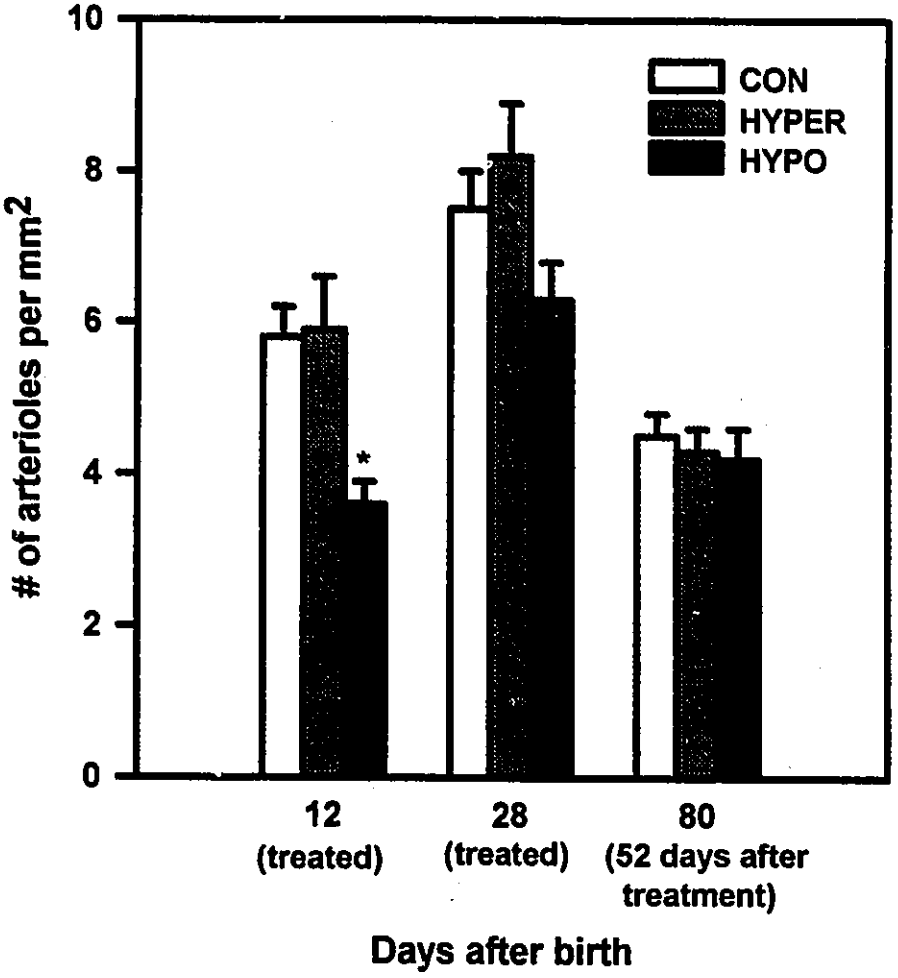
10
8
6
4
2
0
# of arterioles per mm2
CON
HYPER
HYPO
*
12
(treated)
28
(treated)
80
(52 days after
treatment)
Days after birth

Figure 4.5 Total arteriolar length in the left ventricle of hearts from control (CON), hyperthyroid (HYPER), and hypothyroid (HYPO) rats at 12 and 28 days of age, and 52 days after treatment was stopped (80 days of age). The treatment period is indicated at the bottom of the graph. A significant difference at $P<0.01$ was found among 12, 28, and 80 day CON rats, between 12 and 28 day old HYPER, and between 28 day old HYPO and 80 day old previously HYPO rats. * $P<0.05$ v. CON; $^{\delta}$ $P<0.01$ v. CON and HYPER. Results are presented as mean ± SEM.

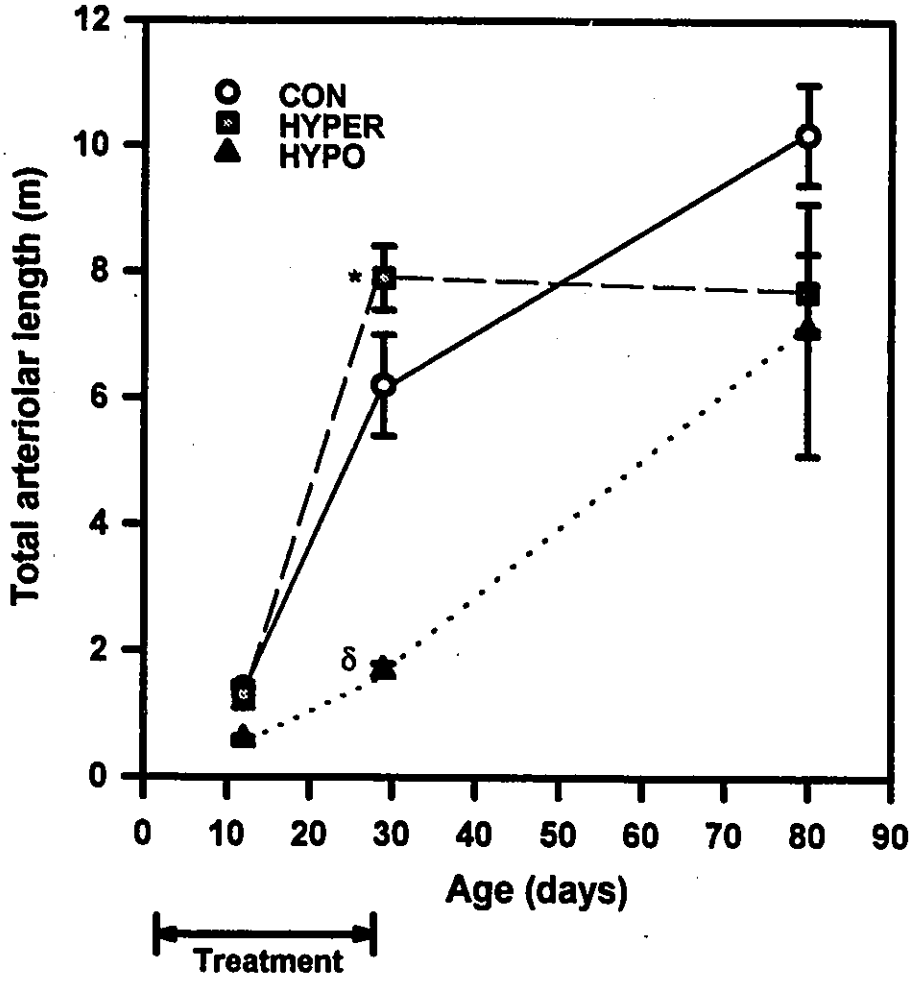
12
10
8
6
4
2
0
CON
HYPER
HYPO
Total arteriolar length (m)
*
δ
0
10
20
30
40
50
60
70
80
90
Age (days)
Treatment

significantly lower ($P<0.01$) in 28 day old hypothyroid rats compared to age-matched control. These results together with arteriolar numerical density results, suggest that neonatal hyperthyroidism stimulated arteriolar growth, whereas neonatal hypothyroidism attenuated arteriolar growth during the early postnatal period. At 80 days of age, total arteriolar length in the LV of previously hyper- and hypothyroid rats were not significantly different to control.

The number of capillaries per arteriole is relatively constant throughout development in control rats (Fig. 4.6), indicating proportional growth of the capillary and arteriolar beds. A similar pattern is observed in hyperthyroid rats suggesting that stimulated arteriolar growth in these hearts is matched by stimulated capillary growth. In hypothyroid rats a significantly greater number of capillaries per arteriole was noted at 12 ($P<0.01$) and 28 days of age ($P<0.05$) compared to controls, reflecting attenuation of arteriolar proliferation relative to capillary proliferation. After return to euthyroidism, the number of capillaries per arteriole was comparable among the three groups.

4.3.8 Arteriolar morphological measurements

No significant differences in any of the morphologic parameters examined (i.e average minimum external and internal diameter, average wall thickness, and length density) were found among the treatment groups at any age (Table 4.2). Developmentally, a significant decrease in average minimum external diameter and

Figure 4.6 Number of capillaries per arteriole in the left ventricle of control (CON), hyperthyroid (HYPER) and hypothyroid (HYPO) rats at 12 and 28 days of age, and 52 days after treatment was stopped (80 days of age). 28 day old HYPO is significantly different from 80 day old previously HYPO at $P<0.01$. * $P<0.05$ v. CON and HYPER; $^{\delta}$ $P<0.01$ v. CON and HYPER. Results are presented as mean + SEM.

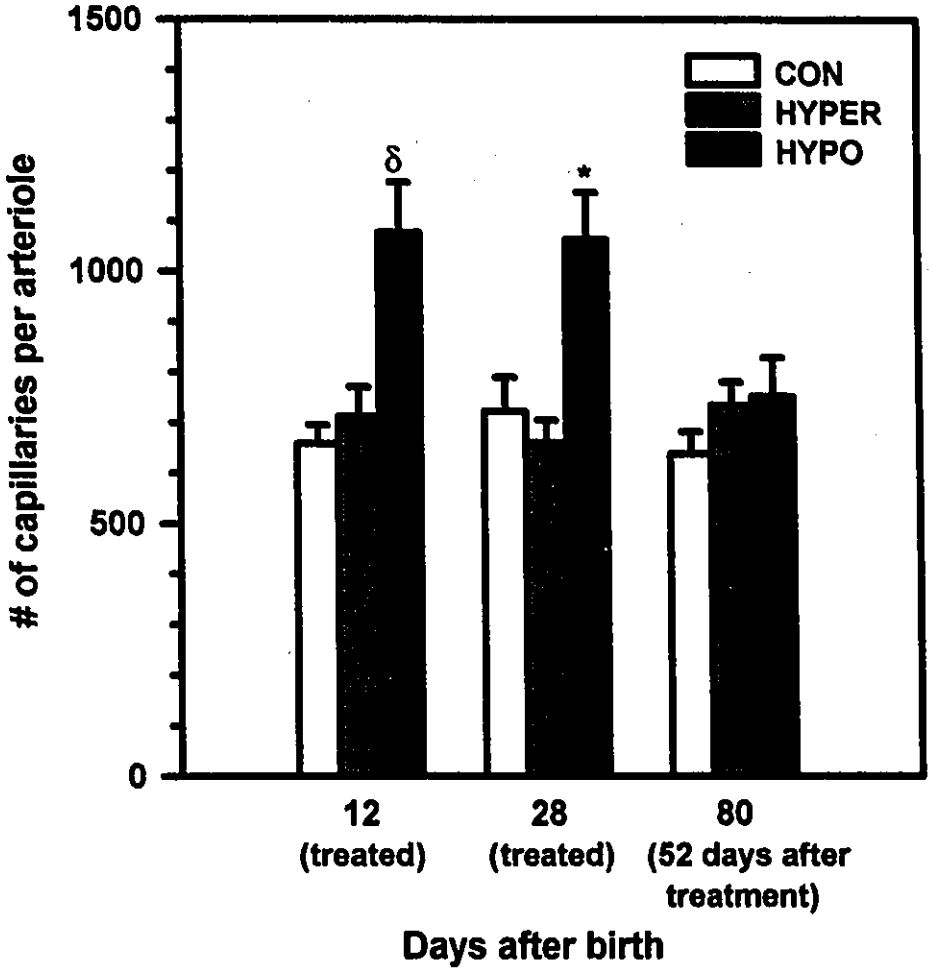
1500
1000
500
0
# of capillaries per arteriole
CON
HYPER
HYPO
δ
*
12
(treated)
28
(treated)
80
(52 days after
treatment)
Days after birth

Table 4.2 **Arteriolar measurements for 12 and 28 day old Control, Hyperthyroid, and Hypothyroid rats and in rats 52 days after treatment was stopped (80 day old)**

Group	Minimum External diameter (μm)	Internal diameter (μm)	Average wall thickness (μm)	Length density (mm/mm^3)
CON-12	17.0 ± 0.5	8.0 ± 0.3	4.2 ± 0.1	13 ± 1
HYPER-12	16.9 ± 0.5	7.9 ± 0.2	4.5 ± 0.2	14 ± 2
HYPO-12	18.1 ± 0.3	8.8 ± 0.2	4.7 ± 0.2	19 ± 2
CON-28	14.4 ± 0.6[1]	6.6 ± 0.2[1]	3.9 ± 0.2	23 ± 3[1]
HYPER-28	15.1 ± 0.5[1]	6.6 ± 0.3[1]	4.3 ± 0.2	23 ± 1[1]
HYPO-28	15.3 ± 0.6[1]	6.3 ± 0.2[1]	4.5 ± 0.2	18 ± 1
CON-80	16.3 ± 0.7	8.2 ± 0.6[2]	4.1 ± 0.3	11 ± 1[2]
HYPER-EU-80	16.1 ± 0.5	8.0 ± 0.3[2]	4.1 ± 0.3	11 ± 1[2]
HYPO-EU-80	15.0 ± 0.7	7.8 ± 0.3[2]	3.5 ± 0.3	12 ± 2[2]

Values are mean ± SEM. CON-12, CON-28, CON-80: 12, 28, and 80 day old control rats; HYPER-12, HYPER-28: 12 and 28 day old hyperthyroid rats; HYPO-12, HYPO-28: 12 and 28 day old hypothyroid rats; HYPER-EU-80: 80 day old previously hyperthyroid rats (52 days after treatment stopped); HYPO-EU-80: 80 day old previously hypothyroid rats (52 days after treatment stopped). [1] $P<0.01$ *v.* 12 day old; [2] $P<0.05$ *v.* 28 day old.

average internal diameter was observed between 12 and 28 days in all groups ($P<0.01$). Thereafter, an increase in average internal diameter was observed ($P<0.05$). With respect to arteriolar length density, a significant increase was noted between 12 and 28 days in control ($P<0.01$), followed by a significant decrease to approximately 12 day old values, between 28 and 80 days ($P<0.05$). A similar developmental pattern was observed in hyperthyroid rats. However, in hypothyroid rats no significant difference in length density was found between 12 and 28 days supporting the postulate of slowed arteriolar growth. No significant changes in arteriolar wall thickness with age were noted in any of the groups.

Since the average values determined for these parameters could have resulted from different changes in the arteriolar population within each experimental groups, we examined the relative frequency of arteriolar sizes (Fig. 4.7). Changes in the arteriolar population at each age are reflected in the general shape of the distribution graph. A significant difference in the overall frequency distributions was observed among all groups at 12, 28, and 80 days of age ($P<0.01$).

The distribution pattern was similar among the different groups at comparable ages. In controls there was an increase in the percentage of smallest arterioles between 12 and 28 days ($P<0.01$) reflecting numerical growth of the smallest arterioles, followed by a decrease in the frequency of this same population and a shift towards larger arterioles at 80 days of age ($P<0.01$), reflecting maturation of the arteriolar bed. A similar distribution pattern was evident in hyper- but not

Figure 4.7 Frequency distribution of left ventricular coronary arterioles as a function of the log of the minimum external diameter for control (CON), hyperthyroid (HYPER), and hypothyroid (HYPO) rats at 12 and 28 days of age, and 52 days after treatment was stopped (80 days of age). All groups are significantly different in their frequency distribution, among 12, 28, and 80 day old rats, at $P<0.01$. Results are presented as percentages.

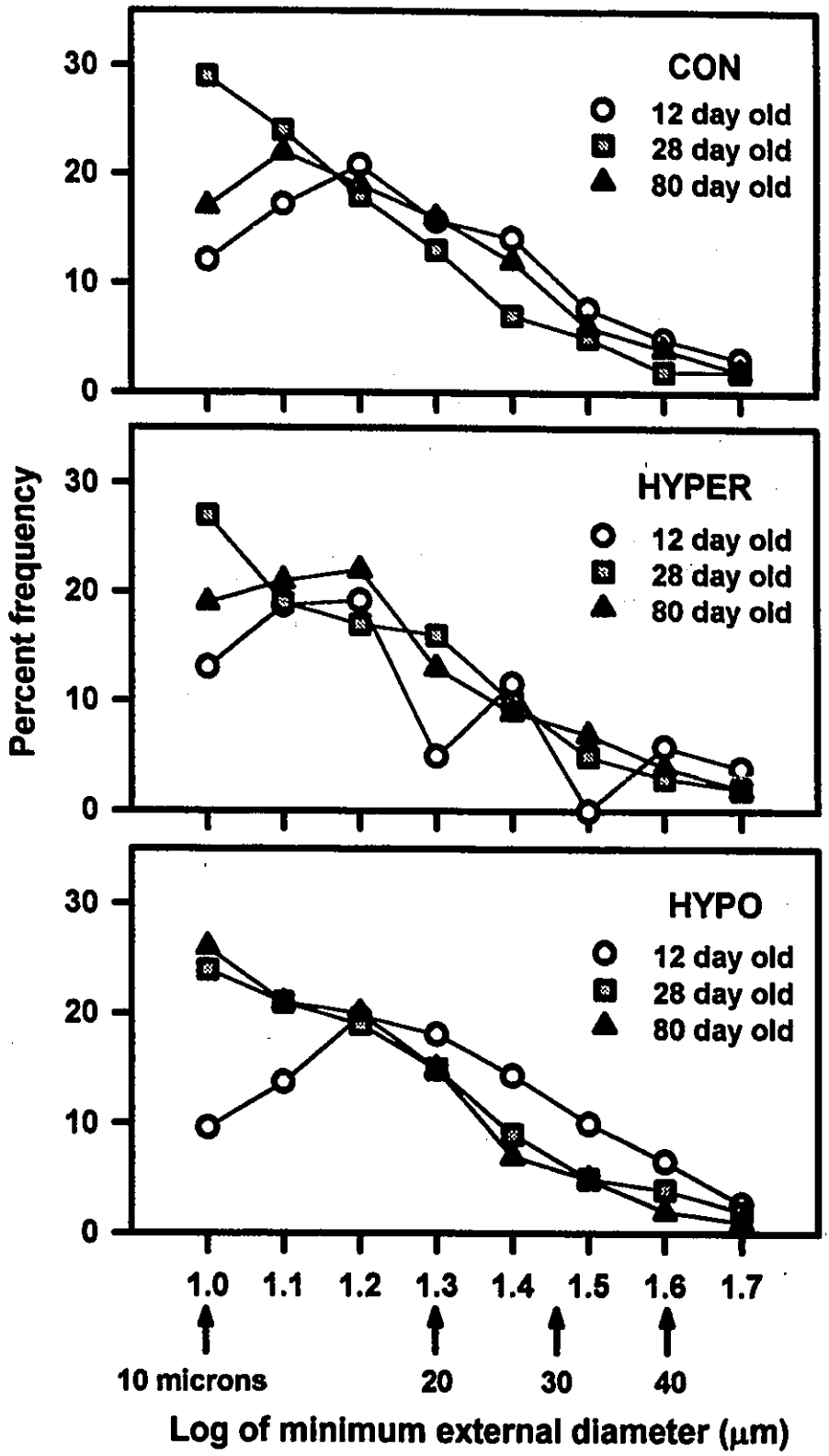
CON
12 day old
28 day old
80 day old
HYPER
12 day old
28 day old
80 day old
HYPO
12 day old
28 day old
80 day old
Percent frequency
30
20
10
0
1.0
1.1
1.2
1.3
1.4
1.5
1.6
1.7
10 microns
20
30
40
Log of minimum external diameter (μm)

hypothyroid rats: the decrease in frequency of smallest arterioles and shift towards larger arterioles was not evident between 28 and 80 days.

4.4 Discussion

Body growth and cardiac development

The results of the present study correspond with reports in the literature, suggesting that neonatal hypothyroidism slows the rate of maturation (Liu et al., 1994; Moussavi et al., 1985) and neonatal hyperthyroidism accelerates the rate of maturation (e.g. Kolar et al., 1992). Delayed eye opening in neonatal hypothyroid rats supports this hypothesis. In this study the body mass of 28 day old neonatal hypothyroid rats was comparable to that of 11 day old control rats. In comparison neonatal hyperthyroidism appeared to hasten the rate of maturation. Observations made during the treatment period: early eye-opening, facilitated fur and ear growth, and better neuromuscular coordination - support this claim. Similar observations were also made in the preceding study (Chapter 3).

As the overall changes in heart mass among the groups, both during and after treatment, were comparable to those of the previous study the reader is referred to the relevant portions of this discussion for comparison of our results with those reported in the literature. Notably, only the heart mass changes in 12 day old hyperthyroid rats were in disagreement. Based on the results in this study it would appear that the hypertrophic affects of excess thyroid hormone were not yet manifest in the heart.

According to serum T_3 analysis and heart rate changes these rats were hyperthyroid, ruling out the possibility that the injections were ineffective as far as inducing a hyperthyroid state. Other than the effect of natural biological variation no other explanations can be provided at this time.

Coronary microvascular geometry

The effect of neonatal hyper- and hypothyroidism was more apparent on the developing arteriolar network than on the developing capillary network. Neonatal hyperthyroidism stimulated arteriolar and capillary proliferation agreeing with findings in adult (Chilian et al., 1985; Tomanek et al., 1995; Wachtlova et al., 1985 - examined capillaries only) and pigs (Breisch et al., 1989). On the other hand, neonatal hypothyroidism markedly attenuated arteriolar proliferation but did not appear to attenuate capillary growth. Attenuated arteriolar growth was not observed in adult hypothyroid rats (Tomanek et al., 1993). Coronary capillary growth was found in adult (Chapter 2) hypo- and hyperthyroid rats from the preceding studies. However, in the previous neonatal study capillary growth was believed to be attenuated with regard to the formation of new capillary branches or connections and less with respect to the elongation of capillary segments. Capillary segment lengths would need to be measured in the present study in order for a complete comparison to be made between studies. At this point, it may be stated that the affect of neonatal hypothyroidism on coronary capillaries is variable. The possible reasons for this variability are discussed

in Chapter 5 (General Discussion).

Long-term effects of neonatal hyper- and hypothyroidism

Following discontinuation of treatment, increased cardiac mass, decreased arteriolar numerical density, and maintenance of total arteriolar length found in previously hyperthyroid rats indicate that no arteriolar growth occurred after the period of hyperthyroidism. On the other hand, changes in these same parameters suggest that compensatory arteriolar growth occurred after the period of hypothyroidism. It thus appears that enhanced maturation by neonatal hyperthyroidism, may hasten the period of postnatal arteriolar proliferation and once this stimulus is removed subsequent arteriolar growth is minimal. Neonatal hypothyroidism delays maturation, thereby slowing the period of arteriolar proliferation and possibly not compromising compensatory arteriolar growth.

Changes in arteriolar frequency distributions, during development in control rats, were similar to those observed in humans (Rakusan et al., 1994b). Larger arteriolar branches are formed early, possibly already present at birth, while smaller arterioles continue to proliferate postnatally. With age formation of new arterioles declines, the vascular bed continues to mature, arterioles increase in size and the relative frequency of larger arterioles increases. Neonatal hyperthyroidism did not appreciably affect this developmental pattern even after return to euthyroidism. The persistence of a large number of smaller arterioles and no apparent corresponding shift

towards larger arterioles in 80 day old previously hypothyroid rats, likely reflects delayed maturation and compensatory arteriolar growth.

Constant arteriolar wall thickness despite increasing age agrees with other studies in mammals (Rakusan and Nagai, 1994; Tomanek et al., 1995). A constant wall thickness suggests that abnormal smooth muscle cell hypertrophy (resulting in thicker walls) or atrophy (resulting in thinner walls) was not induced by either neonatal thyroid condition. In comparison, a thickening of arteriolar walls has been associated with hypertension in senescent rats (Rakusan and Wicker, 1990; Tomanek, 1990; Vitullo et al., 1993). Length density estimates in 80 day old rats from our study, were between those of Anversa and co-workers (1991) in one year old rats, and Tomanek and co-workers (1991) in 5 month old rats, though closer to the latter study. The lack of significant changes in morphological parameters with treatment suggests that the effect of altered thyroid hormone levels on arteriolar growth occurs primarily by indirect mechanisms, as one would expect changes in arteriolar wall morphology by the direct effect of thyroid hormones on vascular smooth muscle cells.

Summary

This study represents the first time that the response of the developing coronary arteriolar network to neonatal hypothyroidism or hyperthyroidism has been morphometrically analyzed in rats. The results of this study indicate that thyroid hormones play an important regulatory role in development of the arteriolar network

during the neonatal period. Neonatal hypothyroidism, which delayed maturation, markedly attenuated cardiac and arteriolar growth. On the other hand, neonatal hyperthyroidism, which hastened maturation, stimulated capillary and arteriolar growth in parallel with the increase in cardiac mass. Notably, both neonatal conditions induced long-term changes in cardiac growth and arteriolar geometry - neonatal hyperthyroidism, by hastening maturation of the arteriolar bed, markedly limited subsequent arteriolar growth, and neonatal hypothyroidism, by delaying maturation did not appreciably compromise subsequent arteriolar growth. The plasticity of arterioles and their sensitivity to atrophic or hypertrophic influences arising during the neonatal period, was evident. Interestingly, plasticity of the arteriolar network has also been observed during the normal aging process (Rakusan and Nagai, 1994).

CHAPTER 5

GENERAL DISCUSSION

The response of the coronary microvasculature to adult- or neonatal-onset hyperthyroidism or hypothyroidism was studied, using comprehensive morphometric methods, in order to gain insight into: (1) whether the response of the coronary capillary network to adult-onset hyper- or hypothyroidism preserves the geometrical conditions for oxygen supply to the hypertrophied or atrophied myocardium; (2) how neonatal hyper- or hypothyroidism influences the developing coronary microvasculature; and (3) whether geometrical changes in the coronary microvasculature, induced by either neonatal thyroid condition, persist after re-establishment of euthyroidism.

The first portion of this chapter focuses on the implications of our principal findings as they relate to the geometrical conditions for myocardial oxygenation in the neonatal and adult heart. In the second portion, the general mechanisms of angiogenesis during normal development and as it is influenced by accelerated (hyperthyroidism) or retarded (hypothyroidism) maturation will be considered.

Coronary capillary geometry in adult-onset hyperthyroidism and hypothyroidism

In both adult-onset hyperthyroidism and hypothyroidism the geometrical conditions for myocardial oxygenation were maintained or even improved. In adult hypothyroidism, capillary numerical density increased and capillary domain areas in

both regions of the capillary network decreased; the heterogeneity in capillary spacing was unchanged. Capillary segment lengths and the volume of tissue supplied by a capillary segment (i.e. capillary supply unit volume) decreased. Based strictly on these changes it appears that the geometrical conditions for oxygen diffusion and supply within the myocardium were improved. Considering the reduced cardiac workload and decreased myocardial oxygen consumption associated with hypothyroidism (Beznak, 1963; reviewed in Morkin et al., 1983), it is even more likely that myocardial oxygenation was, in the very least, maintained if not improved.

In adult hyperthyroidism, capillary numerical density and the heterogeneity of capillary spacing was maintained despite the increased cardiac mass. Domain areas in proximal regions of the capillary bed were decreased, whereas in distal regions their size was maintained. These results suggest that the geometrical conditions for oxygen diffusion within tissue cross-sections, were improved in proximal and maintained in distal regions. On their own, improved geometrical conditions for oxygen supply in proximal regions seem surprising if one considers that PO_2 is higher in this portion of the capillary network. In fact, it has recently been shown that in low-flow ischemia areas of hypoxic tissue are found primarily in the distal portions of the capillary bed (Vetterlein et al., 1995). Capillary segment lengths decreased throughout the capillary network though segment lengths were longer in proximal than in distal portions. One may speculate that a greater reduction in proximal capillary domains is a way of compensating for longer proximal segment lengths.

In thyroid hormone induced cardiac hypertrophy changes in microvascular geometry within cross-sections were accompanied by alterations along the longitudinal axis, which together maintained the capillary supply unit volume in both regions of the capillary bed. In light of an increased coronary blood flow (Breish et al., 1989; Weiss and Grover, 1987; Weiss and Tse, 1995) conservation of the volume of tissue supplied by a capillary segment maintains the geometrical conditions for myocardial oxygen supply. One may speculate that the response of the coronary capillary network in adult-onset hyperthyroidism, is directed towards maintaining a normal optimal tissue supply volume throughout the capillary bed.

A close relationship between the capillary supply unit and myocyte volumes was noted in both hypo- and hyperthyroid adult hearts. This same association was also observed in hearts from adult SHR and nifedipine-treated adult SHR (Rakusan et al., 1994c) and during normal development (Rakusan et al., 1994b). Though the significance of this relationship is not understood it does suggest the possibility that myocardial oxygen supply may be regulated at the level of an individual myocyte, and as a consequence quantitative changes in cardiac myocytes may be closely coupled to changes in the capillary network. Based on this premise a possible mechanism for regulating capillary geometry may be proposed: under normal conditions, for a given capillary segment length a critical tissue supply volume would exist beyond which adequate oxygen supply would be compromised. An increase in the volume of cardiac myocytes beyond this critical volume, either due to cardiac hypertrophy or

postnatal growth, would evoke a signal from either the myocyte or endothelial cells that would stimulate a growth response in the capillary network. The capillaries would adapt so as to return the volume of tissue supplied to an optimal level.

Coronary capillary geometry in neonatal-onset hyperthyroidism and hypothyroidism

In general coronary capillary geometry, as assessed by capillary numerical density and segment lengths, was maintained in both neonatal-onset hyper- and hypothyroidism. Even though capillary numerical density results were not always in agreement between the two neonatal studies (c.f. Chapter 3 and 4), it may be said that the geometrical conditions for oxygen diffusion were never impaired with either neonatal hyper- or hypothyroidism, that is, capillary numerical density never decreased. For both neonatal thyroid conditions, capillary segment lengths in both regions of the capillary bed were comparable to those in normal hearts. As capillary domain areas could not be determined for proximal and distal capillaries, the capillary supply unit volumes for proximal and distal capillary segments could likewise not be determined. Though it would be convenient to assume that since the capillary numerical density and segment lengths were similar to normal capillary supply unit volumes would also be similar to normal, this would not be correct. For instance, in adult hyperthyroid hearts capillary numerical density was found to be similar to control yet the domain area for proximal capillaries was smaller than control. Thus, being able to evaluate the geometry in both regions of the capillary network is

important for a complete appreciation of its potential consequences on myocardial oxygenation.

Though a rigid comparison cannot be made between the data from adult and neonatal studies, one may propose that the overall response of the coronary capillary network to hyper- or hypothyroidism is primarily directed towards preserving the geometrical conditions for adequate myocardial oxygenation in both young and adult hearts.

Factors involved in the observed microvascular growth response

The fact that capillary growth was induced in both adult hyper- and hypothyroid rats suggests that a common mechanism must be responsible. Many different types of stimuli are known to promote capillary angiogenesis. Metabolic factors, such as hypoxia, low pH, and increased lactate concentration have been considered stimuli for capillary growth (please see review by Hudlicka, et al., 1992), especially during wound healing (Knighton et al., 1981). In hyperthyroidism the increased work of the heart (Beznak, 1962) and myocardial oxygen consumption (Talafih et al., 1983, 1984; Weiss and Tse, 1995) predispose the myocardium to hypoxia especially in distal portions of the capillary network. However, in hypothyroidism the work of the heart and myocardial oxygen consumption are reduced (Beznak, 1963; reviewed in Morkin et al., 1983), thus the likelihood of hypoxia is small.

The direct effect of thyroid hormones may be another stimulus for capillary growth. In this case, one would expect enhanced capillary growth with hyperthyroidism, but reduced capillary growth in hearts of hypothyroid rats. This may be a reasonable explanation for the observed changes in neonatal rats but would not explain the response in adults.

The direct effect of growth-regulating factors, in particular angiotensin II (AII), is another possible explanation for the stimulated capillary proliferation in both adult hyperthyroid and hypothyroid rats. Angiotensin II is an important factor for normal postnatal cardiac growth (Beinlich et al., 1991) and may on its own stimulate capillary growth. Plasma levels of AII have been shown to increase with hyperthyroidism and decrease with hypothyroidism (Marchant et al., 1993). Thus, increased AII levels in hyperthyroid rats would stimulate capillary proliferation. Similarly, decreased levels of AII have also been implicated in stimulating capillary growth. Studies examining treatment of myocardial infarction with ACE inhibitors (Canby and Tomanek, 1989; Unger et al., 1992) or the AT_1 receptor antagonist losartan, which mimics the condition of low circulating AII levels but does not produce increased bradykinin levels, (Schieffer et al., 1994; Sladek et al., 1996), have reported capillary proliferation. Results of these studies and those of Marchant and co-workers (1993) would suggest that the low AII levels induced by hypothyroidism would also stimulate capillary growth.

One can not rule out the involvement of other growth factors (e.g. VEGF,

PDGF, TGF-β, bFGF, IGF-I, etc.) in stimulating capillary growth, however not all of these factors have been characterized with respect to changes in their levels during hyper- or hypothyroidism. For instance, IGF-I mRNA levels have been shown to decrease in the absence of thyroid hormones and increase in thyroid hormone treated hypophysectomized neonatal rats (Kupfer and Rubin, 1992).

Another likely stimulus for capillary proliferation in adult-onset hyper- and hypothyroidism is an increase in the mechanical forces acting on the microvascular wall. In hyperthyroidism, increased mechanical stress arises from an increase in myocardial blood flow (Talafih et al., 1983, 1984) and possibly from increased blood viscosity (Kossler et al., 1987). In hypothyroidism, resultant bradycardia prolongs the diastolic period. As coronary blood flow occurs principally during diastole, a longer diastolic period increases the time during which shear stress and stretch act on the vascular endothelium (Wright and Hudlicka, 1981; Hudlicka et al., 1988; Tomanek et al., 1993). Increased plasma viscosity resulting from hypothyroidism (Kossler et al, 1987) may also contribute to this increased mechanical stress.

Mechanical factors may also be implicated as playing a role in the response elicited by the developing coronary capillary network to altered neonatal thyroid status. This explanation is in accordance with the observed capillary changes in hyperthyroid rats. However, in hypothyroid rats the variability in the observed response is greater than would be expected if mechanical stimulus on its own influenced the capillary growth response. The inconsistency in capillary response in

neonatal hypothyroid rats, while probably having to do in part with biological variation, may reflect the interaction of many factors which affect capillary growth. For instance, in neonatal hypothyroidism it may be proposed that decreased thyroid hormone levels may directly or indirectly attenuate capillary growth. However, as mechanical factors may at the same time be providing a stimulus for capillary growth, the overall capillary response may be a result of these influences, and as such would be variable. In the case of neonatal hyperthyroidism, both the excess in thyroid hormones and mechanical factors stimulate capillary growth, and therefore a consistent growth response is noted.

The direct effect of thyroid hormones on expression levels of growth factors and hormones, which are involved in vascular smooth muscle cell proliferation and differentiation is the most likely explanation for the observed changes in arteriolar growth. During the early postnatal period, growth of arterioles may depend on the normal expression of specific growth factors. Increases or decreases in the expression of these factors resulting from neonatal hyper- or hypothyroidism may thus enhance or attenuate arteriolar growth. For example, angiotensin II (AII) is known to stimulate expression of many proto-oncogenes and growth factors within cultured vascular smooth muscle cells (Dzau, 1993). Depending on the interaction of these expressed growth factors, AII can stimulate smooth muscle cell hyperplasia (Gibbons et al., 1992). In postnatal development, plasma ACE levels are regulated by thyroid hormones (Costerousse et al., 1994). Consequently, neonatal hyperthyroidism would

increase plasma ACE levels and likely AII levels. An increase in plasma AII may enhance growth factor expression within smooth muscle cells resulting in AII promotion of vascular smooth muscle cell hyperplasia and ultimately arteriolar proliferation. The converse scenario may be proposed for neonatal hypothyroidism.

To date, studies assessing the postnatal growth of the microvasculature have expressed these changes as a function of age and rate of heart growth. However, closely related to an increase in age and development is the process of maturation. Maturation involves a series of changes through which a young organism must pass, as it approaches the adult phenotype. During normal postnatal development it is difficult to dissociate the effect due to rate of cardiac growth or to maturation. Results from the model of altered neonatal thyroid hormone status suggested that the observed decline in capillary proliferation may depend more on maturation than rate of cardiac growth. Furthermore, it was apparent that accelerated or attenuated maturation can induce long-term changes in subsequent arteriolar and cardiac growth and probably even in heart function.

One possible mechanism which may contribute to the decline in capillary proliferation involves the development or establishment of cardiac sympathetic innervation. Establishment of the sympathetic innervation in the heart during early postnatal development is a normal process of maturation that is independent of the rate of cardiac growth. Sympathetic innervation has been associated with the inhibition, either directly or indirectly, of coronary capillary proliferation (Tomanek,

1989). Based on this, it may be suggested that establishment of sympathetic innervation would be enhanced with neonatal hyperthyroidism and thus, the decline or cessation of capillary proliferation would be accelerated. With neonatal hypothyroidism likely the establishment of sympathetic innervation would be attenuated resulting in a delay in the decline in capillary proliferation.

Long-term effects of altered neonatal thyroid status

Associated with the maturation of cardiac tissue, is a coordinated series of changes in the expression of certain enzymes, growth-regulating factors, and hormones. The discrete developmental pattern of changes in expression levels of these substances with time has been associated with specific processes during cardiac development (for review please see MacLellan et al., 1993). Long-term changes may result after introduction of a stimulus which alters the normal expression pattern of growth-regulating factors. Both neonatal hyper- and hypothyroidism resulted in a long-term deficit in left ventricular growth.

It has been proposed that the normal surge in thyroid hormones, which occurs approximately during the second postnatal week (Samels, 1967) and is temporally associated with transition from cardiac myocyte hyperplasia to hypertrophy, is accelerated with neonatal hyperthyroidism (Gerdes et al., 1983; Dubeck et al., 1989). After return to euthyroidism, the number of myocytes in hearts from previously hyperthyroid rats remained reduced (Gerdes et al., 1983). Thus, it may be that the

smaller number of myocytes are not capable of producing the same increase in cardiac mass compared to normal hearts and this may provide an explanation for the reduced heart mass observed in previously hyperthyroid rats (Chapter 3 and 4). With neonatal hypothyroidism, slowing of the cardiac growth rate and decreases in the level of important growth-regulating factors, such as somatotropin, may also have potentially reduced the number of cardiac myocytes in these hearts.

Long-term positive chronotropic and inotropic effects were noted in the hearts of previously hyperthyroid rats. The explanation of these observations is unclear and many possible mechanisms may be taken into account. Thyroid hormones are known to induce a variety of direct effects on cardiac muscle as well as influence heart function indirectly, e.g. via effects on peripheral circulation or interaction with the adrenergic nervous system (Polikar et al., 1993). However, these changes have been shown to return to normal after stopping treatment, at least in adult animals (Cihak et al., 1992).

As in adults, excess thyroid hormone during the neonatal period induces positive chronotropic and inotropic effects on the heart that are associated for example, with altered calcium transport by cardiac membranes (Kolar et al., 1992; Wibo et al., 1995) and changes at the level of the contractile apparatus (Chizzonite and Zak, 1984; Dieckman and Solaro, 1990). It is unknown whether these changes are reversible as those induced during adulthood. One may even speculate that at the time these rats were examined (i.e. 52 days after stopping treatment), some of the

changes induced during the neonatal period may not have been completely reversed. An alternative explanation for these findings may be an increased sensitivity of these rats to the anaesthetic used. To the best of our knowledge however, no other studies in hyperthyroid rats have reported any anomalous responses to anaesthesia.

A similar scenario to the one proposed for long-term effects on heart mass may be advanced for the long-term 'inhibitory' effect of neonatal hyperthyroidism on subsequent arteriolar growth. The period of neonatal arteriolar growth is accelerated due to hyperthyroidism however, arteriolar growth is not compromised during this time because hyperthyroidism also increases the expression levels of important vascular smooth muscle cell growth-regulating factors (see previous discussion). However, it is possible that the accelerated maturation may have hastened a critical developmental process (e.g. transition from smooth muscle cell hyperplasia to hypertrophy; prematurely induced the expression of a growth factor, etc.), which results in the lack of subsequent arteriolar growth. For example, down-regulation of mRNA for AT_1 receptors on vascular smooth muscle cells in culture has been shown to occur when these cells are exposed to epidermal growth factor, basic fibroblast growth factor, or platelet-derived growth factor-BB (Nickenig and Murphy, 1994). Plasma thyroid hormone levels, either directly or indirectly, may influence the expression of any one of these growth factors during early postnatal development. If this is true then one may speculate that during the period of hyperthyroidism, even though AT_1 receptors may be affected, ACE activity and angiotensinogen levels would

be higher (Marchant et al., 1993; Michel et al., 1994) and ultimately arteriolar growth would not be compromised. However, when euthyroidism is re-established the changes in receptor expression may persist, yet ACE activity and angiotensinogen levels would no longer be increased, ultimately resulting in the inhibition of subsequent arteriolar growth. A summary of these principal findings and the primary conclusions which were reached may be found in the following section.

SUMMARY

Previous studies have shown that the response of the microvasculature to a hypertrophic stimulus depends on the age at which that stimulus is introduced, as well as the nature of the stimulus itself. The magnitude of changes in the microvascular geometry, in relation to the associated changes in cardiac myocytes, determines the maintenance or impairment of adequate myocardial oxygen supply. The research presented in this dissertation focused on the quantitative assessment of the coronary microvascular response to hypothyroidism and hyperthyroidism, induced during two characteristically different stages of development - the neonatal period and adulthood.

In the first part of this work, changes in coronary capillary geometry induced by adult-onset hyper- or hypothyroidism were examined using more advanced morphometric methods, in combination with a unique histochemical stain (Alkaline phosphatase/Dipeptidyl peptidase IV), which distinguished between proximal and distal regions of the capillary network. This approach enabled the comprehensive evaluation of capillary geometry in two regions of the capillary network having different oxygen supply conditions. In addition, a new immunohistochemical method for the detection of Proliferating Cell Nuclear Antigen (PCNA) protein expression, was used for the first time in cardiac tissue, for the direct identification of proliferating endothelial, myocyte, or other cell types.

Adult-onset hyperthyroidism stimulated capillary growth in proportion to the resultant cardiomegaly. This capillary growth served to preserve the geometrical

conditions for adequate myocardial oxygen supply throughout the capillary network. Capillary numerical density, the heterogeneity in capillary spacing, and the capillary supply unit volume were maintained. Capillary segment lengths were shorter in both regions of the capillary network. In comparison, adult-onset hypothyroidism induced changes in the capillary bed which improved the geometrical conditions for tissue oxygen supply. Capillary numerical density increased, yet capillary segment lengths and capillary supply unit volumes all decreased, and the heterogeneity in capillary spacing was unchanged. Notably, capillary growth was observed in both adult thyroid states.

Based on the importance of normal plasma thyroid hormone levels during the neonatal period of cardiac development, and the observed responses in adults, the affect of altered thyroid hormone status on the developing coronary capillary and arteriolar networks was examined. In neonatal hearts, the problem of non-functional enzymes or reduced activity of the Alkaline phosphatase or Dipeptidyl peptidase IV enzyme was overcome by using a recently introduced method, *Bandeiraea simplicifolia I* lectin. This method enabled identification and localization of capillaries within a cross-section, in the hearts of young rats. The AP/DPP method was employed in older rats for the evaluation of capillary segment lengths. A routine Silver-methenamine stain was employed to facilitate morphometric assessment of the developing coronary arteriolar network.

Neonatal-onset hyperthyroidism enhanced cardiac growth, whereas neonatal

hypothyroidism attenuated this growth. In comparison, adult-onset hyperthyroidism induced cardiac hypertrophy and neonatal hypothyroidism induced cardiac atrophy. The response of the coronary capillary bed to alterations in thyroid hormone status during the neonatal and adult period, seemed to be directed towards maintaining the geometrical conditions for myocardial oxygen supply.

Hyperthyroidism and hypothyroidism induced during the early neonatal period, accelerated or attenuated maturation, respectively. With neonatal hyperthyroidism, cardiac hypertrophy was matched by capillary and arteriolar growth. Conversely neonatal hypothyroidism attenuated cardiac and coronary arteriolar growth. The response in coronary capillary growth was more varied, though provided evidence of attenuated growth. The influence of hyper- or hypothyroidism on the coronary arteriolar network was more apparent than on the capillary network. Based on the microvascular and cardiac changes observed in this neonatal model, it was suggested that the normal postnatal decline in capillary growth may be more dependent on the rate of tissue maturation than on the rate of cardiac growth. After return to a euthyroid status, cardiac mass was lower in both previously hypo- and hyperthyroid rat compared to normal. A significantly greater proportion of small arterioles was observed in previously hypothyroid rats, suggesting proliferation of smaller arterioles or lack of growth of larger ones. Further growth of the arteriolar bed was not observed in previously hyperthyroid rats. Moreover, lasting positive inotropic and chronotropic effects on heart function were induced by neonatal hyperthyroidism.

CONCLUSIONS

The data presented in this dissertation has served to address several important questions concerning the response of the coronary microvascular network to hyper- or hypothyroidism, induced during the neonatal or adult stage of development. The following principal conclusions may be drawn:

- Age did not appreciably affect the response of the coronary capillary network to altered thyroid status. However, it was a more prominent factor in the response of the developing coronary arteriolar network.

- Adult-onset hypo- and hyperthyroidism stimulated capillary growth in both regions (proximal and distal) of the capillary network. The elicited changes either maintained or improved the geometrical conditions for myocardial oxygen supply.

- Neonatal-onset hyperthyroidism enhanced capillary proliferation in proportion to the significant increase in cardiac mass. Whereas, the affect of neonatal hypothyroidism on capillary growth was variable.

- Neonatal-onset hyperthyroidism enhanced the growth of coronary arterioles whereas neonatal-onset hypothyroidism attenuated this growth.

- Neonatal-onset hyperthyroidism inhibited subsequent arteriolar growth and induced lasting positive chronotropic and inotropic effects on cardiac function, after return to euthyroidism. Neonatal-onset hypothyroidism resulted in a greater proportion of smaller arterioles, after return to euthyroidism.

REFERENCES

Anversa, P., Ricci, R. and Olivetti, G. (1986) Coronary capillaries during normal and pathological growth. *Can.J.Cardiol.* **2**:104-113

Anversa, P., Capasso, J.M., Ricci, R., Sonnenblick, E.H. and Olivetti, G. (1989) Morphometric analysis of coronary capillaries during physiologic myocardial growth and induced cardiac hypertrophy: A review. *Int.J.Microcirc.* **8**:353-363

Anversa, P., and Sonnenblick, E. H. (1990) Ischemic cardiomyopathy: pathophysiologic mechanisms. *Prog. Cardiovasc. Dis.* **33**:49-70.

Anversa, P. and Capasso, J.M. (1991) Loss of intermediate-sized coronary arteries and capillary proliferation after left ventricular failure in rats. *Am.J.Physiol.* **260**:H1552-H1560

Batra, S., Kuo, C. and Rakusan, K. Spatial distribution of coronary capillaries: A-V segment staggering. In: *Oxygen Transport to Tissue XI*, edited by Rakusan, K., Biro, G.P., Goldstick, T.K. and Turek, Z. New York/London: Plenum Press, 1989, p. 241-247.

Batra, S., Rakusan, K. and Campbell, S.E. (1991) Geometry of capillary networks in hypertrophied rat heart. *Microvasc.Res.* **42**:29-39

Batra, S. and Rakusan, K. (1991) Geometry of capillary networks in volume overloaded rat heart. *Microvasc.Res.* **42**:40-50

Batra, S. and Rakusan, K. (1992) Capillary network geometry during postnatal growth in rat hearts. *Am.J.Physiol.* **262(31)**:H635-H640

Beinlich, C.J., White, G.J., Baker, K.M. and Morgan, H.E. (1991) Angiotensin II and left ventricular growth in newborn pig heart. *J.Mol.Cell.Cardiol.* **23**:1031-1038

Beznak, M. (1962) Cardiovascular effects of thyroxine treatment in normal rats. *Can.J.Biochem.Physiol.* **40(12)**:1647-1654

Beznak, M. (1963) Cardiovascular effects of thyroxine treatment of hypophysectomized rats. *Circ.Res.* **12 (4)**:333-340

Brasel, J. and Winick, M. (1970) Differential Cellular Growth in the Organs of Hypothyroid Rats. *Growth* **34**:197-207

Bravo, R. and Macdonald-Bravo, H. (1987) Existence of two populations of cyclin/proliferating cell nuclear antigen during the cell cycle: association with DNA replication sites. *J.Cell.Biochem.* **105**:1549-1554

Breisch, E.A., White, F.C., Hammond, H.K., Flynn, S. and Bloor, C.M. (1989) Myocardial characteristics of thyroxine stimulated hypertrophy. A structural and functional study. *Basic Res.Cardiol.* **84**:345-358

Brent, G.A., Moore, D.D. and Larsen, P.R. (1991) Thyroid hormone regulation of gene expression. *Annu.Rev.Physiol.* **53**:17-35

Campbell, S.E. and Gerdes, A.M. (1988) Regional changes in myocyte size during the reversal of thyroid-induced cardiac hypertrophy. *J.Mol.Cell.Cardiol.* **20**:379-387

Campbell, S., Korecky, B. and Rakusan, K. (1991) Remodelling of myocyte dimensions in hypertrophic and atrophic rat hearts. *Circ.Res.* **68**:984-996

Canby, C.A. and Tomanek, R.J. (1989) Role of lowering arterial pressure on maximal coronary flow with and without regression of cardiac hypertrophy. *Am. J. Physiol.* **257**:H1110-H1118.

Casasco, A., Giordano, M., Danova, M., Casasco, M., Icaro Cornaglia, A. and Calligaro, A. (1993) PC10 monoclonal antibody to proliferating cell nuclear antigen as probe for cycling cell detection in developing tissues. A combined immunocytochemical and flow cytometric study. *Histochem.* **99(3)**:191-199

Chen, Y., Torry, R.J., Baumbach, G.L. and Tomanek, R.J. (1994) Proportional arteriolar growth accompanies cardiac hypertrophy induced by volume overload. *Am.J.Physiol.* **267**:H2132-H2137

Chilian, W.M., Wangler, R.D., Peters, K.G., Tomanek, R.J. and Marcus, M.L. (1985) Thyroxine-induced left ventricular hypertrophy in the rat. Anatomical and physiological evidence for angiogenesis. *Circ.Res.* **57**:591-598

Chilian, W.M. and Marcus, M.L. (1987) Coronary vascular adaptations to myocardial hypertrophy. *Annu.Rev.Physiol.* **49**:477-487

Chizzonite, R.A., and Zak, R. (1984) Regulation of myosin isozyme composition in fetal and neonatal rat ventricle by endogenous thyroid hormones. *J. Biol. Chem.* **259**:12628-12632.

Christie, K.N. and Thomson, C. (1989) Bandeiraea simplicifolia lectin demonstrates significantly more capillaries in rat skeletal muscle than enzyme methods. *J.Histochem.Cytochem.* **37(8)**:1303-1304

Cihak, R., Kolar, F., Pelouch, V., Prochazka, J., Ostadal, B. Widimsky, J. (1992) Functional changes in the right and left ventricle during the development of cardiac hypertrophy and after its regression. *Cardiovasc. Res.* **26(9)**:845-850.

Coleman, P.S., Parmacek, M.S., Lesch, M. and Samarel, A.M. (1989) Protein synthesis and degradation during regression of thyroxine-induced cardiac hypertrophy. *J.Mol.Cell.Cardiol.* **21**:911-925

Costerousse, O., Alegrini, J., Huang, H., Bounhik, J. and Alhenc-Gelas, F. (1994) Regulation of ACE gene expression and plasma levels during rat postnatal development. *Am.J.Physiol.* **267**:E745-E753

Craft-Cormney, C. and Hansen, J.T. (1980) Early ultrastructural changes in the myocardium following thyroxine-induced hypertrophy. *Virchows Arch.B Cell Path.* **33**:267-273

Dbaly, J. (1973) Postnatal development of coronary arteries in the rat. *Z.Anat.Entwickl.-Gesch.* **141**:89-101

Dieckman, L.J., and Solaro, R.J. (1990) Effect of thyroid status on thin-filament Ca^{2+} regulation and expression of troponin I in perinatal and adult rat hearts. *Circ. Res.* **67**:344-351.

Dietrich, D.R. (1993) Toxicological and pathological applications of proliferating cell nuclear antigen (PCNA), a novel endogenous marker for cell proliferation. *Crit.Rev.Toxicol.* **23**:77-109

Dillman, W.H. (1990) Biochemical basis of thyroid hormone action in the heart. *Am.J.Med.* **88**:626-630

Dubeck, J.K., Penney, D.G., Brown, T.R. and Sharma, P. (1989) Thyroxine treatment of neonatal rats suppresses normal and stress-stimulated heart cell hyperplasia and abolishes persistent cardiomegaly. *J.Appl.Cardiol.* **4**:195-205

DuPont Co: Sorval, *Microtomes: Instruction Manual*, Wilmington, Delaware:1979. pp. 27.

Dzau, V.J. Local expression and pathophysiological role of renin-angiotensin in the blood vessels and heart. In: *Angiotensin and the Heart*, edited by Grobecker, H., Heusch, G. and Strauer, B.F. Darmstadt: Steinkopff Verlag, 1993, p. 2-14.

Engerman, R.L., Pfaffenbach, D. and Davis, M.D. (1967) Cell turnover of capillaries. *Lab.Invest.* **17(6)**:738-743

Erzen, I. and Maravic, V. (1993) Simultaneous histochemical demonstration of capillaries and muscle fibre types. *Histochem.* **99**:57-60

Fagg Sanford, C., Griffin, E.E. and Wildenthal, K. (1978) Synthesis and degradation of myocardial protein during the development and regression of thyroxine-induced cardiac hypertrophy in rats. *Circ.Res.* **43(5)**:688-694

Flanagan, M.F., Aoyagi, T., Currier, J.J., Colan, S. and Fujii, A.M. (1994) Effect of young age on coronary adaptations to left ventricular pressure overload hypertrophy in sheep. *J.Am.Coll.Cardiol.* **24(7)**:1786-1796

Florini, J.R., Saito, Y. and Manowitz, E.J. (1973) Effect of age on thyroxine-induced cardiac hypertrophy in mice. *J.Gerontol.* **28(3)**:293-297

Gadeau, A., Campan, M. and Desgranges, C. (1991) Induction of cell cycle-dependent genes during cell cycle progression of arterial smooth muscle cells in culture. *J.Cell.Physiol.* **146**:356-361

Gerdes, M.A., Callas, G. and Kaster, F.H. (1979) Differences in regional capillary distribution and myocyte sizes in normal and hypertrophic rat hearts. *Am.J.Anat.* **156**:523-532

Gerdes, A.M., Kriseman, J. and Bishop, S.P. (1983) Changes in myocardial cell size and number during the development and reversal of hyperthyroidism in neonatal rats. *Lab.Invest.* **48(5)**:598-602

Gibbons, G.H., Prott, R.E., Dzau, V.J. (1992) Vascular smooth muscle cell hypertrophy vs. hyperplasia. Autocrine transforming growth factor-beta1 determines growth response to angiotensin II. *J. Clin. Invest.* **90**:456-461

Gordon, D., Reidy, M.A., Benditt, E.P. and Schwartz, S.M. (1990) Cell proliferation in human coronary arteries. *Proc.Natl.Acad.Sci.* **87**:4600-4604

Gratzner, H.G. (1982) Monoclonal antibody to 5-bromo- and 5-iododeoxy-uridine: a new reagent for detection of DNA replication. *Science* **218**:474-475.

Grim, M. and Carlson, B.M. (1990) Alkaline phosphatase and dipeptidyl/peptidase IV staining of tissue components of skeletal muscle: a comparative study. *J.Histochem.Cytochem.* **38**:1907-1912

Hansen-Smith, F.M., Watson, L., Lu, D.Y. and Goldstein, I. (1988) Griffonia simplicifolia I: Fluorescent tracer for microcirculatory vessels in nonperfused thin muscles and sectioned muscle. *Microvasc.Res.* **36**:199-215.

Hansen-Smith, F., Banker, K., Morris, L. and Joswiak, G. (1992a) Alternative histochemical markers for skeletal muscle capillaries: a statistical comparison among three muscles. *Microvasc.Res.* **44**:112-116

Hansen-Smith, F.M., Blackwell, L.H. and Joswiak, G.R. (1992b) Expression of muscle capillary alkaline phosphatase is affected by hypoxia. *J.Appl.Physiol.* **73(2)**:776-780

Haynes, R.C., and Murad, F. (1980) Thyroid and antithyroid drugs. In: *The Pharmacological Basis of Therapeutics*, edited by Goodman, A.G., Goodman, L.S., and Gilman, A. New York: MacMillan Publishing Co, Inc., 1980, p.1397-1419.

Hoofd, L., Turek, Z., Kubat, K., Ringnalda, B.E.M. and Kazda, S. Variability of intercapillary distance estimated on histological sections of rat heart. In: *Oxygen Transport to Tissue V11*, edited by Kreuzer, F., Cain, S.M., Turek, Z. and Goldstick, T.K. New York: Plenum Press, 1985, p. 239-247.

Hudlicka, O. and Tyler, K.R. *Angiogenesis: The growth of the vascular system*, New York:Academic Press, 1986. pp. 1-221.

Hudlicka, O., Wright, A.J.A., Hoppeler, H. and Uhlmann, E. (1988) The effect of chronic bradycardial pacing on the oxidative capacity in rabbit hearts. *Resp.Physiol.* **72**:1-12

Hudlicka, O., Brown, M., Egginton, S. (1992) Angiogenesis in skeletal and cardiac muscle. *Physiol. Rev.* **72(2)**:369-416.

Izumo, S. and Mahdavi, V. (1988) Thyroid hormone receptor alpha isoforms generated by alternative splicing differentially activate myosin HC gene transcription. *Nature* **334**:539-542

Kajstura, J., Mansukhani, M., Cheng, W., Reiss, K., Krajewski, S., Reed, J.C., Quaini, F., Sonnenblick, E.H., Anversa, P. (1995) Programmed cell death and expression of the proto-oncogene bcl-2 in myocytes during postnatal maturation of the heart. *Exp.Cell Res.* **219**:110-121

Karimu, A.L. and Burton, G.J. (1994) Significance of changes in fetal perfusion pressure to factors controlling angiogenesis in the human term placenta. *J.Reprod.Fert.* **102**:447-450

Klein, I. and Ojamaa, K. Thyroid hormone and blood pressure regulation. In: *Hypertension: Pathophysiology, Diagnosis, and Management*, edited by Laragh, J.H. and Brenner, B.M. New York: Raven Press, Ltd., 1995, p. 2247-2262.

Knighton, D.R., Silver, I.A., Hunt, T.K. (1981) Regulation of wound healing angiogenesis: effect of oxygen gradients and inspired oxygen concentration. *Surgery St. Louis* **90**:262-270.

Koenig, R.J., Warne, R.L., Brent, G.A., Harney, J.W., Larsen, P.R., and Moore, D.D. (1988) Isolation of a cDNA alone encoding a biologically active thyroid hormone receptor. *Proc. Natl. Acad. Sci USA* **85**:5031-5035.

Kolar, F., Seppet, E.K., Vetter, R., Prochazka, J., Grunermel, J., Zilmer, K., Ostadal, B. (1992) Thyroid control of contractile function and calcium handling in neonatal rat heart. *Eur.J.Physiol.* **421**:26-31

Korecky, B., Zak, R., Schwartz, K. and Aschenbrenner, V. (1987) Role of thyroid hormone in regulation of isomyosin composition, contractility, and size of heterotopically isotransplanted rat heart. *Circ.Res.* **60(6)**:824-830

Kossler, A., Hagmuller, K. and Winkler, R. (1987) The effects of experimental hypo- and hyperthyroidism on blood viscosity and other blood parameters in the rat. *Biorheol.* **24**:769-774

Kreuzer, F. (1982) Oxygen supply to tissues: The Krogh model and its assumptions. *Experientia* **38**:1415-1425

Krogh, A. (1919) The number and distribution of capillaries in muscles with calculations of the oxygen pressure head necessary for supplying the tissue. *J.Physiol.* **52**:409-415

Kupfer, J.M. and Rubin, S.A. (1992) Differential regulation of insulin-like growth factor I by growth hormone and thyroid hormone in the heart of juvenile hypophysectomized rats. *J. Mol. Cell. Cardiol.* **24(6)**:631-639.

Lawrence, M., Watson, L., Pettijohn, T., Doyle, T., Tasca, S.I. and Stoica, G. (1995) Immunohistochemical localization of proliferating cells, basic fibroblast growth factor and Fos protein following iliac artery balloon angioplasty in hypercholesterolemic

rabbits. *in vivo* 9:27-34

Li, H., Waga, S., Hannon, G.J., Beach, D. and Stillman, B. (1995) Differential effects by the p21 CDK inhibitor on PCNA-dependent DNA replication and repair. *Nature* **371**:534-537

Linden, M.D., Torres, F.X., Kubus, J. and Zarbo, R.J. (1992) Clinical application of morphologic and immunocytochemical assessments of cell proliferation. *Am.J.Clin.Pathol.* **97(5) suppl.**:S4-S13

Liu, H., Momotani, N., Yoshimura, J., Ishikawa, N., Takebe, K. and Ito, K. (1994) Maternal hypothyroidism during early pregnancy and intellectual development of the progeny. *Arch.Int.Med.* **154**:785-787

Liu, Z. and Gerdes, A.M. (1990) Influence of hypothyroidism and the reversal of hypothyroidism on hemodynamics and cell size in the adult rat heart. *J.Mol.Cell.Cardiol.* **22**:1339-1348

Lohr, F., Wenz, F., Haas, S. and Flentje, M. (1995) Comparison of proliferating cell nuclear antigen (PCNA) staining and BrdUrd-labelling index under different proliferative conditions in vitro by flow cytometry. *Cell Prolif* **28**:93-104

Lojda, Z. (1979) Studies on dipeptidyl(amino)peptidase IV (glycyl-proline naphthylamidase). *Histochem.* **59**:153-166

Lompre, A., Mercadier, J. and Schwartz, K. (1991) Changes in gene expression during cardiac growth. *Internat.Rev.Cytol.* **124**:137-187

MacLellan, W.R., Brand, T. and Schneider, M.D. (1993) Transforming growth factor-beta in cardiac ontogeny and adaptation. *Circ.Res.* **73**:783-791

Mall, G., Zimmer, G., Baden, S. and Mattfeldt, T. (1990) Capillary neoformation in the rat heart - stereological studies on papillary muscles in hypertrophy and physiologic growth. *Basic Res.Cardiol.* **85**:531-540

Marchant, C., Brown, L. and Sernia, C. (1993) Renin-angiotensin system in thyroid dysfunction in rats. *J.Cell.Physiol.* **22**:449-455

Marino, T.A., Haldar, S., Williamson, E.C., Beaverson, K., Walter, R., Marino, D.R., Beatty, C., Lipson, K.E. (1991) Proliferating cell nuclear antigen in developing and adult rat cardiac muscle cells. *Circ.Res.* **69**:1353-1360

Mathews, M.B., Bernstein, R.M., Franza Jr., B.R. and Garrels, J.L. (1984) Identity of the proliferating cell nuclear antigen and cyclin. *Nature* **309**:374-376

McCallister, L.P. and Page, E. (1973) Effects of thyroxin on ultrastructure of rat myocardial cells: a stereological study. *J.Ultrastructure Res.* **42**:136-155

Meisami, E. (1984) Complete recovery of growth deficits after reversal of PTU-induced postnatal hypothyroidism in the female rat: a model for catch-up growth. *Life Sci.* **34**:1487-1496

Michel, B., Grima, M., Coquard, C., Welsch, C., Barthelmebs, M. and Imbs, J.L. (1994) Effects of triiodothyronine and dexamethasone on plasma and tissue angiotensin converting enzyme in the rat. *Fundam.Clin.Pharmacol.* **8**:366-372

Mirsky, I. and Pasipoularides, A. (1990) Clinical Assessment of diastolic function. *Prog. Cardiovasc. Dis.* **32**:291-318.

Miyachi, K., Fritzler, M.J. and Tan, E.M. (1978) Autoantibody to nuclear antigen in proliferating cells. *J.Immunol.* **121**:2228-2234

Morkin, E., Flink, I.L. and Goldman, S. (1983) Biochemical and physiologic effects of thyroid hormone on cardiac performance. *Prog.Cardiovasc.Dis.* **25(5)**:435-459.

Moussavi, R., Meisami, E. and Timiras, P.S. (1985) Compensatory cell proliferation and growth in the rat heart after postnatal hypothyroidism. *Am.J.Physiol.* **248**:E381-E387

Neter, J., Wasserman, W. and Kutner, M.H. . In: *Applied Linear Statistical Models*, Boston: Irwin, 1990, p. 607-625.

Nickenig, G. and Murphy, T.J. (1994) Down-regulation by growth factors of vascular smooth muscle angiotensin receptor gene expression. *Mol.Pharmacol.* **46**:653-659

Ojamaa, K., Samarel, A.M., Kupfer, J.M., Hong, C. and Klein, I. (1992) Thyroid hormone effects on cardiac gene expression independent of cardiac growth and protein synthesis. *Am.J.Physiol.(Endocrinol.Metab.)* **263**:E534-E540

Olivetti, G., Anversa, P. and Loud, A.V. (1980) Morphometric study of early postnatal development in the left and right ventricular myocardium of the rat. *Circ.Res.* **46**:503-512

Polikar, R., burger, A.G., Scherrer, U. and Nicod, P. (1993) The thyroid and the heart. *Circulation* **87(5)**:1435-1441

Quaini, F., Cigola, E., Lagrasta, C., Saccani, G., Quaini, E., Rossi, C., Olivetti, G., Anversa, P. (1994) End-stage cardiac failure in humans is coupled with the induction of proliferating cell nuclear antigen and nuclear mitotic division in ventricular myocytes. *Circ.Res.* **75**:1050-1063

Rakusan, K. and Poupa, O. (1963) Changes in the diffusion distance in the rat heart muscle during development. *Physiol.Bohemoslov.* **12**:220

Rakusan, K., Jelinek, J., Korecky, B., Soukupova, M. and Poupa, O. (1965) Postnatal development of muscle fibres and capillaries in the rat heart. *Physiol.Bohemoslov.* **14**:32-37

Rakusan, K., Mesnil de Rochemont, W., Braasch, W., Tschopp, H. and Bing, R.J. (1967) Capacity of the terminal vascular bed during normal growth, in cardiomegaly, and in cardiac atrophy. *Circ.Res.* **21**:209-215

Rakusan, K. *Oxygen in the heart muscle*, Springfield:Charles C. Thomas, 1971. pp. 3-98.

Rakusan, K. Cardiac growth, maturation, and aging. In: *Growth of the heart in health and disease*, edited by Zak, R. New York: Raven Press, 1984, p. 131-164.

Rakusan, K. and Turek, Z. (1985) Protamine inhibits capillary formation in growing hearts. *Circ.Res.* **57**:393-398

Rakusan, K. Microcirculation in the stressed heart. In: *The Stressed Heart*, edited by Legato, M.J. Boston: Martinus Nijhoff Publishing, 1987, p. 107-123.

Rakusan, K. Development of cardiac vasculature. In: *Handbook or Human Growth and Developmental Biology*, edited by Meisami, E. and Timiras, P.S. Boston: CRC Press, 1990, p. 101-106.

Rakusan, K. and Wicker, P. (1990) Morphometry of the small arteries and arterioles in rat heart: effects of chronic hypertension and exercise. *Cardiovasc.Res.* **24**:278-284

Rakusan, K., Flanagan, M.F., Geva, T., Southern, J. and Van Praagh, R. (1992) Morphometry of human coronary capillaries during normal growth and the effect of age in left ventricular pressure-overload hypertrophy. *Circulation* **86**:38-46

Rakusan, K., Batra, S. and Heron, M.I. A new approach for quantitative evaluation of coronary capillaries in longitudinal sections. In: *Oxygen Transport to Tissue XVI*, edited by Hogan, M.C., Mathieu-Costello, O., Poole, D.C. and Wagner, P.D. New York: Plenum Press, 1994a, p. 407-415.

Rakusan, K., Cicutti, N. and Flanagan, F. (1994b) Changes in the microvascular network during cardiac growth, development and aging. *Cell.Mol.Biol.Res.* **40(2)**:117-122

Rakusan, K., Cicutti, N., Kazda, S. and Turek, Z. (1994c) Effect of nifedipine on coronary capillary geometry in normotensive and hypertensive rats. *Hypertension* **24**:205-211.

Rakusan, K. and Nagai, J. (1994) Morphometry of arterioles and capillaries in hearts of senescent mice. *Cardiovasc.Res.* **28**:969-972

Rakusan, K. and Heron, M.I. (1996) The effect of developmental stage on cardiac growth response. In: *The Developing Heart*, edited by Ostadal, B., Nagano, M., Takeda, N., and Dhalla, N.S., New York: Lippincott-Raven Publishers (in press).

Rakusan, K., Heron, M.I. and Sladek, T. (1996) The effect of losartan on endothelial cell proliferation in infarcted rat hearts (PCNA study). *Int.J.Microcirc.* (Abstract: Munich)

Read, L.C., Wallace, P.G. and Berry, M.N. (1987) Effects of thyroid state on respiration of perfused rat and guinea pig hearts. *Am.J.Physiol.* **253**:H519-H523

Reiss, K., Kajstura, J., Capasso, J.M., Marino, T.A., and Anversa, P. (1993) Impairment of myocyte contractility following coronary artery narrowing is associated with activation of the myocyte IGF1 autocrine system, enhanced expression of late growth related genes, DNA synthesis, and myocyte nuclear mitotic division in rats. *Exp.Cell Res.* **207**:348-360

Roberts, J.T. and Wearn, J.R. (1941) Quantitative changes in the capillary-muscle relationship in human hearts during normal growth and hypertrophy. *Am.Heart J.* **21**:617-633

Rongish, B.J., Torry, R.J. and Tomanek, R.J. (1995) Coronary neovascularization of embryonic rat hearts cultured in oculo is independent of thyroid hormones. *Am.J.Physiol.* **268 (37)**:H811-H816

Rosenblatt, J.D., Kuzon, W.M., Plyley, M.J., Pynn, B.R. and McKee, N.H. (1987) A histochemical method for the simultaneous demonstration of capillaries and fibre type in skeletal muscle. *Stain Technol.* **62(2)**:85-92

Samels, M. (1968) Thyroid function during postnatal development in the rat. *Gen. Comp. Endocrinol.* **10**:229-234

Samuels, H.H., Forman, B., Horowitz, Z.D. and Ye, Z. (1989) Regulation of gene expression by thyroid hormone. *Annu.Rev.Physiol.* **51**:623-639

Sap, J., Munoz, A., Damm, K., Goldberg, Y., Chysdael, J., Leutz, A., Beug, H., Vennstrom, B. (1986) The c-erb-A protein is a high-affinity receptor for thyroid hormone. *Nature* **324**:635-640

Sasaki, R., Morishita, T. and Yamagata, S. (1968) Mitosis of heart muscle cells in normal rats. *Tohoku J.Exp.Med.* **96**:405-411

Schieffer, B., Wirger, A., Meybrun, M., Seitz, S., Holtz, J., Riede, U.N. and Drexler, H. (1994) Comparative effects of chronic angiotensin-converting enzyme inhibition on angiotensin II type I receptor blockade on cardiac remodelling after myocardial infarction in the rat.*Circulation* **89**:2273-2282.

Segal, J., Troen, B.R., Ingbar, S.H. (1982) Influence of age and sex on the concentrations of thyroid hormone in serum in the rat. *J. Endocrinol.* **93**:177-181

Seiden, D., Navidad, P. and Weiss, H. (1988) Oxygen diffusion distance in thyroxine-induced hypertrophic rabbit myocardium. *J.Mol.Cell.Cardiol.* **20**:917-930

Seppet, E.K., Kolar, F., Dixon, I.M.C., Hata, T. and Dhalla, N.S. (1993) Regulation of cardiac sarcolemmal Ca^{2+} channels and Ca^{2+} transporters by thyroid hormone. *Mol.Cell.Biochem.* **129**:145-159

Shipley, R.A., Shipley, L.J. and Wearn, J. (1937) The capillary supply in normal and hypertrophied hearts of rabbits. *J.Exp.Med.* **65**:29-44

Shivji, M.K.K., Podust, V.N., Hubscher, U. and Wood, R.D. (1995) Nucleotide excision repair DNA synthesis by DNA polymerase E in the presence of PCNA, RFC, and RPA. *Biochem.* **34**:5011-5017

Sholley, M.M., Ferguson, G.P., Seibel, H.R., Montour, J.L. and Wilson, J.D. (1984) Mechanisms of neovascularization. Vascular sprouting can occur without proliferation of endothelial cells. *Lab.Invest.* **51(6)**:624-634

Sillau, A.H. and Banchero, N. (1977) Visualization of capillaries in skeletal muscle by the ATPase reaction. *Eur.J.Physiol.* **369**:269-271

Sladek, T., Sladkova, J., Kolar, F., Papousek, F., Cicutti, N., Korecky, B., Rakusan, K. (1996) The effect of AT_1 receptor antagonist on chronic cardiac response to coronary artery ligation in rats. *Cardiovasc. Res.* (in press)

Suzuki, K., Katoh, R. and Kawaoi, A. (1992) Immunohistochemical demonstration of proliferating cell nuclear antigen (PCNA) in formalin-fixed, paraffin-embedded sections from rat and human tissues. *Acta.Histochem.Cytochem.* **25 (1&2)**:13-21

Talafih, K., Briden, K.L. and Weiss, H.R. (1983) Thyroxine-induced hypertrophy of the rabbit heart. Effect on regional oxygen extraction, flow, and oxygen consumption. *Circ.Res.* **52**:272-279

Talafih, K., Grover, G.J. and Weiss, H.R. (1984) Effect of T4-induced cardiac hypertrophy on O_2 supply-consumption balance during normoxia and hypoxia. *Am.J.Physiol.* **246**:H374-H379

Tomanek, R.J. (1989) Sympathetic nerves modify mitochondrial and capillary growth in normotensive and hypertensive rats. *J. Mol. Cell. Cardiol.* **21**:755-764.

Tomanek, R.J. (1990) Response of the coronary vasculature to myocardial hypertrophy. *J.Am.Coll.Cardiol.* **15**:528-533

Tomanek, R.J., Barlow, P.A., Connell, P.M., Chen, Y. and Torry, R.J. (1993) Effects of hypothyroidism and hypertension on myocardial perfusion and vascularity in rabbits. *Am.J.Physiol.* **265**:H1638-H1644

Tomanek, R.J., Connell, P.M, Butters, C.A. and Torry, R.J. (1995) Compensated coronary microvascular growth in senescent rats with thyroxine-induced cardiac hypertrophy. *Am.J.Physiol.* **268**:H419-H425

Torres, A. and Tucker, D.C. (1993) Effects of thyroid hormones on cardiac development in oculo. *Am. J. Physiol.* **264**:H244-H251.

Turek, Z. and Rakusan, K. (1981) Lognormal distribution of intercapillary distance in normal and hypertrophic rat heart as estimated by the method of concentric circles: its effect on tissue oxygenation. *Eur.J.Physiol.* **391**:17-21

Unger, T., Mattfeldt, T., Lamberty, V., Bock, P., Mall, G., Linz, W., Schoulkens, B.A. and Gohlke, P. (1992) Effect of early onset angiotensin converting enzyme inhibition

on myocardial capillaries. *Hypertension* **20**:478-482.

van Dierendonck, J.H., Wijsman, J.H., Keijzer, R., van de Velde, C.J.H. and Corneliss, C.J. (1991) Cell-cycle-related staining patterns of anti-proliferating cell nuclear antigen monoclonal antibodies. Comparison with BrdUrd labelling and Ki-67 staining. *Am.J.Pathol.* **138(5)**:1165-1172

Vetterlein, F., Prange, M., Lubrich, D., Pedina, J., Neckel, M. and Schmidt, G. (1995) Capillary perfusion pattern and microvascular geometry in heterogeneous hypoxic areas of hypoperfused rat myocardium. *Am.J.Physiol.* **268(37)**:H2183-H2194

Vitullo, J.C., Penn, M.C., Rakusan, K. and Wicker, P. (1993) Effects of hypertension and aging on coronary arteriolar density. *Hypertension* **21**:406-414

Wachtlova, M., Ostadal, B. and Mares, V. (1985) Thyroxine-induced cardiomegaly in rats of different age. *Physiol.Bohemoslov.* **34**:385-394

Wallenstein, S., Zucker, C.L., Fleiss, J.L. (1980) Some statistical methods useful in circulation research. *Circ. Res.* **47**:1-9

Weinberger, C., Thompson, C.C., Ong, E.S., Lebo, R., Gruol, D.J. and Evans, R.M. (1986) The c-erb-A gene encodes a thyroid hormone receptor. *Nature* **324**:641-646

Weiss, H.R. and Grover, G.J. (1987) T4-induced cardiac hypertrophy and the perfused and total microvasculature of the heart. *Can.J.Physiol.Pharmacol.* **65**:1848-1855

Weiss, H.R. and Tse, J. (1995) Myocardial metabolic and functional responses to acetylcholine are altered in thyroxine-induced cardiac hypertrophy. *Can.J.Physiol.Pharmacol.* **73**:729-735

Wibo, M., Kolar, F., Zheng, L. and Godfraind, T. (1995) Influence of thyroid status on postnatal maturation of calcium channels, beta-adrenoceptors and cation transport ATPases in rat ventricular tissue. *J.Mol.Cell.Cardiol.* **27**:1731-1743

Wickline, K.M. and Fischer, V.W. (1985) Incorporation of [^{3}H]-thymidine into myocardial capillary cells in streptozotocin-diabetic rats. *Exp.Mol.Pathol.* **43**:135-141

Woeber, K.A. (1992) Thyrotoxicosis and the heart. *N.Eng.J.Med.* **327**:94-98

Wright, A.J.A. and Hudlicka, O. (1981) Capillary growth and changes in heart performance induced by chronic bradycardial pacing in the rabbit. *Circ.Res.* **49**:469-478

Yao, J. and Eghbali, M. (1992) Decreased collagen gene expression and absence of fibrosis in thyroid hormone-induced myocardial hypertrophy. *Circ.Res.* **71**:831-839

Yu, C.C.-W., Woods, A.L. and Levison, D.A. (1992) The assessment of cellular proliferation by immunohistochemistry: a review of currently available methods and their applications. *Histochem.J.* **24**:121-131

Zeymer, U., Fishbein, M.C., Forrester, J.S. and Cercek, B. (1992) Proliferating cell nuclear antigen immunohistochemistry in rat aorta after balloon denudation. Comparison with thymidine and bromodeoxyuridine labelling. *Am.J.Pathol.* **141(3)**:685-690

Zimmer, H.G. and Zierhut, W. Effects of thyroid hormones on the heart. Functional alterations and development of hypertrophy. In: *Cardiac Dilatation*, edited by Jacob, Seipel, and Zucker, Stuttgart: Gustav Fischer Verlag, 1990, p. 68-80.

Zimmer, H.G. *Heart Function in Heart and Disease*, London:Kluwer Academic Publishers, 1993. pp. 239-250.

CURRICULUM VITAE

Marcia Indranee Heron

EDUCATION

1991- present	University of Ottawa Ottawa, Ontario Graduate student - Physiology
1987-1991	Queen's University Kingston, Ontario Honours Bachelor of Science - Life Science

SCHOLARSHIPS & AWARDS

1994-1996	**Heart and Stroke Foundation of Canada Traineeship**
1994-1996	**Entrance Scholarship** - Graduate Studies and Research, University of Ottawa
1994-1996	**Ontario Graduate Scholarship** - Government of Ontario (declined 1994-1995 and 1995-1996)
July 1995	**Finalist in poster competition** - XV World Congress of the ISHR, Prague, Czech Republic
July 1995	**Travel Award - International Society for Heart Research**, XV World Congress of the ISHR, Prague, Czech Republic
1994-1995	**Gerald Taichman Award** - Best Research Achievement by a Graduate

Student (Ph. D. Program), Department of Physiology, University of Ottawa

SCHOLARSHIPS AND AWARDS CONT.

1993-1994	**Entrance Scholarship** - Graduate Studies and Research, University of Ottawa
1993-1994	**Graduate Studies and Research Award** - University of Ottawa
1992-1993	**Gerald Taichman Award** (M. Sc. Program), Department of Physiology, University of Ottawa
1991-1992	**Gerald Taichman Award** (M. Sc. Program), Department of Physiology, University of Ottawa
1991-1992	**Entrance Scholarship** - Faculty of Medicine, University of Ottawa

RESEARCH EXPERIENCE

1991 - current	**Graduate student (Ph. D. program)** - Department of Physiology, University of Ottawa Supervisor: Dr. Karel Rakusan
1990 and 1991	**Summer studentship** - Department of Physiology, Queen's University - MRC Group in Sensory-Motor Physiology Supervisor: Dr. Frances J.R. Richmond
1990 - 1991	**B. Sc. Honours Thesis** - Departments of Anatomy and Physiology, Queen's University. Thesis title: *Analysis of Single Muscle Fibre Lengths in Human gracilis and sartorius Muscles.* Supervisors: Dr. W. Forest and Dr. F.J.R. Richmond

TEACHING EXPERIENCE

1995-1996	**Teaching assistant** - Cardiovascular and respiratory physiology in first year ANP 1101 and 1301 course.
November/December 1995	**Tutor in Physiology** to second year nursing student
1993 - 1996	**Scientific Liaison** with area High Schools for the "Let's Talk Science" Program at the University of Ottawa
February - April 1994	**Tutor in Physiology** to second year nursing student
May 1993	**Teaching Assistant (Physiology)** - Ottawa/Hull Region Secondary School Science Week
October 1992	**Coordinator** of Shad Valley Student Enrichment Group, Health Sciences Tour and Conference
1991-1994	**Laboratory Demonstrator** - Medical Physiology Labs, University of Ottawa

MEMBERSHIPS, COMMITTEES AND POSITIONS HELD

1994-1996	Member - Canadian Physiological Society
1994-1996	Member - International Society for Heart Research, North American Section.
1993-1996	Graduate Student Representative - Human Research Ethics Committee of the Faculty of Medicine, University of Ottawa

1992-1993	Department of Physiology Representative on the Graduate Student Council, University of Ottawa

PEER REVIEWED PUBLICATIONS

Rakusan, K., **Heron, M.I.**, Kolar, F., Korecky, B. (1996) Transplantation induced atrophy of normal and hypertrophic rat hearts: effect on cardiac myocytes and capillaries. *Circulation* (submitted)

Heron, Marcia I., and Rakusan, Karel (1996) Effect of Neonatal Hypo- and Hyperthyroidism on Coronary Capillary Geometry and Long-term Cardiac Function in Rats. *Cardiovasc. Res.* (submitted)

Heron, Marcia I., and Rakusan, Karel (1996) Short and Long-term Effects of Neonatal Hypo- and Hyperthyroidism on Coronary Arterioles in Rat. *Am. J. Physiol. (Heart Circ. Physiol.)* (accepted)

Heron, Marcia I., and Rakusan, Karel (1995) Proliferating Cell Nuclear Antigen (PCNA) Detection of Cellular Proliferation in Hypothyroid and Hyperthyroid Rat Hearts. *J. Mol. Cell. Cardiol. 27(7)*:1393-1403

Heron, Marcia I. and Rakusan, Karel (1994) Geometry of Coronary Capillaries in Hyperthyroid and Hypothyroid Rat Heart. *Am. J. Physiol.* 267 (*Heart Circ. Physiol.* 36): H1024-H1031.

Rakusan, K., Batra, S., and **Heron, Marcia I.**, (1994) A New Approach for Quantitative Evaluation of Coronary Capillaries in Longitudinal Sections. In: *Oxygen Transport to Tissue XVI* , Eds. MC.Hogan et. al., Plenum Press, New York, p.407-415.

Heron, Marcia I., and Richmond, Frances J. R., (1993) In-Series Fibre Architecture in Long Human Muscles. *J. Morph.* 216: 35-45.

BOOK CHAPTERS

Rakusan, Karel and **Marcia I. Heron** (1996) The Effect of Developmental Stage on Cardiac Growth Response. In: *The Developing Heart*, Eds. B. Ostadal, M. Nagano, N. Takeda, and N. S. Dhalla, Lippincott-Raven Publishers, New York. (in press)

PUBLISHED ABSTRACTS

Heron, M.I., Kolar, F., Papousek, F., and Rakusan, K. (1995) Coronary Microvasculature in Neonatal Hypo- and Hyperthyroid Rats. Changes in Morphometry and Cardiac Function after Return to Euthyroidism. *J. Mol. Cell. Cardiol. 27(6): A230*
(presented by M. Heron at the 1995 World Congress of the International Society for Heart Research, Prague, Czech Republic). Presentation selected as Finalist in Poster Competition.

Rakusan, Karel and **Heron, Marcia I.** (1995) Postnatal Development of the Mammalian Heart: Growth of the Vascular Structures. *J. Mol. Cell. Cardiol. 27(6): A275*
(presented by K. Rakusan at the 1995 World Congress of the International Society for Heart Research, Prague, Czech Republic)

Heron, Marcia I., Kolar, F., Papousek, F., and Rakusan, K. (1995) Neonatal Hypo- and Hyperthyroidism and its Correction: Effect on Ventricular Hemodynamics in Rat Heart. *J. Mol. Cell. Cardiol. 27(6): A312*
(presented by M. Heron at the 1995 Otto-Frank Satellite Symposium to the World Congress of the International Society for Heart Research, Munich, Germany)

Rakusan, Karel and **Heron, Marcia I.** (1995) The Effect of Developmental Stage on Cardiac Growth Response (Morphometric Study). *J. Mol. Cell. Cardiol. 27(5): A11*
(presented by K. Rakusan at the 1995 Annual Meeting of the International Society for Heart Research, Perdido Beach, Alabama)

Heron, Marcia I. and Rakusan, Karel (1994) Proliferating Cell Nuclear Antigen (PCNA) Detection of Cellular Proliferation in Hypo- and Hyperthyroid Rat Heart. *J. Mol. Cell. Cardiol.* 26(7):CLIX
(presented by M. Heron at the 1994 Annual Meeting of the International Society for Heart Research, London, Ontario)

Rakusan, Karel and **Heron, Marcia I.**, (1993) A New Approach for Quantitative Evaluation of Coronary Capillaries in Longitudinal Sections.
(presented by K. Rakusan at the 1993 Annual Meeting of the International Society for Oxygen Transport to Tissue, San Diego, California)

Heron, M.I. and Rakusan, K., (1993) The Effect of Thyroid Hormone Status on

Coronary Capillaries in Rat Myocardium. *Can. J. Physiol. Pharmacol.* 71(2):Avii **(ORAL)**
(presented by M. Heron at The Canadian Physiological Society 1993 Annual Winter Meeting, Mt. Tremblant, Quebec)

Heron, Marcia I., Parry, D. J., and Rakusan, Karel, (1992) The Influence of Differing Skeletal Muscle Fibre Types on Capillary Domain Areas in Rat Gastrocnemius Muscle. *J. Mol. Cell. Cardiol.* 24(Suppl. III): 64
(presented by M. Heron at the 1992 Annual Meeting of the International Society for Heart Research, Burlington, Vermont)

Smits, E., **Heron, M.I.**, Rose, P.K., Gordon, T.T., and Richmond, F.J.R. (1991) Motor-Unit Distribution in Feline Anterior Sartorius Muscle. *Soc. Neurosci. Abs.* #555.11
(presented by E. Smits at the 21st Annual Meeting of The Society for Neuroscience, Louisiana, New Orleans)